Title
Frequency Modulation Processing in Primary Auditory Cortex

Author
Heiser, Marc

Publication Date
2008-06-10

Frequency Modulation Processing In Primary Auditory Cortex

by

Marc Aaron Heiser

DISSERTATION

Submitted in partial satisfaction of the requirements for the degree of

DOCTOR OF PHILOSOPHY

in

Neuroscience

in the

GRADUATE DIVISION

of the

UNIVERSITY OF CALIFORNIA, SAN FRANCISCO

[redacted]

Dedication

For my grandparents, my parents, my sister, and my wife to be…

Abstract:

Frequency-modulated (FM) are important components of animal vocalizations, human speech, and music. The representation of these important sounds in the auditory cortex of awake animals remains unknown, as do the effect of background noise on the representation of these sounds. Here, we determine the encoding of FM sweeps in primary auditory cortex (AI) of awake squirrel monkeys. We also examine the effects of varying the level of a white noise masker on the responses of AI neurons to FM sweeps. We find that FM sweeps are represented differently in different populations of neurons. Some neurons have sustained responses and a rate code for FM sweeps while others have brief responses and a temporal code. Background noise produced a variety of effects on the responses of AI neurons to FM sweeps. While noise degraded the responses of some neurons, the responsiveness of many AI neurons increased in the presence of noise. These results advance our understanding of the processing of frequency modulations in auditory cortex.

Table of Contents

Chapter 1

Introduction

Introduction to Thesis

Understanding the relation between communication sounds, the neuronal responses they generate in auditory cortex, and their perception is a fundamental goal of auditory neuroscience. In particular this is important in the context of determining where in the auditory system is a transition between external, stimulus-based information processing to a more conceptual, object-based processing framework that is more suitable to interface with higher cognitive functions, such as the language system in humans. A number of experimental approaches have been developed to address this issue. Many studies have examined the selectivity of cortical neurons for vocalizations themselves (Z. Wollberg and J. D. Newman, 1972; J. D. Newman and Z. Wollberg, 1973b, a; X. Wang et al., 1995; X. Wang and S. C. Kadia, 2001; L. M. Romanski and P. S. Goldman-Rakic, 2002; L. Qin et al., 2008). These experiments asked whether neurons behave as vocalization detectors or are selective for features of vocalizations, where selectivity is defined as an increased firing rate for a particular value or range of values of a stimulus parameter. In general, neurons that are selective for a sensory stimulus may carry relevant information for performance of a perceptual task in which that stimulus must be detected or discriminated from other stimuli (A. J. Parker and W. T. Newsome, 1998). If neurons are selective for particular vocalizations or other sounds, then they likely play a critical role in the perception of those sounds. Yet, because of their spectro-temporal complexity, it is difficult to determine the aspects of communication sounds for which auditory cortical neurons are selective. Therefore, another approach to the question of the relation between communication sounds, neuronal responses, and behavior is to determine the cortical representation of synthetic components of vocalizations. This approach will be discussed in more detail in the following section.

Neuronal responses to communication sounds are often complex and the question of which aspects of responses are critical for performance of auditory tasks remains unanswered (I. Nelken et al., 2005). For example, playback of vocalizations elicits changes in the firing rate of AI neurons. These changes in firing rate have a highly specific temporal structure that varies between vocalization stimuli (X. Wang et al., 1995; S. S. Nagarajan et al., 2002; I. Nelken et al., 2005; J. W. Schnupp et al., 2006; N. Mesgarani et al., 2008). The temporal window over which variations in the firing rate of neurons is integrated to produce changes in the perception of vocalizations, however, is not known, and, therefore, the importance of these temporal variations in neuronal responses is unknown. Furthermore, it is unknown how sensitive downstream areas are to specific combinations or patterns of spike times. Analytical techniques have been developed which determine the theoretical limits of sensory discrimination based upon either the stimulus driven spike count (or long term firing rate) of neurons or the precise temporal pattern of neuronal responses (F. Rieke et al., 1997; J. Victor and K. Purpura, 1999; S. Panzeri and S. R. Schultz, 2001; M. C. van Rossum, 2001; G. Foffani and K. A. Moxon, 2004; E. E. Thomson and W. B. Kristan, 2005). These estimates of sensory detection/discrimination performance based upon neuronal responses can then be compared with psychophysical performance in order to understand how responses are integrated into behavioral decisions.

The goal of this thesis is to identify strategies that form the basis of the representation of components of communication sounds in primary auditory cortex (AI). Towards this goal, we have examined the encoding of a class of sounds, frequency modulated (FM) sweeps, in different background noise conditions in AI of awake squirrel monkeys. FM sweeps are pure tones the frequency of which changes over time. These sounds are defined by four parameters: the start frequency, the end frequency, the direction of modulation, and the rate, or speed of modulation. Importantly, FM sweeps are critical elements of communication sounds and music. Formant transitions in human speech, for example, consist of rapid shifts in the spectral peaks (or formants) over time and determine the perceptual categories that distinguish some phonemes (A. M. Liberman et al., 1967; B. E. Lindblom and M. Studdert-Kennedy, 1967; F. G. Zeng et al., 2005). The vocalizations of many non-human primates are composed of single or repeated phrases of FM sweeps (P. Winter et al., 1966; J. D. Newman, 1978; T. Riede and K. Zuberbuhler, 2003), and FM sweeps in bat bio-sonar signals are used for the determination of target distance (N. Suga, 1989). Because of their prevalence in communications sounds, a complete understanding of the processing of FM sweeps will systematically advance our understanding of more general signal encoding in the central auditory system.

In addition, communication sounds must be detected, discriminated, and categorized in the presence of other background sounds. The acoustic conditions in which signals are presented will affect their representation in auditory cortex, and yet at some processing stage, neuronal responses to signals must tolerate variations in acoustic conditions. Determining the effects of the level of background noise on the representation of FM sweeps will reveal the principles of stimulus encoding in AI that may contribute to the processing of complex sounds across conditions.

The Representation of FM Sweeps in the Central Auditory System

Experiments have examined the responses of neurons throughout the central lemniscal auditory system to FM sweeps. The responses of most auditory neurons to FM sweeps are largely determined by their frequency tuning. In general, auditory neurons are selective for the frequency of acoustic stimuli, a property predominately inherited from the spatial distribution of frequency responsiveness of the basilar membrane of the cochlea. By presenting pure tones with varying frequency and intensity, experimenters determine the frequency response area (FRA) of auditory neurons (Fig 1A). When FM sweeps are presented, neurons begin firing action potentials when the instantaneous sweep frequency is within the FRA (S. D. Erulkar et al., 1968; P. Heil et al., 1992a; P. Heil and D. R. Irvine, 1998; B. Godey et al., 2005) (Fig 1B). The length of the response varies between auditory stations and is affected by the state of alertness (awake vs. anesthetized). In the cochlear nucleus, neurons often respond as long as the instantaneous sweep frequency is within the FRA, while in the medial geniculate nucleus and AI of anesthetized animals, FM sweeps often produce onset responses.

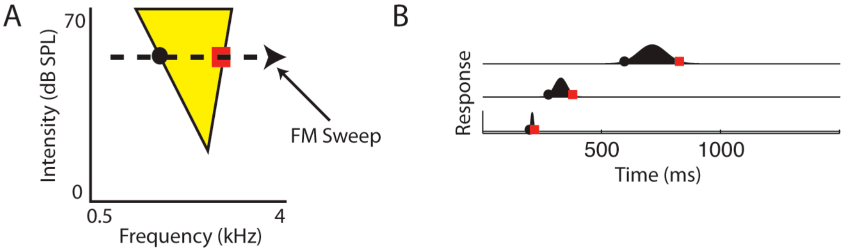

Figure 1. Relation between frequency tuning and FM sweep responses. A. Schematic of an FRA from an AI neuron. The dashed arrow represents an upward FM sweep (frequency increasing over time). The black circle and red square represent the frequency at which the FM response begins and ends respectively. B. Schematic PSTHs of responses to FM sweeps with different speeds. The bottom PSTH represents the response to a fast modulation rate while the uppermost represents the response to a slower modulation rate. The sweep frequency is within the tonal receptive field for a longer duration for slower modulation rates. This produces a longer response.

Most studies of FM processing in the central auditory system have focused on the selectivity of central auditory neurons for the direction and speed of FM sweeps and suggest that neurons in higher auditory stations are more sensitive to the to these parameters. The majority of Eighth nerve neurons have symmetric responses to up (increasing frequency) and down (decreasing frequency) FM sweeps (R. Britt and A. Starr, 1976). Many neurons have increased firing rates as the modulation rate increases indicating some sensitivity to the speed of the modulation. In the cochlear nucleus of cats, neurons have more complex responses to FM sweeps of varying speed and direction that depend on the response class of the neuron under study (N. Suga, 1964, 1965; S. D. Erulkar et al., 1968; R. Britt and A. Starr, 1976). In general, primary-like neurons are not direction selective while many onset units respond only to one direction of modulation. Build-up and pauser neurons had mixed direction sensitivity. Neurons in the inferior colliculus (IC) are often direction selective and tuned to the speed of frequency sweeps (A. Rees and A. R. Moller, 1983; P. W. Poon et al., 1991; C. Felsheim and J. Ostwald, 1996; H. J. Lee et al., 2002). Most neurons in the ventral division of the medial geniculate nucleus (MGNv) respond best to fast or medium FM speeds and many neurons are direction selective (O. Creutzfeldt et al., 1980; B. Lui and J. R. Mendelson, 2003). Figure 2 shows peri-stimulus time histograms (PSTHs) of responses to linear FM sweeps for a direction/speed selective MGNv neuron. Overall, the MGN is thought to contain more direction selective neurons than the IC.

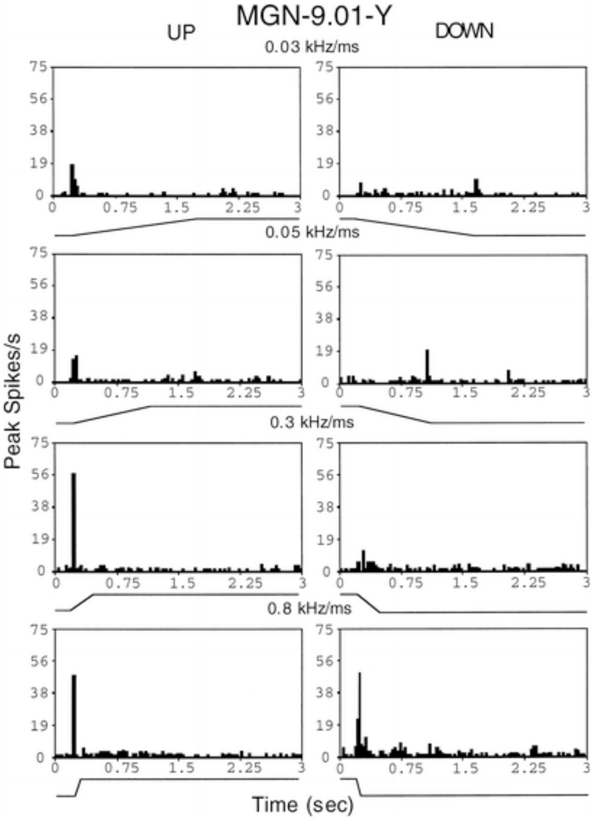

Figure 2. FM sweep responses in the auditory thalamus. PSTHs of responses to FM sweeps with slow modulation speeds are shown in the upper part of the figure. The modulation speed

increases as you move down. Responses to up and down sweeps are shown in the left and right columns respectively. This neuron responded best to fast up sweeps. From Lui and Mendelson (2003).

Studies in a number of species have examined the responses of AI neurons to FM sweeps. Many of these studies have demonstrated that AI neurons are sensitive to the rate of change of frequency, or sweep speed. Selectivity for the speed of frequency modulation is likely influenced by cortical inhibition. In AI of anesthetized pallid bats, late-arriving high frequency inhibition confers selectivity for fast modulation speeds (K. A. Razak and Z. M. Fuzessery, 2006). In this study, AI neurons were more broadly tuned for FM rate than neurons in the IC. In anesthetized AI of several species, neurons have been shown to be direction selective and several studies have demonstrated a relation between the pure tone best frequency (BF) or center frequency (CF) of the neuron and the preference for up or down modulation such that neurons with lower BFs prefer up sweeps while neurons with higher BFs prefer down sweeps (D. P. Phillips and M. S. Cynader, 1985; P. Heil et al., 1992b; P. Heil et al., 1992a; S. A. Shamma et al., 1993; B. Tian and J. P. Rauschecker, 1994; I. Nelken and H. Versnel, 2000; P. W. Poon and P. P. Yu, 2000; L. I. Zhang et al., 2003; B. Godey et al., 2005). To quantify the direction selectivity of cortical neurons a direction selectivity index (DSI) is used. The DSI is defined as,

$\mathrm{DSI} = \frac{r_{up} - r_{down}}{r_{up} + r_{down}}$ where r_{up} is the response to an increasing FM sweep, r_{down} is the response to a decreasing FM sweep. The relationship between the frequency tuning and direction preference of neurons in AI of the anesthetized rats is illustrated in

Figure 3, which shows a tonotopic frequency map (Fig. 3A) and a corresponding distribution of direction selectivity index values across the surface of AI (Fig. 3B). CF and DSI were highly correlated (Fig. 3C). Zhang et al. (2003) demonstrated that this relationship could be partially explained by systematic differences in cortical synaptic excitation and inhibition: neurons with low CFs had stronger excitatory and inhibitory currents on the low frequency side of the synaptic FRA while neurons with high CFs had greater currents on the high frequency side of the synaptic FRA. Asymmetric synaptic input produced asymmetric FM sweep responses because FM sweeps in the non-preferred direction evoked weak subthreshold excitatory currents and inhibitory currents that reduced the probability of spiking before the onset of stronger excitatory currents. In the preferred direction strong excitatory currents produce a spiking response before the onset of inhibition.

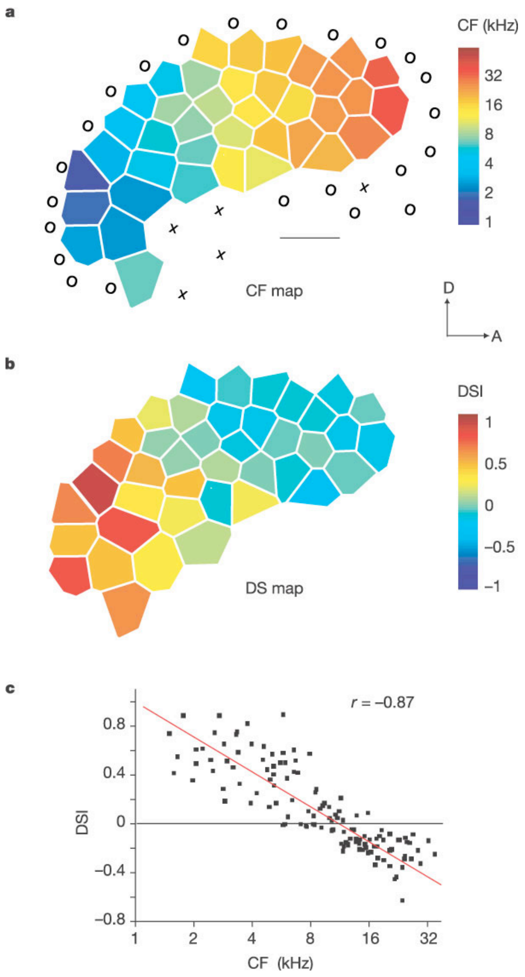

Figure 3. Relation between frequency preference and direction selectivity in AI. A. The spatial distribution of CFs for neurons in AI of an anesthetized rat are shown by color. 'o' and 'x' represent locations that were not responsive or not tuned to frequency. Scale bar = 0.5mm, 'A' = anterior, 'D' = dorsal. B. Spatial map of DSI values AI in the same rat. Colors indicate DSI value. C. Correlation between CF and DSI from 5 rats. Red line is least squares fit. From Zhang et al. (2003).

That cortical inhibition enhances direction selectivity in AI suggests that computation of the direction of frequency modulation may be an import function of auditory cortex. An intact AI is necessary for the perception and discrimination of species-specific vocalizations suggesting that AI involved in the processing of temporally complex sounds (H. E. Heffner and R. S. Heffner, 1984, 1986; I. A. Harrington et al., 2001). In addition, lesions of the right auditory cortex impair the ability of animals to discriminate the direction of FM sweeps (F. W. Ohl et al., 1999; N. Rybalko et al., 2006; W. Wetzel et al., 2008). Therefore, auditory cortex plays a critical role in the extraction of modulation direction from complex sounds. Yet, the relation between the selectivity of AI neurons for parameters of FM sweeps and behavioral discrimination has not been determined nor have the theoretical limits of FM sweep parameter discrimination and identification based upon AI responses been examined. Furthermore, the specific aspects of AI neuronal responses that contribute to behavioral decisions about FM sweep parameters remain unknown.

Species Similarity and Response Diversity in AI

Neurophysiological experiments have demonstrated a surprising correspondence between the responses to simple stimuli in AI of a number of mammalian species. As discussed above, there is a topographically organized distribution of frequency modulation direction preference in AI of rats, cats, ferrets, and primates. The preference and selectivity of neurons for the speed of frequency modulation are also clustered spatially across the surface of AI in several species (J. R. Mendelson et al., 1993; B. Godey et al., 2005). In fact, AI neurons across species represent a wide range of simple stimulus parameters including tone frequency, spectral bandwidth, sound intensity, and temporal modulation rate, among others, and many of these stimulus parameters are topographically organized such that neurons that prefer similar values of a parameter are spatially clustered or organized into modules in a manner analogous to the orientation selectivity of neurons in primary visual cortex (C. E. Schreiner and J. R. Mendelson, 1990; C. E. Schreiner and M. L. Sutter, 1992; M. P. Kilgard and M. M. Merzenich, 1999; G. H. Recanzone et al., 1999; S. W. Cheung et al., 2001; D. B. Polley et al., 2007; N. Mesgarani et al., 2008). Such functional similarity of AI across species suggests that, at this early cortical stage, sound processing is more general and that AI is suited to represent a wide range of sounds. Therefore, the principles of sound representation in animal AI likely apply to the processing of complex sounds in human AI.

The selectivity of different neurons for different ranges of a stimulus parameter produces a distributed representation of sounds in cortex. Most studies of the representation of sound parameters in auditory cortex have been conducted in anesthetized animals. Neurophysiological experiments in AI of awake animals have also revealed a diversity of preferences for simple stimuli including tones and amplitude modulation sounds (I. O. Volkov and A. V. Galaziuk, 1985; G. H. Recanzone, 2000; T. Lu et al., 2001; X. Wang et al., 2005; B. J. Malone et al., 2007; T. Hromadka et al., 2008). Furthermore, these experiments demonstrated an increased prevalence of sustained responses in awake animals in contrast to anesthetized animals. As most studies of FM processing in AI were conducted in anesthetized animals, the significance of the response diversity in awake animals for the representation of FM sweep remains unknown. Furthermore, the relation between fundamental response properties such as response threshold, spectral integration, and response latency, and sustained and onset response modes has not been determined. In both AI and the IC of anesthetized cats, fundamental properties such as firing rate are related to the selectivity of neurons for stimulus features and in the transmission of stimulus-related information (M. A. Escabi et al., 2005; C. A. Atencio and C. E. Schreiner, 2008). Knowledge of relations among various response modes and other neuronal properties will reveal general encoding strategies used by the auditory cortex and provide clues as to the synaptic mechanisms that generate response diversity in awake animals.

Effects of Background Noise on AI Neurons

Because most sounds do not occur in silence, it is essential to determine the effects of background noise on the representation of sounds in auditory cortex. Background noise produces a variety of effects on the responses of AI neurons. Responses to noise itself depend upon the intensity tuning of neurons; Neurons with monotonic rate-level functions for pure tones usually respond to wide-band noise while neurons with non-monotonic rate-level function do not (D. P. Phillips et al., 1985). Because monotonic and non-monotonic neurons are spatially segregated in AI (D. P. Phillips et al., 1985; C. E. Schreiner et al., 1992; D. B. Polley et al., 2007), responsiveness to noise also varies across cortex. In addition, noise responses are related to the more general property of spectral integration. Neurons with narrowband spectral tuning often do not respond to broadband noise while broadband neurons respond to broadband sounds. The response to noise illustrates the complex relation between the selectivity of cortical neurons to multiple features of a sound. The result is that noise produces non-uniform effects distributed across the population of AI neurons.

The consequences of the non-uniform distribution of responses to noise on the representation of sounds at the population level in auditory cortex remain to be determined. At the single unit level, neurons adapt to the presence of noise (D. P. Phillips, 1990; G. Ehret and C. E. Schreiner, 2000). Neuronal thresholds for tone responses increase, and rate-level functions derived from tone responses are shifted towards higher intensities. These studies, however, were conducted in anesthetized animals where responses to noise are not sustained in contrast to awake animals (G. H. Recanzone, 2000). Furthermore, the population response to signals in the context of noise is unknown. Using adaptation or other encoding strategies, AI may produce a population response that is normalized across background noise conditions. This would aid in the establishment of context invariant signal representations and in the ability of animals to recognize sounds in different environments.

Thesis Organization

All of the studies in this thesis were conducted in awake squirrel monkeys (*Saimiri sciureus*). Squirrel monkeys are arboreal primates that live in large colonies and maintain group contact using a complex repertoire of vocalizations (L. A. Rosenblum and R. W. Cooper, 1968; D. Todt et al., 1988). AI in the squirrel monkey is easily accessible, lying primarily on the lateral surface of the temporal gyrus (H.

Burton and E. G. Jones, 1976; E. G. Jones and H. Burton, 1976; S. W. Cheung et al., 2001). The importance of sounds for the behavior of squirrel monkeys and the accessibility of AI makes them ideally suited for studies of the auditory cortex.

In chapter 2, we examine the relation between tone responses, FM sweeps, and other fundamental neuronal properties such as the threshold and frequency tuning bandwidth of neurons in AI of awake squirrel monkeys. The response mode (sustained or onset) of AI neurons has been hypothesized to be highly stimulus specific and a consequence of the optimality of the stimulus under study (X. Wang et al., 2005; X. Wang, 2007). Here, we examine the generality of the response mode and the functional significance of sustained and onset responses for the encoding of FM sweeps.

In Chapter 3 we use information theory (T. M. Cover and J. A. Thomas, 2006) to determine the theoretical limits for the identification of FM sweep stimuli based upon the temporal pattern of responses in AI and the spike count of AI neurons. Using this technique, we can determine the information these aspects of the response carry about FM sweeps.

The effects of background noise on the representation of FM sweeps in AI are examined in Chapter 4. We determine the response magnitude and response selectivity for FM sweep parameters in different levels of background noise. The information contained in the temporal response pattern and in the firing rate of AI neurons is also quantified as a function of background noise level. Furthermore, the population representation of FM sweeps in different background noise levels is determined.

Lastly, in chapter 5, we summarize our results and discuss directions for future research.

References:

Atencio CA, Schreiner CE (2008) Spectrotemporal processing differences between auditory cortical fast-spiking and regular-spiking neurons. J Neurosci 28:3897-3910.

Britt R, Starr A (1976) Synaptic events and discharge patterns of cochlear nucleus cells. II. Frequency-modulated tones. J Neurophysiol 39:179-194.

Burton H, Jones EG (1976) The posterior thalamic region and its cortical projection in New World and Old World monkeys. J Comp Neurol 168:249-301.

Cheung SW, Bedenbaugh PH, Nagarajan SS, Schreiner CE (2001) Functional organization of squirrel monkey primary auditory cortex: responses to pure tones. J Neurophysiol 85:1732-1749.

Cover TM, Thomas JA (2006) Elements of information theory, 2nd Edition. Hoboken, N.J.: Wiley-Interscience.

Creutzfeldt O, Hellweg FC, Schreiner C (1980) Thalamocortical transformation of responses to complex auditory stimuli. Exp Brain Res 39:87-104.

Ehret G, Schreiner CE (2000) Regional variations of noise-induced changes in operating range in cat AI. Hear Res 141:107-116.

Erulkar SD, Butler RA, Gerstein GL (1968) Excitation and inhibition in cochlear nucleus. II. Frequency-modulated tones. J Neurophysiol 31:537-548.

Escabi MA, Nassiri R, Miller LM, Schreiner CE, Read HL (2005) The contribution of spike threshold to acoustic feature selectivity, spike information content, and information throughput. J Neurosci 25:9524-9534.

Felsheim C, Ostwald J (1996) Responses to exponential frequency modulations in the rat inferior colliculus. Hear Res 98:137-151.

Foffani G, Moxon KA (2004) PSTH-based classification of sensory stimuli using ensembles of single neurons. J Neurosci Methods 135:107-120.

Godey B, Atencio CA, Bonham BH, Schreiner CE, Cheung SW (2005) Functional organization of squirrel monkey primary auditory cortex: responses to frequency-modulation sweeps. J Neurophysiol 94:1299-1311.

Harrington IA, Heffner RS, Heffner HE (2001) An investigation of sensory deficits underlying the aphasia-like behavior of macaques with auditory cortex lesions. Neuroreport 12:1217-1221.

Heffner HE, Heffner RS (1984) Temporal lobe lesions and perception of species-specific vocalizations by macaques. Science 226:75-76.

Heffner HE, Heffner RS (1986) Hearing loss in Japanese macaques following bilateral auditory cortex lesions. J Neurophysiol 55:256-271.

Heil P, Irvine DR (1998) Functional specialization in auditory cortex: responses to frequency-modulated stimuli in the cat's posterior auditory field. J Neurophysiol 79:3041-3059.

Heil P, Rajan R, Irvine DR (1992a) Sensitivity of neurons in cat primary auditory cortex to tones and frequency-modulated stimuli. I: Effects of variation of stimulus parameters. Hear Res 63:108-134.

Heil P, Langner G, Scheich H (1992b) Processing of frequency-modulated stimuli in the chick auditory cortex analogue: evidence for topographic representations and possible mechanisms of rate and directional sensitivity. J Comp Physiol [A] 171:583-600.

Hromadka T, Deweese MR, Zador AM (2008) Sparse representation of sounds in the unanesthetized auditory cortex. PLoS Biol 6:e16.

Jones EG, Burton H (1976) Areal differences in the laminar distribution of thalamic afferents in cortical fields of the insular, parietal and temporal regions of primates. J Comp Neurol 168:197-247.

Kilgard MP, Merzenich MM (1999) Distributed representation of spectral and temporal information in rat primary auditory cortex. Hear Res 134:16-28.

Lee HJ, Wallani T, Mendelson JR (2002) Temporal processing speed in the inferior colliculus of young and aged rats. Hear Res 174:64-74.

Liberman AM, Cooper FS, Shankweiler DP, Studdert-Kennedy M (1967) Perception of the speech code. Psychol Rev 74:431-461.

Lindblom BE, Studdert-Kennedy M (1967) On the role of formant transitions in vowel recognition. J Acoust Soc Am 42:830-843.

Lu T, Liang L, Wang X (2001) Temporal and rate representations of time-varying signals in the auditory cortex of awake primates. Nat Neurosci 4:1131-1138.

Lui B, Mendelson JR (2003) Frequency modulated sweep responses in the medial geniculate nucleus. Exp Brain Res 153:550-553.

Malone BJ, Scott BH, Semple MN (2007) Dynamic amplitude coding in the auditory cortex of awake rhesus macaques. J Neurophysiol 98:1451-1474.

Mendelson JR, Schreiner CE, Sutter ML, Grasse KL (1993) Functional topography of cat primary auditory cortex: responses to frequency-modulated sweeps. Exp Brain Res 94:65-87.

Mesgarani N, David SV, Fritz JB, Shamma SA (2008) Phoneme representation and classification in primary auditory cortex. J Acoust Soc Am 123:899-909.

Nagarajan SS, Cheung SW, Bedenbaugh P, Beitel RE, Schreiner CE, Merzenich MM (2002) Representation of spectral and temporal envelope of twitter vocalizations in common marmoset primary auditory cortex. J Neurophysiol 87:1723-1737.

Nelken I, Versnel H (2000) Responses to linear and logarithmic frequency-modulated sweeps in ferret primary auditory cortex. Eur J Neurosci 12:549-562.

Nelken I, Chechik G, Mrsic-Flogel TD, King AJ, Schnupp JW (2005) Encoding stimulus information by spike numbers and mean response time in primary auditory cortex. J Comput Neurosci 19:199-221.

Newman JD (1978) Perception of sounds used in species-specific communication: the auditory cortex and beyond. J Med Primatol 7:98-105.

Newman JD, Wollberg Z (1973a) Multiple coding of species-specific vocalizations in the auditory cortex of squirrel monkeys. Brain Res 54:287-304.

Newman JD, Wollberg Z (1973b) Responses of single neurons in the auditory cortex of squirrel monkeys to variants of a single call type. Exp Neurol 40:821-824.

Ohl FW, Wetzel W, Wagner T, Rech A, Scheich H (1999) Bilateral ablation of auditory cortex in Mongolian gerbil affects discrimination of frequency modulated tones but not of pure tones. Learn Mem 6:347-362.

Panzeri S, Schultz SR (2001) A unified approach to the study of temporal, correlational, and rate coding. Neural Comput 13:1311-1349.

Parker AJ, Newsome WT (1998) Sense and the single neuron: probing the physiology of perception. Annu Rev Neurosci 21:227-277.

Phillips DP (1990) Neural representation of sound amplitude in the auditory cortex: effects of noise masking. Behav Brain Res 37:197-214.

Phillips DP, Cynader MS (1985) Some neural mechanisms in the cat's auditory cortex underlying sensitivity to combined tone and wide-spectrum noise stimuli. Hear Res 18:87-102.

Phillips DP, Orman SS, Musicant AD, Wilson GF (1985) Neurons in the cat's primary auditory cortex distinguished by their responses to tones and wide-spectrum noise. Hear Res 18:73-86.

Polley DB, Read HL, Storace DA, Merzenich MM (2007) Multiparametric auditory receptive field organization across five cortical fields in the albino rat. J Neurophysiol 97:3621-3638.

Poon PW, Yu PP (2000) Spectro-temporal receptive fields of midbrain auditory neurons in the rat obtained with frequency modulated stimulation. Neurosci Lett 289:9-12.

Poon PW, Chen X, Hwang JC (1991) Basic determinants for FM responses in the inferior colliculus of rats. Exp Brain Res 83:598-606.

Qin L, Wang JY, Sato Y (2008) Representations of cat meows and human vowels in the primary auditory cortex of awake cats. J Neurophysiol 99:2305-2319.

Razak KA, Fuzessery ZM (2006) Neural mechanisms underlying selectivity for the rate and direction of frequency-modulated sweeps in the auditory cortex of the pallid bat. J Neurophysiol 96:1303-1319.

Recanzone GH (2000) Response profiles of auditory cortical neurons to tones and noise in behaving macaque monkeys. Hear Res 150:104-118.

Recanzone GH, Schreiner CE, Sutter ML, Beitel RE, Merzenich MM (1999) Functional organization of spectral receptive fields in the primary auditory cortex of the owl monkey. J Comp Neurol 415:460-481.

Rees A, Moller AR (1983) Responses of neurons in the inferior colliculus of the rat to AM and FM tones. Hear Res 10:301-330.

Riede T, Zuberbuhler K (2003) The relationship between acoustic structure and semantic information in Diana monkey alarm vocalization. J Acoust Soc Am 114:1132-1142.

Rieke F, Warland D, Ruyter van Stevenick R, Bialek W (1997) Spikes: exploring the neural code. Cambridge, MA.

Romanski LM, Goldman-Rakic PS (2002) An auditory domain in primate prefrontal cortex. Nat Neurosci 5:15-16.

Rosenblum LA, Cooper RW (1968) The squirrel monkey. New York,: Academic Press.

Rybalko N, Suta D, Nwabueze-Ogbo F, Syka J (2006) Effect of auditory cortex lesions on the discrimination of frequency-modulated tones in rats. Eur J Neurosci 23:1614-1622.

Schnupp JW, Hall TM, Kokelaar RF, Ahmed B (2006) Plasticity of temporal pattern codes for vocalization stimuli in primary auditory cortex. J Neurosci 26:4785-4795.

Schreiner CE, Mendelson JR (1990) Functional topography of cat primary auditory cortex: distribution of integrated excitation. J Neurophysiol 64:1442-1459.

Schreiner CE, Sutter ML (1992) Topography of excitatory bandwidth in cat primary auditory cortex: single-neuron versus multiple-neuron recordings. J Neurophysiol 68:1487-1502.

Schreiner CE, Mendelson JR, Sutter ML (1992) Functional topography of cat primary auditory cortex: representation of tone intensity. Exp Brain Res 92:105-122.

Shamma SA, Fleshman JW, Wiser PR, Versnel H (1993) Organization of response areas in ferret primary auditory cortex. J Neurophysiol 69:367-383.

Suga N (1964) Recovery Cycles and Responses to Frequency Modulated Tone Pulses in Auditory Neurones of Echo-Locating Bats. J Physiol 175:50-80.

Suga N (1965) Analysis of frequency-modulated sounds by auditory neurones of echo-locating bats. J Physiol 179:26-53.

Suga N (1989) Principles of auditory information-processing derived from neuroethology. J Exp Biol 146:277-286.

Thomson EE, Kristan WB (2005) Quantifying stimulus discriminability: a comparison of information theory and ideal observer analysis. Neural Comput 17:741-778.

Tian B, Rauschecker JP (1994) Processing of frequency-modulated sounds in the cat's anterior auditory field. J Neurophysiol 71:1959-1975.

Todt D, Goedeking P, Symmes D (1988) Primate vocal communication. Berlin ; New York: Springer-Verlag.

van Rossum MC (2001) A novel spike distance. Neural Comput 13:751-763.

Victor J, Purpura K (1999) Estimation of information in neuronal responses. Trends Neurosci 22:543.

Volkov IO, Galaziuk AV (1985) [Reactions of neurons of the auditory cortex of unanesthetized cats to tones of a characteristic frequency]. Neirofiziologiia 17:500-508.

Wang X (2007) Neural coding strategies in auditory cortex. Hear Res 229:81-93.

Wang X, Kadia SC (2001) Differential representation of species-specific primate vocalizations in the auditory cortices of marmoset and cat. J Neurophysiol 86:2616-2620.

Wang X, Merzenich MM, Beitel R, Schreiner CE (1995) Representation of a species-specific vocalization in the primary auditory cortex of the common marmoset: temporal and spectral characteristics. J Neurophysiol 74:2685-2706.

Wang X, Lu T, Snider RK, Liang L (2005) Sustained firing in auditory cortex evoked by preferred stimuli. Nature 435:341-346.

Wetzel W, Ohl FW, Scheich H (2008) Global versus local processing of frequency-modulated tones in gerbils: an animal model of lateralized auditory cortex functions. Proc Natl Acad Sci U S A 105:6753-6758.

Winter P, Ploog D, Latta J (1966) Vocal repertoire of the squirrel monkey (Saimiri sciureus), its analysis and significance. Exp Brain Res 1:359-384.

Wollberg Z, Newman JD (1972) Auditory cortex of squirrel monkey: response patterns of single cells to species-specific vocalizations. Science 175:212-214.

Zeng FG, Nie K, Stickney GS, Kong YY, Vongphoe M, Bhargave A, Wei C, Cao K (2005) Speech recognition with amplitude and frequency modulations. Proc Natl Acad Sci U S A 102:2293-2298.

Zhang LI, Tan AY, Schreiner CE, Merzenich MM (2003) Topography and synaptic shaping of direction selectivity in primary auditory cortex. Nature 424:201-205.

Chapter 2

Sustained and Transient Response Modes in Primary Auditory Cortex

Abstract:

In primary auditory cortex (AI) of awake animals, neurons respond to static tones with sustained, onset, or onset-sustained responses. The relation between these response types and the responses to other sounds remains unknown as does the mechanism that generates them. One possibility is that they are stimulus specific. Another possibility is that these response types reflect more general processing differences in distinct populations. Variation in the strength and timing of cortical inhibition and synaptic depression may create neurons with sustained or onset-sustained responses across most stimuli. Here, we demonstrate that response diversity is consistent with a difference in more general synaptic mechanisms. AI neurons in awake squirrel monkeys had similar response types to a variety of stimulus classes including broadband noise and frequency sweeps. As predicted by our descriptive model, the responses of sustained and onset neurons were anti-correlated functions of the modulation speed of frequency sweeps: onset neurons preferred fast speeds while sustained neurons preferred slow speeds. Finally, tone response classes differed in several fundamental properties; Onset neurons had lower spontaneous activity, greater frequency selectivity, and higher thresholds than sustained neurons. These results suggest that diversity in the temporal profile of suppression creates different functional classes of neurons with complementary stimulus preferences. Such mechanisms are similar to those that sharpen orientation selectivity in primary visual cortex and produce the diversity of selectivity found therein.

Introduction

It has long been known that the responses of neurons in primary auditory cortex (AI) of anesthetized animals occur predominately at the onset of tonal stimuli. This result stands in contrast to studies in alert animals which have demonstrated that neurons can respond to static pure tones with sustained responses in which the firing rate is high throughout the stimulus duration, onset-sustained responses for which the response is strongest at the stimulus onset but the firing rate remains elevated for the stimulus duration, as well as onset responses (G. L. Gerstein and N. Y. Kiang, 1964; I. C. Whitfield and E. F. Evans, 1965; M. Abeles and M. H. Goldstein, Jr., 1972; J. F. Brugge and M. M. Merzenich, 1973; J. M. Miller et al., 1974; I. O. Volkov and A. V. Galaziuk, 1985; G. H. Recanzone, 2000; D. Bendor and X. Wang, 2005; T. Hromadka et al., 2008). Despite knowledge of the existence of these response types, little is known about their function or the mechanisms that generate them.

One possibility that explains the existence of different response types in AI is that the temporal response pattern for pure tones is not related to that for other stimuli. In this case, all neurons respond to some select subset of stimuli with sustained responses (D. Bendor and X. Wang, 2005; X. Wang, 2007). A related possibility is that tone response types reflect differences in general properties of a neuron such as differences in cortico-cortical synaptic inhibition or in the adaptation kinetics of inputs (M. Atzori et al., 2001). Studies in AI of the anesthetized rat using in vivo whole cell voltage clamp demonstrated that synaptic inhibitory currents immediately followed tone evoked excitatory depolarization (M. Wehr and A. M. Zador, 2003; A. Y. Tan et al., 2004). These inhibitory currents limited the spiking response to the onset of stimuli. The increased prevalence of sustained responses in alert AI suggests that the strength of tone evoked inhibition may vary considerably between neurons. This notion is supported by a study in the auditory cortex of awake squirrel monkeys in which responses to two-tone stimuli demonstrated the existence of populations with and without inhibitory sidebands (S. A. Shamma and D. Symmes, 1985). Neurons without inhibitory sidebands responded continuously to tones and noise while those with strong inhibitory sidebands either had sustained responses to tones alone or onset tone responses. Rapid onset cortico-cortical synaptic inhibition is also thought to sharpen the orientation tuning of neurons in primary visual cortex (V1) (R. Shapley et al., 2007). Additionally, variability in the amount of such inhibition is thought to produce the diversity of orientation selectivity observed within V1.

Importantly, the mechanisms outlined above make specific predictions regarding other properties of AI neurons. The sensitivity to certain stimulus parameters or in the preferred range of a stimulus parameter should differ between AI neurons with onset and sustained tone responses. Onset neurons should be generally more sensitive to rapid fluctuations of energy within the receptive field that produce synchronous depolarization strong enough to reach threshold before inhibition or rapid adaptation occurs. These neurons would be less responsive to slower modulations of energy within receptive field because inhibition clamps down immediately and suppresses spiking. Neurons with sustained tone responses (less inhibition and/or slower adaptation) should, in contrast, respond continuously to sounds in general and track the stimulus envelope via changes in instantaneous firing rate. Furthermore, the increased strength of balanced inhibition should create sharper frequency tuning and may also increase the threshold of neurons with onset tone responses (M. Wehr and A. M. Zador, 2003).

In this study, we compared the tone response types of AI neurons in awakes squirrel monkeys with the responses to frequency sweeps and broadband noise. Varying the speed of modulation of the frequency sweeps allowed us to test whether or not there was a difference in the responses to slow versus fast modulations between tone response types. We also compared the tone response type with basic properties of neurons such as the spontaneous firing rate and spectral integration.

Methods

Animal Preparation

All procedures related to the maintenance and use of animals in this study were approved by the Institutional Animal Care and Use Committee at the University of California, San Francisco, and were consistent with national and state animal welfare guidelines.

The preparation for awake recording procedures were adapted for the squirrel monkey from those used in the awake marmoset monkey (T. Lu et al., 2001b). Two adult female squirrel monkeys (*Saimiri sciureus*) were trained to sit quietly in a restraint chair over several weeks. Animals were then implanted with a head post to allow for head fixation during physiological recording. After using ketamine (25mg/kg) and midazolam (0.1mg/kg) for induction, the animals were maintained in a steady plane of anesthesia using isoflurane gas (0.5-5%). Implants were secured to the skull using bone screws and dental acrylic. Animals were then trained based on positive reinforcement methods to sit in the primate chair with their head fixed to a frame over the course of several weeks after which they underwent a second surgery to implant a recording chamber of auditory cortex. During this procedure, animals were anesthetized using the protocol above. The bone overlying auditory cortex was exposed and an 8-10mm diameter ring was secured using bone screws and dental acrylic. To expose the auditory cortex, a 1-3mm burr hole was placed under magnification with a surgical microscope. A small slit was made in the dura using microsurgical instruments after application of 1% lidocaine. Under sterile conditions, 5-10 electrode penetrations were made in each burr hole after which another region of cortex was exposed and the recording process repeated.

Electrophysiology

All recordings were made in a soundproof chamber (Industrial Acoustics Company, Bronx, New York). During each recording session, the animal was seated comfortably in a custom-built primate chair with its head fixed to a frame. Animals were not required to perform tasks but had to remain awake and received randomly-timed juice rewards during the recording sessions. Data were obtained using 16-channel linear electrodes (177μm ^{2} contact size, 100 or 150μm spacing; 1-3MOhm impedance) from NeuroNexus Technologies (Ann Arbor, MI). An electrode was advanced into cortex using a microdrive (David Kopf Instruments, Tujunga, CA) to the depth at which most channels were active (tip depth of ~1-2mm from the depth of first spontaneous activity identified audio-visually). Penetrations were made perpendicular to the surface of AI when possible, though it was often impossible to see the surface through such the small craniotomy and dural incision. Electrical signals from the brain were amplified using a 16-channel pre-amplifier (RA16 Medusa; Tucker-Davis Technologies, Alachua, FL), filtered (600-7000Hz band-pass) and recorded using an RX-5 amplifier and Brainware software (Tucker-Davis Technologies, Alachua, FL) on a personal computer. Brainware was used for online estimation of neural responsiveness and tuning, and the raw waveform was recorded (25 kHz sampling rate). Single neurons were sorted offline using Spikesort (written by Mark Kvale) which uses a Bayesian algorithm (M. S. Lewicki, 1994) to derive spike templates. In the squirrel monkey, AI is located on the surfaces of the temporal gyrus and in the supratemporal plane of the lateral sulcus. The precise location of our recordings were determined physiologically by the characteristics of AI neurons including vigorous pure tone responses, latency, and tonotopic gradient in the rostrocaudal dimension (S. W. Cheung et al., 2001). A terminal mapping experiment in the anesthetized animal confirmed the location and extent of AI.

Acoustic Stimulation

All sounds were presented using a Sony SS-MB150H free field speaker positioned 50cm in front of the animal. The sound delivery system was calibrated using a sound-level meter (Model 2209, Brüel & Kjær, Norcross, GA) and SigCal software (Tucker-Davis Technologies, Alachua, FL). Tone bursts (50-500 ms duration, 5 ms on/off cosine gate, 500 ms inter-stimulus interval) were generated using SigGen software (Tucker-Davis Technologies, Alachua, FL). For measurement of frequency response areas (FRA), randomized tone bursts were played while frequency and intensity were varied. The range of frequencies used varied from 1-4 octaves (semitone or tone spacing) centered on the estimated center frequency of the neurons. Tone intensities spanned 0-70 dB in 10 dB steps. 2-5 repetitions were presented for each frequency-level combination.

Logarithmic frequency sweeps were created in Matlab (The MathWorks, Natick, MA) and written as .wav files for delivery using SigGen and Brainware (Tucker-Davis Technologies, Alachua, FL). The sweep frequency ranged from 50 to 21,000 Hz in upward and downward directions with rates of frequency change of 5, 10, 20, 35, 60, 85, and 110 octaves/s (Fig. 1). Thus, there were a total of 14 frequency sweep direction-speed combinations. Because the sweep frequency range was held constant, the length of the stimuli changed as sweep speed was varied. Corresponding sweep lengths were the following: 1743, 871, 436, 249, 145, 103, and 79 ms. Each sweep also contained a 100 ms constant tone at the start and end frequencies. These constant frequency portions had a 5 ms cosine ramp up and ramp down at the beginning and end of the stimulus. Sweeps were played at 60 dB sound-pressure level (SPL). Each sweep was repeated 20 times in a random order with a minimum of 500 ms inter-trial interval.

Data Analysis

Analysis of pure tone responses

To quantify the sustained or onset nature of the responses to characteristic frequency pure tones, we used a *Tone Response Ratio* (TRR) defined as:

$\frac{\mathrm{Response}_{\mathrm{1st\ half}}}{\mathrm{Response}_{\mathrm{2nd\ half}}}$ where $\mathrm{Response}_{\mathrm{1st\ half}}$ was the firing rate-spontaneous rate during the first 25 ms of the stimulus, and $\mathrm{Response}_{\mathrm{2nd\ half}}$ was the firing rate-spontaneous rate during the second half of the stimulus. Thus, a higher TRR indicated a more sustained tone response. Because we used different stimulus lengths and were interested in comparing the onset response with sustained responses, for tone lengths longer than 50 ms, we determined the firing rate during the first 100 ms and during the remainder of the stimulus. The TRR could then be compared with other parameters of the frequency response area, sweep responses and noise responses.

For each neuron, the responses to the pure tones with different levels and frequencies determined the frequency response area (FRA). Several measures were derived from each FRA (C. E. Schreiner and J. R. Mendelson, 1990). Threshold was defined as the lowest sound intensity (in 10 dB steps) that evoked a response to the tones. CF was the frequency of the tone that evokes a response at threshold. The high and low frequency edges of the FRA at 10, 20, 40 and 60 dB SPL and the bandwidth at 10, 20, 40, and 60 dB SPL were extracted. Q20, a center frequency normalized measure of the sharpness of frequency tuning, was defined as $Q20 = \frac{CF}{BW20}$, where BW20 was the bandwidth 20 dB above threshold. The latency to tone responses was also determined by finding the times of the first spikes of a tone response.

Analysis of frequency sweep responses

To determine whether or not the tone response types were specific to pure tones or whether they were more general response classes, we compared the tone responses to frequency sweep responses. The response magnitude, response length, and response latency for each frequency sweep was determined by finding consecutive times during which the firing rate in the cumulative PSTH (10 ms bins) was 3 standard deviations above the mean spontaneous rate. Response magnitude was defined as the number of spikes during this time and response length was the duration of the significant response time.

Three measures were used to quantify the selectivity of neurons for frequency the speed and direction of the frequency sweeps. To quantify sensitivity to the direction of modulation, we used the *Direction Selectivity Index* (DSI) which was defined as $DSI = \frac{\sum R_{up} - \sum R_{down}}{\sum R_{up} + \sum R_{down}}$ where R_{up} is the response to all up sweeps and R_{down} is the sum of responses to downward sweeps. The DSI ranges from -1, for neurons that responded only to down sweeps, to +1, for neurons that responded only to up sweeps. The *Speed Tuning* (ST) of a neuron had the form $ST = \frac{n}{n-1} \times \left[\frac{1 - mean(R)}{\max(R)} \right]$ where ***n*** was the number of speeds used (7), and ***R*** was the response to speeds. The speed tuning was determined using the responses to speeds in the preferred direction. The *Best Speed* (BS) of a neuron was determined using a centroid measure of the form $BS = \frac{\sum_i (speed_i \times R_i)}{\sum_i R_i}$ where $speed_i$ was a specific sweep speed and R_i was the response to that speed.

Because we were interested in comparing the timing of sweep responses with the tonal receptive field of neurons, we determined the instantaneous sweep frequency that triggered the start of the sweep response, the trigger frequency (Fig. 9A,B, black circles) (P. Heil et al., 1992; P. Heil and D. R. Irvine, 1998; B. Godey et al., 2005). For each neuron, the latency to sweep response from the above analysis is plotted as a function of the inverse of the sweep speed for both up and down directions. Linear least squares lines were then computed to fit the data points for each direction. The slope of lines with significant ($p < 0.05$) positive regression fits were considered. The slope is the number of octaves above the starting sweep frequency that caused the start of the neural response. The trigger frequency for up sweeps could be calculated from the equation $F_{up} = 50 \times 2^{S}$, where *S* is the slope of the line fit to the up sweep responses latencies. The trigger frequency for down sweeps was calculated from the relationship $F_{down} = 21000 x 2^{-S}$, where *S* is the slope of the line fit to down sweep response latencies. We extended this analysis to determine the sweep frequency that occurred when the response ended which we called the *end frequency* (Fig. 9A,B, red squares). The procedure used to calculate the end frequency was the same as for the trigger frequency except that rather than using the latency to the start of each response we used the latency to the end of each response. Thus for each neuron, we calculated two trigger frequencies and two end frequencies: $\mathrm{Trigger}_{\mathrm{up}}$, $\mathrm{Trigger}_{\mathrm{down}}$, $\mathrm{End}_{\mathrm{up}}$, $\mathrm{End}_{\mathrm{down}}$. From the trigger frequency and end frequency for up sweeps ($\mathrm{Start}_{\mathrm{up}}$ and $\mathrm{End}_{\mathrm{up}}$, respectively), we calculated a bandwidth using the following: $FMBW_{up} = End_{up} - Trigger_{up}$. We also calculated a bandwidth for the trigger and end frequencies from down sweeps by subtracting the end frequency from the trigger frequency from the equation $FMBW_{down} = Trigger_{down} - End_{down}$. These estimated bandwidths could then be compared with the actual bandwidth of the FRA of each neuron.

Response to continuous broadband noise

To asses the relation between pure tone response type and broadband static stimuli, we recorded responses to continuous white noise at various levels (60 dB - 80 dB, in 5 dB steps) for some AI neurons. Not all intensities were played for every neuron (these stimuli were part of another study). The mean firing rate during each noise stimulus was compared with the spontaneous firing rate of the neuron. The effect of the noise for every neuron was categorized as one of three possibilities. First, if for any level the mean noise response was two standard deviations greater than the mean spontaneous rate, we considered the neuron to have a sustained response to the noise. Second, if the mean noise response was one standard deviation below the mean spontaneous rate, the neuron was considered to be inhibited by the noise. Third, the neuron was classified as having no change in firing rate from the noise if the noise response was not significantly different from the spontaneous rate.

Results

The following results are based on recordings of 129 neurons from the left and right hemispheres of two female adult squirrel monkeys. There were no significant differences in any of the described response parameters between animals. Therefore, the data was combined.

Tone responses in awake AI range from onset to sustained

We examined the temporal pattern of the responses to pure tones of AI neurons. Figure 1 shows the FRA and cumulative PSTH (10 ms bins) of several representative examples of the kinds of responses that we observed. Neurons in the column labeled Onset responded only at the beginning of the tones after which the firing rate returned to spontaneous or suppressed levels. Neurons in the column labeled Onset-sustained had a large response at the tone onsets followed by an elevated firing rate throughout most or all of the remainder. The neurons in the column labeled Sustained had elevated firing rates throughout the stimuli. These response classes are similar to those of Recanzone (2000) in AI of the awake macaque monkey and Chimoto *et al.* (2002) in AI of the awake cat both of which, in turn, are similar to those of Young (1984) in the cochlear nucleus and Nudig et al. (1999) in the inferior colliculus. The similarity in tonal responses between all of these studies suggests that these response categories generalize across central auditory stations and across species.

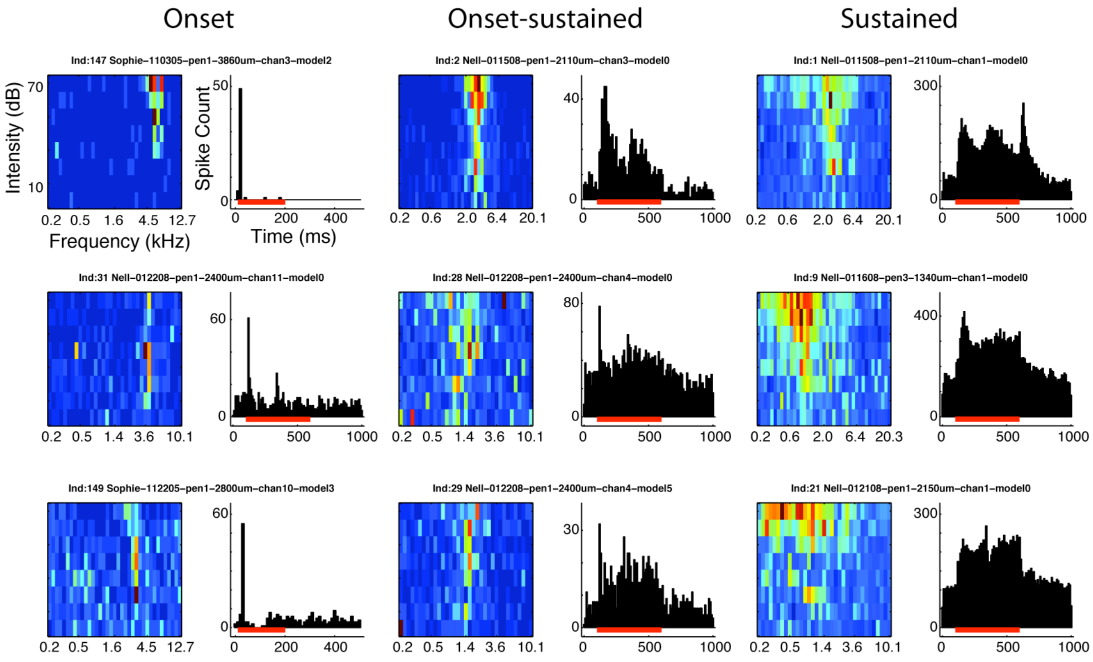

Figure 1. Frequency Response Areas (FRA) and pure tone cumulative PSTH's for representative AI neurons. The FRA plots the firing rate of a neuron for each frequency/intensity combination used (see Methods). Each FRA characterizes the frequency selectivity of a single neuron. The PSTH's shown are derived from the responses to all pure tones presented. The stimulus length is depicted by the red bar under the PSTH. Each column shows the FRA and PSTH of three representative neurons from each tone response class.

To quantify the differences between the tonal response types described above, we used a *Tone Response Ratio* (TRR, see Methods). For sustained responses, the TRR could be close to one or greater. For onset responses, the TRR was lower than 0.5. Figure 2 presents a histogram of the TRRs of all neurons which had significant tone responses. The distribution had a large peak at ≥ 1 and a second hump centered at 0.4. We divided this distribution into 3 categories corresponding to the response categories described above: Onset, Onset-sustained, and Sustained. TRRs ≥ 0.9 were considered Sustained. TRRs < 0.5 were defined as Onset responses. TRRs in between these were considered Onset-sustained. According to this classification, 38% (49/129) of tonal responses were Sustained, 29% (38/129) were Onset-sustained, and 33% (42/129) were Onset. The percentage of sustained responses in this study fell between that reported by Recanzone (2000) in the awake macaque (30%) and the awake cat (50%) reported by Chimoto *et al.* (2002). The broad distribution of TRRs in Fig. 2, however, suggests that these response types lie along a continuum. Furthermore, the exact boundaries of these categories did not significantly affect the results presented below.

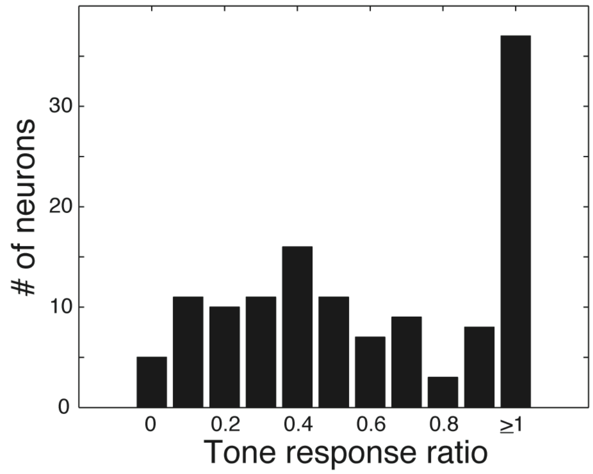

Figure 2. Histogram for Tone Response Ratios (TRR) for all 129 AI neurons. The TRR was used to classify neurons into one of three groups: *Onset*, *Onset-sustained*, and *Sustained*.

Responses to dynamic sweeps are similar to static tone responses

If pure tone temporal response profiles are consequences of general differences in the strength and/or timing suppression, then neurons should respond to multiple stimuli with response types that are similar to the response to static tones. To determine whether neurons with sustained tone responses also had sustained responses to other stimuli, we compared pure tone responses to responses to frequency sweeps that varied in the speed and direction of modulation (see Methods). Figures 3, 4, and 5 show the pure tone PSTH and the sweep PSTH's for several Onset, Onset-sustained, and Sustained neurons, respectively. The Onset neurons in Figure 3 also had brief responses to frequency sweeps. The Onset-sustained neurons in Figure 4 had mixed responses to sweeps with the neuron in Fig. 4A having a somewhat longer response to the slowest sweep speed. The neuron in Fig. 4B had more onset-like sweep responses. Finally, both of the Sustained neurons in Fig. 5 had sustained responses to sweeps. For these neurons, the length of the response followed the length of the stimulus. To quantify the relation between the tone response type and the sustained or onset nature of the sweep response, we compared the mean length of the longest response to the sweep stimuli for all neurons across the tone response categories. Mean longest response length differed significantly across groups (Fig 6., One-way ANOVA, $F(95, 2) = 10.05$, $p < 0.0005$). Neurons with Sustained tone responses had longer sweep responses than Onset-sustained neurons (Tukey's honest significant difference criterion, $p < 0.005$) and Onset neurons (Tukey's honest significant difference criterion, $p < 0.005$).

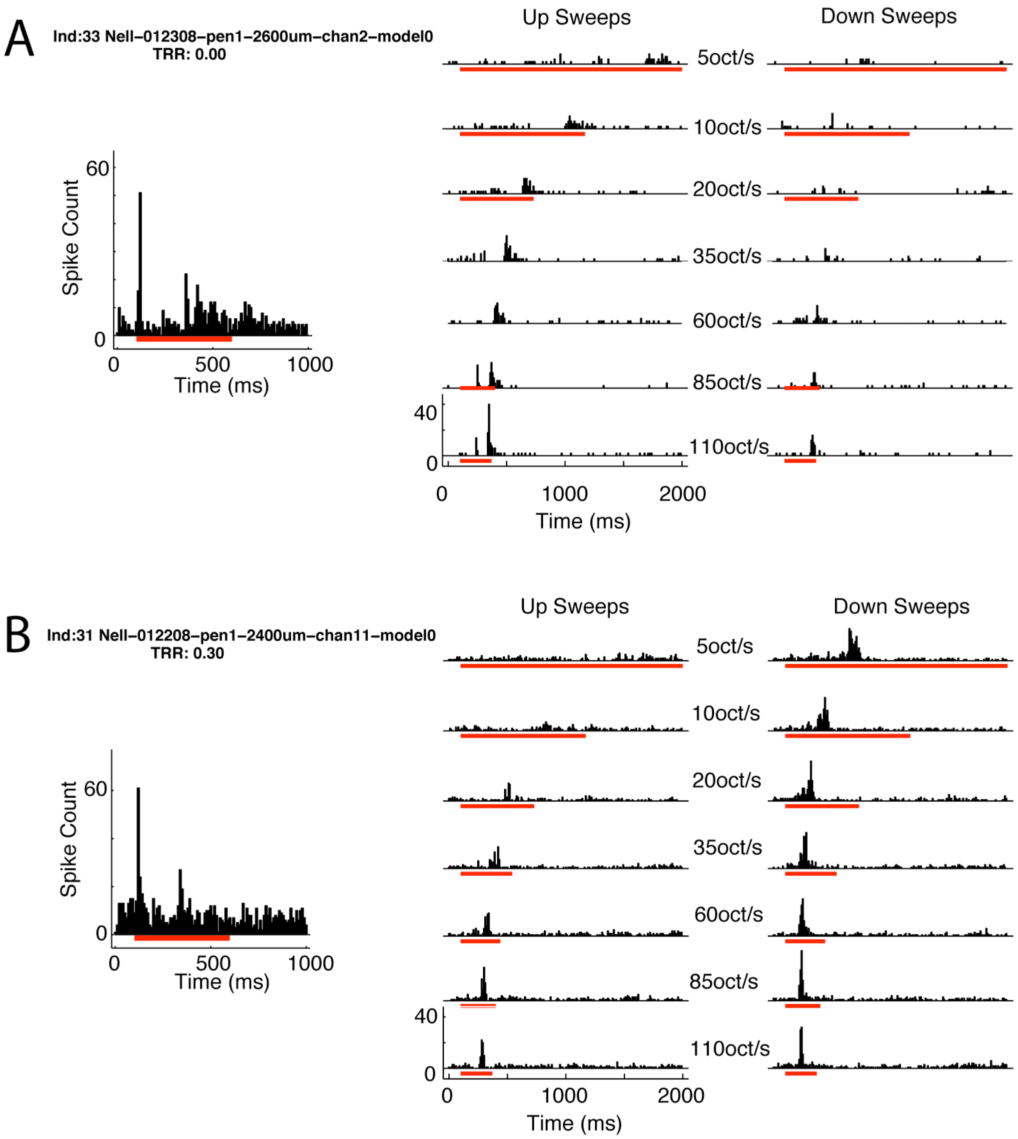

Figure 3. Neurons with onset tone responses have onset sweep responses. A., B. Right column shows tone response PSTHs for two Onset neurons. The middle and left columns plot PSTHs for responses to frequency sweeps of speeds and directions indicated by text.

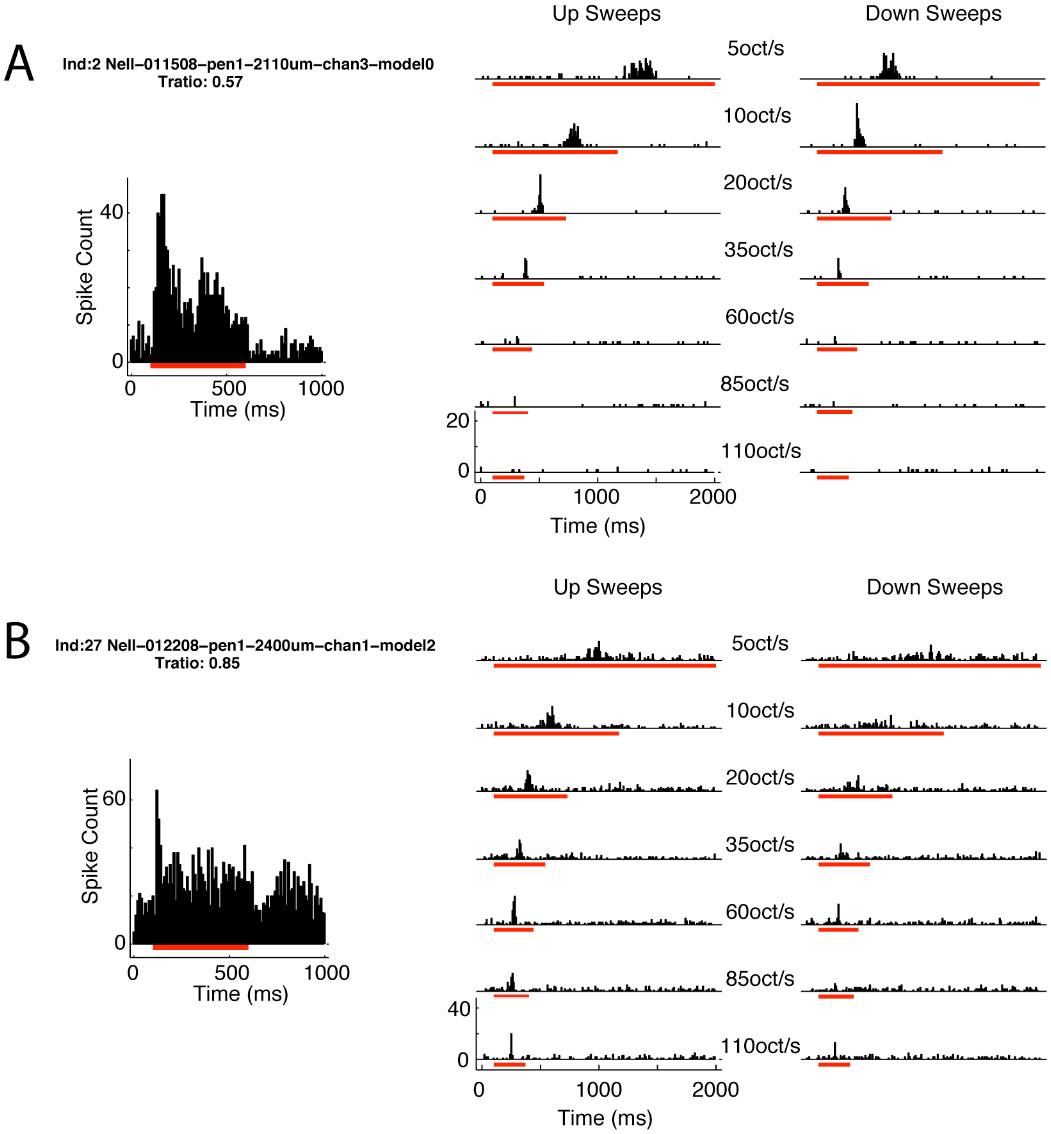

Figure 4. Neurons with Onset-sustained responses have mixed responses to frequency sweeps. This figure has the same format as Fig 3.

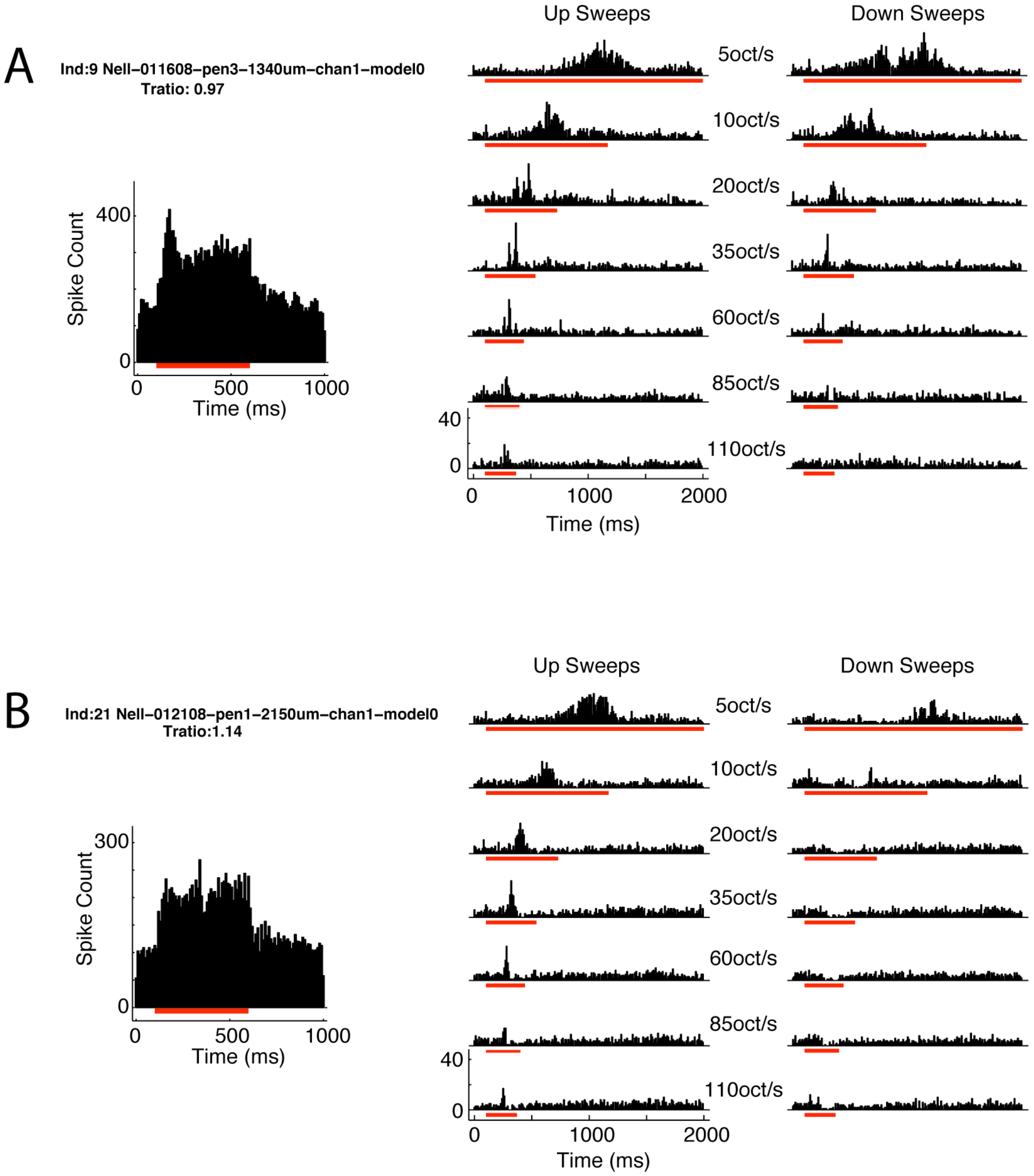

Figure 5. Neurons with Sustained tone responses have sustained sweep responses. This figure has the same format as Fig. 3 and 4.

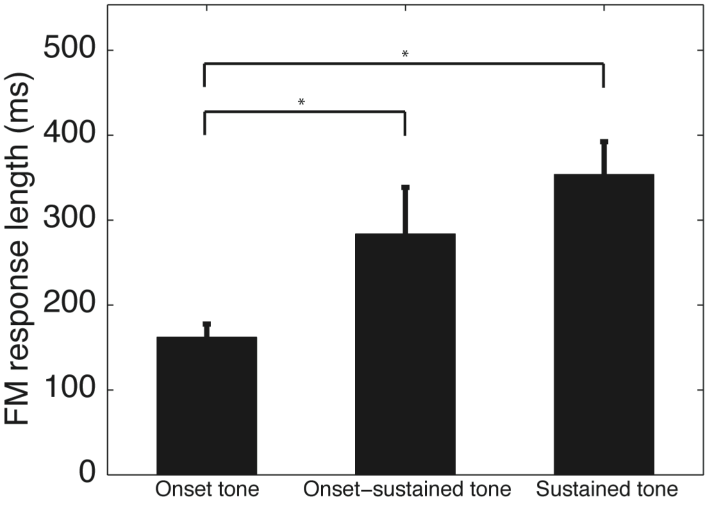

Figure 6. Sustained tone and Onset-sustained tone neurons have longer responses to sweeps than Onset neurons. Bar plot of the mean longest response length to frequency sweeps for each tone response category. For each neuron, the longest response to all sweeps was used to calculate the mean response length for each category. Statistically significant differences between groups are indicated by asterisks (see Results).

While Figure 6 demonstrates that neurons with sustained responses to static tones also have longer responses to dynamic tones, this difference could be due to a difference in the frequency tuning bandwidth of these neurons. To determine whether or not the length of sweep responses matched the time that the instantaneous sweep frequency was within the tonal receptive field, we compared the spectral bandwidths measured from the FRA's of AI neurons with the bandwidths estimated from the timing of the sweep responses (see Methods). To do this, we determined the sweep frequency at the beginning and end of the sweep responses from least-squares fits to response start or end latency versus 1/sweep velocity. Figures 7C and D show the plots of the latency to the response start versus

1/sweep velocity (black circles) and latency to the response end versus 1/sweep velocity (red squares) for a Sustained tone neuron and an Onset tone neuron, respectively (upward sweeps only). The functions for Sustained neuron in Fig. 7C have different slopes: the response start line is a lower slope than the response end line. The start and end frequencies were 276 Hz and 1710 Hz, respectively which matched well the low and high frequency edges of the tuning curve at 60 dB (224 Hz and 1700 Hz, respectively). In contrast, the start and end frequencies were 3379 Hz and 1987 Hz which did not match the edges of the FRA (635 Hz and 2016 Hz). The estimated bandwidth was the difference between the sweep response start and end frequencies.

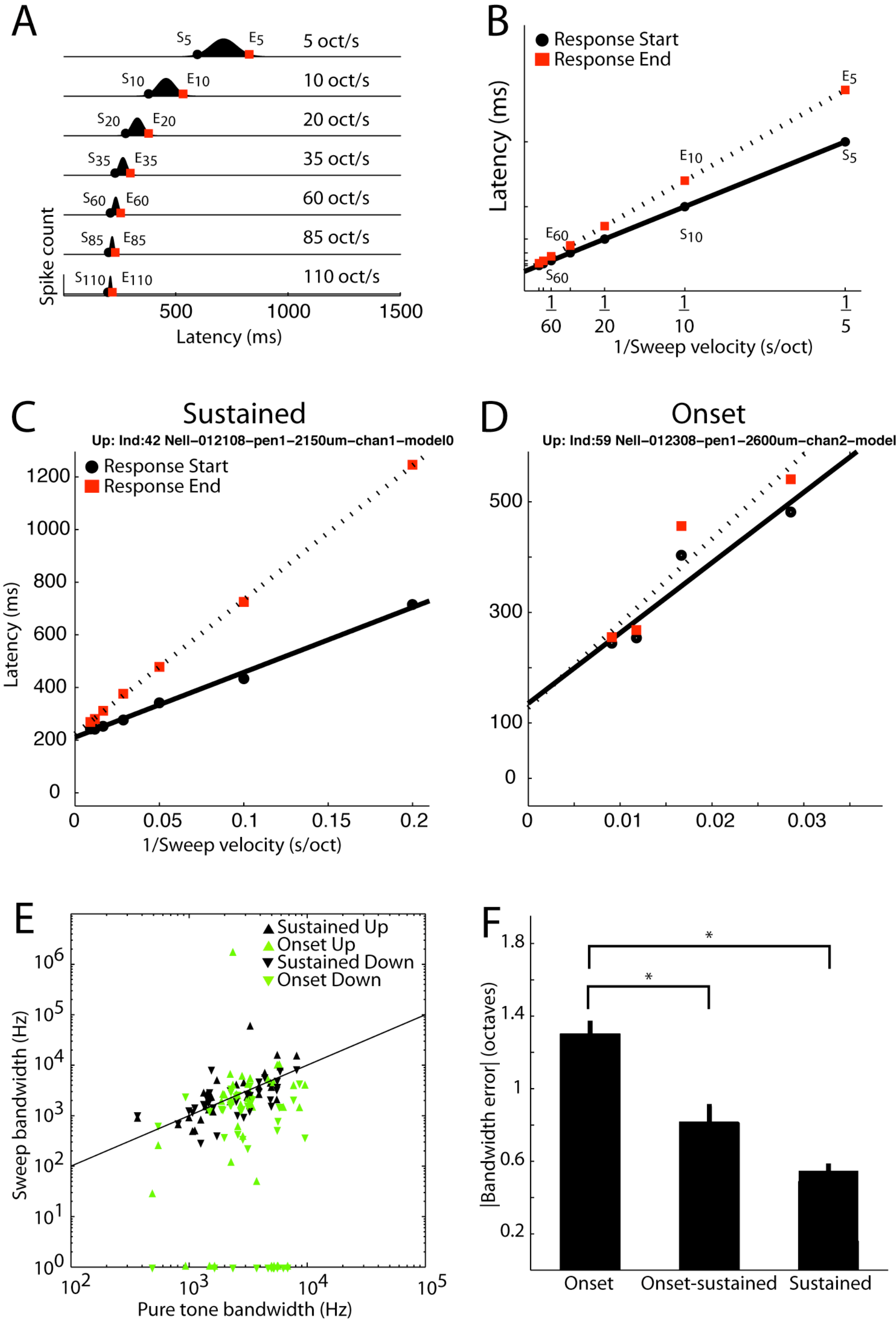

Figure 7. Sustained tone neurons respond while the sweep frequency is within the tonal receptive field. A. Schematic for the determination of trigger frequency and end frequency (see Methods). Filled Gaussians represent PSTHs of a neuronal response to frequency sweeps

with different velocities. Black circles represent the latency to the beginning of the sweep response. Red squares represent the latency to the end of the sweep response. B. Schematic of the determination of trigger frequencies and end frequencies from the plot of latency to start of sweep responses vs. 1/sweep velocity (black line with filled black circles) and the plot of latency to the end of sweep responses vs. 1/sweep velocity (dashed line with red squares). C., D. Example functions of latency to start of sweep responses vs. 1/sweep velocity (solid line, black circles) and latency to the end of sweep responses vs. 1/sweep velocity (dashed line, red squares) for two AI neurons. The neuron in C had sustained tone responses while the neuron in D had Onset tone responses. E. Spectral bandwidth estimated from sweep responses plotted as a function of the true FRA bandwidth. Values for neurons with Sustained tone responses are shown by black filled triangles (pointed up for upward sweeps, inverted for downward sweeps). Values for Onset neurons are shown by green triangles. F. Mean absolute value of the bandwidth estimation error for each tone response category. The bandwidth estimation error was the difference between the estimated and actual bandwidth in octaves. Significant differences between groups are indicated by asterisks.

Figure 7E plots the bandwidth estimated from the up and down sweep responses as a function of the actual FRA bandwidth. Sustained tone response neurons are shown in black triangles and Onset tone response neurons are shown in green triangles. This plot shows that Onset neurons frequently fall below the unity line and many have an estimated bandwidth of 1 Hz (estimated bandwidths equal to zero were changed to one for plotting purposes). For these neurons, the response duration does not match the length of time that the sweep is within the FRA. For Sustained neurons, the estimated and actual bandwidths are more closely matched. This data is summarized for all neurons in Figure 7F which plots the difference between estimated and actual bandwidths (in octaves) for Sustained, Onset-sustained, and Onset neurons. The average error varied with tone response type (One-way ANOVA, $F(171, 2) = 13.85$, $p < 1x10^{-5}$). The mean error for neurons with Onset tone responses was larger than that of Onset-sustained (Tukey's honest significant difference criterion, $p < 0.001$) and Sustained neurons (Tukey's honest significant difference criterion, $p < 0.001$). From this data, we can conclude that neurons with onset tone responses also have brief responses to dynamic tones. Conversely, neurons with sustained tone responses also have sustained sweep responses. These static narrowband tone response classes therefore generalize to dynamic narrowband stimuli.

Preference for sweep parameters differs greatly between tone response types

Systematic variation of rapid onset synaptic inhibition reported between Sustained and Onset neurons should confer different preferences for the rate of stimulus modulation. Neurons with rapid onset inhibition may respond best to stimuli with fast rises in amplitude or rapid entry into the receptive field. Such fast energy changes could cause strong synchronous excitation that reach threshold before the onset of inhibition. As shown above, Sustained neurons respond well to slower modulations which spend more time in the receptive field as demonstrated above. Thus Sustained and Onset neurons may represent complementary ranges of stimulus parameters relating to the rate of change of energy. We compared the selectivity of Sustained tone and Onset tone neurons for the parameters of frequency sweeps. The Direction Selectivity Index (DSI) measures how sensitive neurons are to whether the frequency of the tone was increasing (up sweeps) or decreasing (down sweep). The DSI of neurons with Onset and Sustained tone responses was not different (Fig. 8A, t-test, two-tailed, $p > 0.05$). This indicates that the asymmetry of FRA's and selectivity of thalamic input which contribute to direction selectivity (L. I. Zhang et al., 2003) are similar between tone response types. However, neurons with Sustained tone responses had greater speed tuning (Fig. 8B, Wilcoxon rank-sum test, $p < 1\text{x}10^{-5}$, $n = 88$) and preferred slower sweep speeds (Fig. 8C, Wilcoxon rank-sum test, $p < 1\text{x}10^{-8}$, $n = 88$) than neurons with Onset tone responses. Sustained neurons preferred slow sweep speeds which had longer durations and therefore spent more time within the FRA. The distribution of best speeds for Onset tone neurons was shifted toward higher values and went beyond the best speeds of Sustained neurons. As expected from our hypothesis, Onset neurons responded strongest to rapid entry of energy into the receptive field. Importantly, when the response magnitude was normalized by the length of each response, the speed tuning of sustained neurons decreased dramatically and became lower than that of onset neurons (Fig. 8E, Wilcoxon rank-sum test, $p < 0.005$, $n = 88$). When the length of the stimulus was factored out of the response, the speed tuning of sustained neurons decreased. This demonstrates that the difference in response magnitude between sweep speeds in sustained neurons was truly caused by the length of the stimulus. Furthermore, the preferred speeds of sustained neurons remained lower than the preferred speeds of onset neurons (Fig. 8F, Wilcoxon rank-sum test, $p < 0.001$, $n = 88$).

Figure 8D shows the normalized firing rate of the population of neurons separated according to pure tone response for each sweep speed. This figure demonstrates that the population of neurons with Sustained tone responses fires maximally for slow speeds while the population with Onset tone responses fires maximally for the fastest speeds. Therefore, these two populations represent different ranges of sweep speeds as predicted by differences in the strength and timing of suppression.

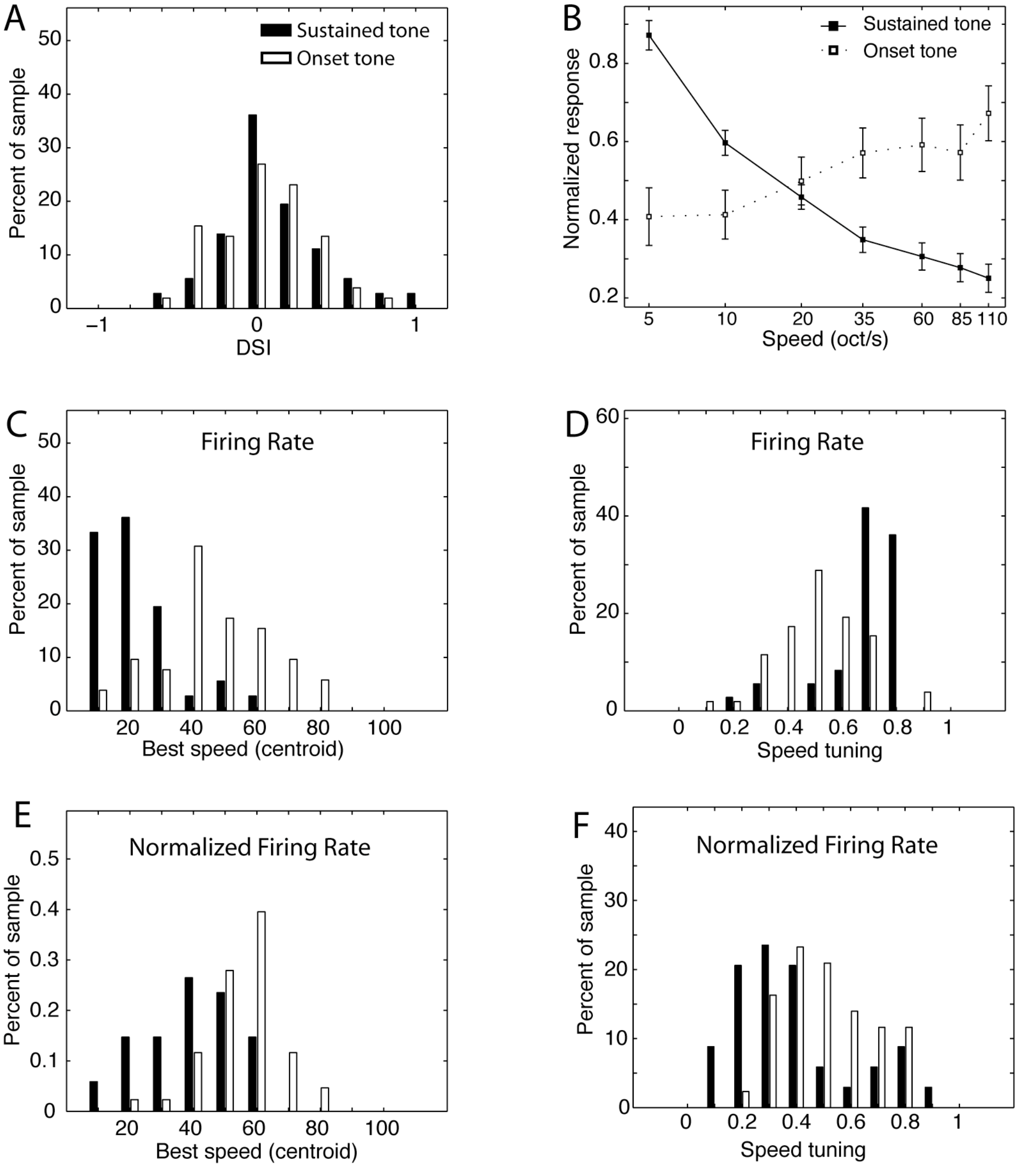

Figure 8. Frequency sweep selectivity differs between Sustained and Onset tone neurons. A. Histogram of Direction Selectivity Index (DSI) values for Sustained tone and Onset tone neurons. B. Histogram of Speed Tuning values for Sustained tone and Onset tone neurons. C. Histogram of Best Speed values for Sustained tone and Onset tone neurons. D. Mean normalized response as a function of sweep speed for Sustained tone neurons (filled squares) and Onset tone neurons (open squares).

Effects of broadband noise vary among tone response categories

We also tested whether or not the responses of AI neurons to a broadband static stimulus differed across the tone response categories. To do this, we compared the firing rate of AI neurons in response to continuous white noise (see Methods) with the spontaneous firing rate. Responses to noise were placed in one of three classes (see Methods): 1. No change, 2. Sustained response, and 3. Inhibited. Figures 9A and B show color plots of PSTH's of two AI neurons in silence and at different noise levels. The activity of the neuron in Fig. 9A was inhibited by the addition of white noise while the neuron in Fig. 9B had an increasing sustained response. In total, 52.9% of neurons were not affected by the noise, 25.9% had sustained responses, and 21.2% were inhibited. Figure 9C shows that the majority of neurons with Onset tone responses were not affected by the noise stimulus. In contrast, many Onset-sustained and Sustained neurons had sustained increases in firing rate when the noise was played. The broadband noise did inhibit some of these neurons, likely via stimulation of inhibitory sidebands. Together, this data demonstrates that neurons with sustained responses to static pure tones also often have sustained responses to broadband noise.

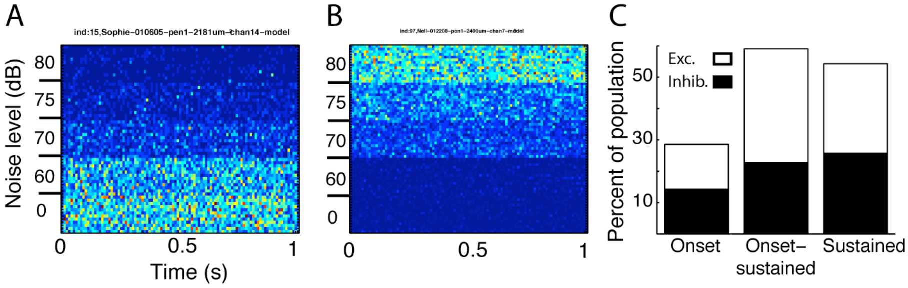

Figure 9. Sustained tone neurons and Onset-sustained tone neurons have more sustained responses to continuous white noise than Onset tone neurons. A., B. PSTHs of responses to 280 1 second continuous segments of white noise. Each row is the PSTH for 20 1 s segments. Responses to different noise intensities are shown along with spontaneous activity (0 dB noise level). The neuron in A was suppressed by the noise. The noise in B had a continuous elevation of firing rate to the noise. C. Bar plot of the percent of each tone response category that had an inhibited firing rate to noise, a sustained response to noise, or no change in response to noise.

Tone response type is correlated with general neuronal properties

In addition to conferring the temporal pattern of responses to multiple stimuli and different preferred modulation rates, variation in the strength and dynamics of balanced inhibition and adaptation between populations of neurons produced differences in other neuronal properties such as the level of spontaneous activity, minimum threshold, and sharpness of frequency tuning. Neurons with sustained tone responses had greater spontaneous activity than neurons with onset (Fig. 10A, Kolmogorov-Smirnov test, $p < 0.015$) and onset-sustained responses (Fig. 10A, Kolmogorov-Smirnov test, $p < 0.015$). Co-tuned excitation and inhibition may also increase the threshold for spiking and the sharpness of frequency tuning for

Onset neurons via an iceberg effect (M. Wehr and A. M. Zador, 2003). The threshold for tone responses varied between tone response types (one-way ANOVA, $F(126, 2) = 3.1$, $p < 0.01$). Figure 10B shows that the average threshold of Sustained neurons was significantly lower than that of Onset neurons (Tukey's honest significant difference criterion, $p < 0.01$). The threshold of Onset-sustained neurons lies between Sustained and Onset neurons. The sharpness of frequency tuning, measured using Q20 (see Methods), also differed across tone response categories (One-way ANOVA, $F(126, 2) = 4.66$, $p < 0.01$). Figure 10C shows that the mean Q20 value for Onset neurons was greater than that for Sustained neurons (Tukey's honest significant difference criterion, $p < 0.01$). The Q20 values of Onset-sustained neurons were between that of the other two response classes. Thus, Onset neurons are more frequency selective than Sustained neurons. The CF of AI neurons was also negatively correlated with the TRR ($p < 0.05$, $r = -0.31$, $n = 126$). Neurons with low CF's tended to be more sustained than neurons with high CF's. The relation between these basic properties of AI neurons and the tone response type suggest that the tone response ratio is the product of fundamental aspects of neuronal processing and supports the notion that these differences arise from differences in cortical inhibition.

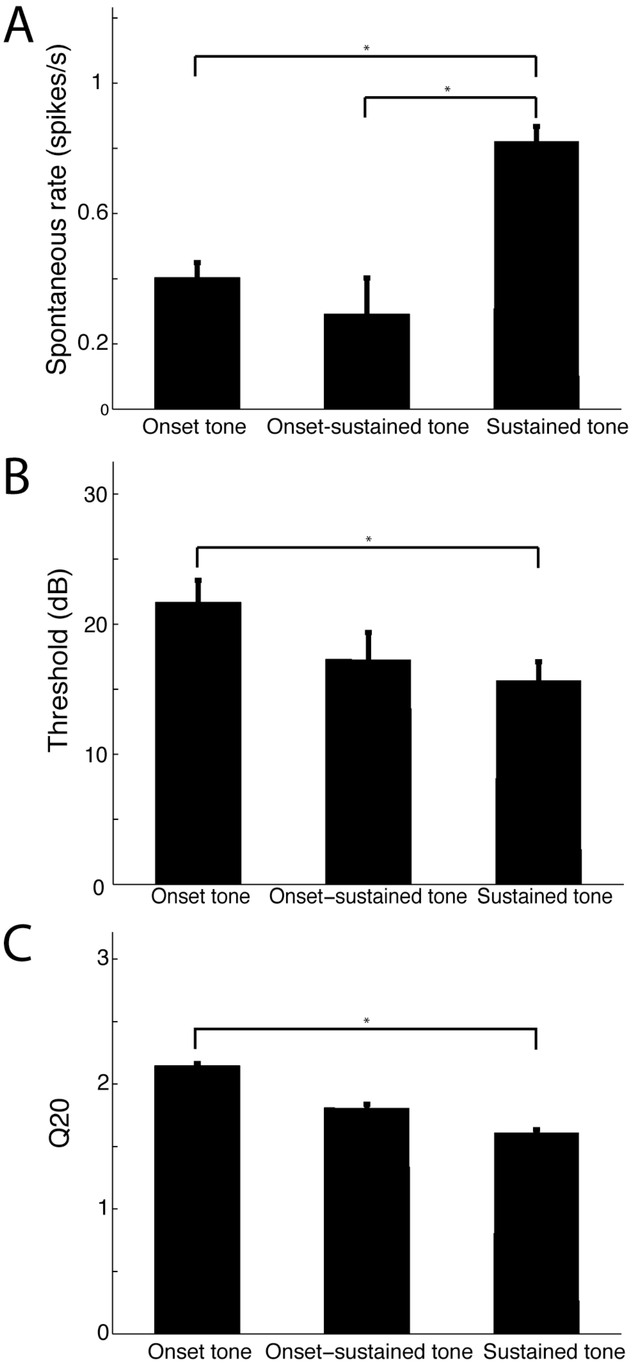

Figure 10. Relation between temporal pattern of tone response and other parameters of AI neurons. *A.* Bar graph showing the mean spontaneous firing rate for neurons in each of the three tone response classes. Asterisks denote significant differences between groups. *B.* Bar graph showing the mean threshold sound intensity level for AI neurons of each tone response group. *C.* Bar graph showing the mean Q20 for AI neurons in each tone response group.

Tone response types are locally clustered

Many fundamental receptive field properties of sensory neurons are organized into spatial gradients or modules across the surface of AI, or show local spatial clustering (see Schreiner and Winer (2007) for review). As demonstrated above, the temporal response pattern of AI neurons is related to a number of parameters some of which show spatial clustering in AI of the anesthetized squirrel monkey (S. W. Cheung et al., 2001). While the recording procedure in the awake monkey prevented us from collecting dense maps of AI, we were able to determine whether there was local clustering of the tone response type by comparing the TRR of neurons recorded simultaneously along the electrodes of our 16-channel linear array (see Methods). We created a *Cluster Index* (CI) which was defined as follows. Neurons with sustained and onset responses were assigned values of +1 and -1 respectively. In penetrations for which more than one neuron was recorded on the same or multiple channels, the value of the category number was summed across all neurons and divided by the number of neurons. Thus the *Cluster Index* ranged from +1 for penetrations in which all neurons had sustained responses to -1 for penetrations for which all neurons had onset responses. CI values between +-1 meant that the penetration had mixed response types. If there was no local clustering of tone response types, the distribution should have a large peak at CI = 0. Figures 11A and B show PSTHs from two example penetrations that had all Onset or all Sustained/Onset-sutained neurons. These two examples had CI values of -1 and

+1 for Figures 11A and B respectively. The majority of electrode penetrations (16/27) had CI values of either -1 or +1 (Fig. 11C). Importantly, the peaks of the distribution of CI values were at +1 and -1 meaning that along a penetration, neurons tend to have similar response types. This result differs from that of Hromadka *et al.* (2008) who did not show clustering of response types along serial recordings from an electrode track. Their data, however, was recorded in the awake rat in which columnar organization appears less robust than in the primate, as the authors acknowledge.

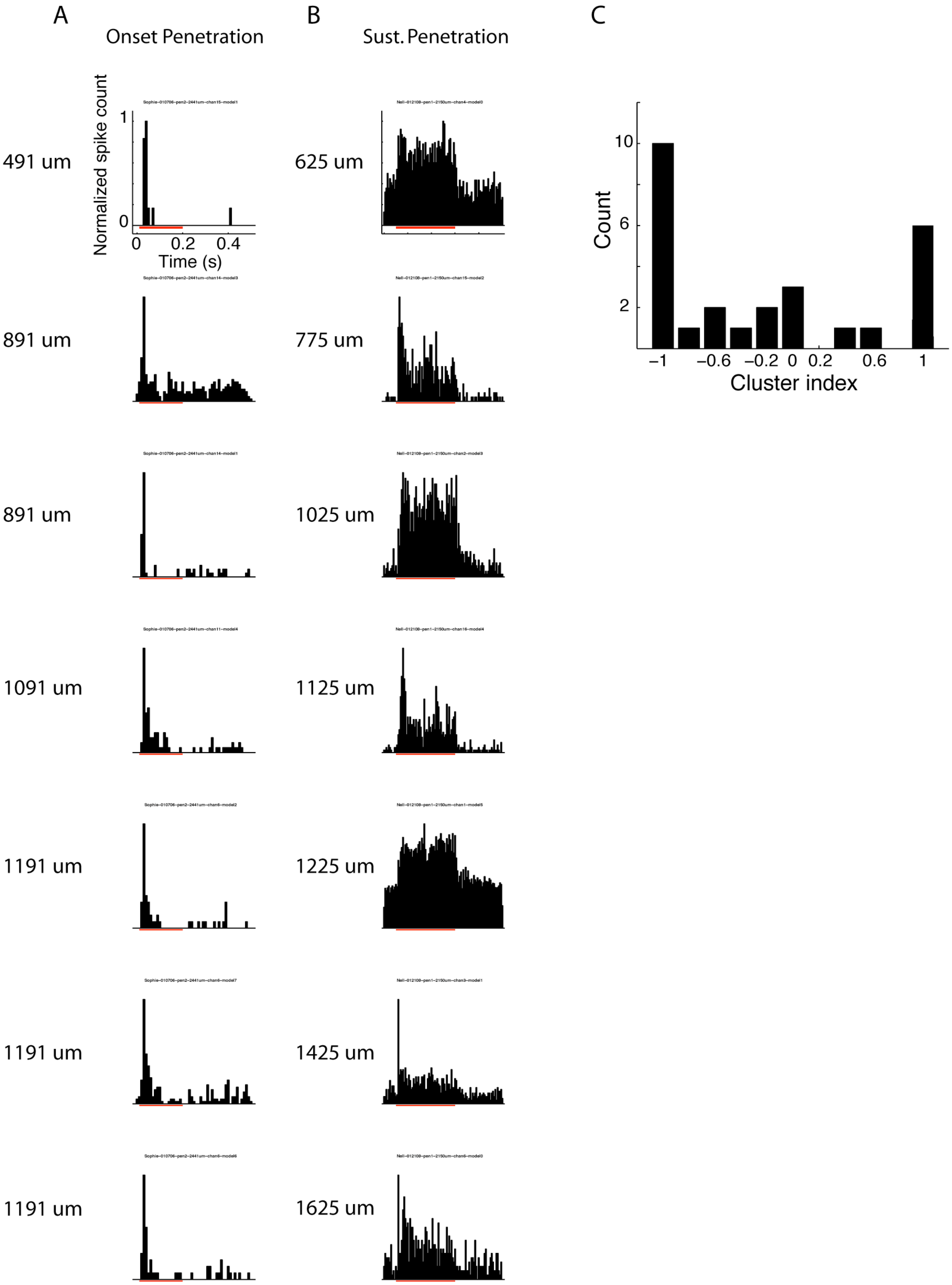
A
Onset Penetration
B
Sust. Penetration
C
Sophie–010706–pen2–2441um–chan15–model1
491 um
Normalized spike count
1
0
0
0.2
0.4
Time (s)
Nell–012108–pen1–2150um–chan4–model0
625 um
Count
10
6
2
–1
–0.6
–0.2
0
0.2
0.6
1
Cluster index
Sophie–010706–pen2–2441um–chan14–model3
891 um
Nell–012108–pen1–2150um–chan15–model2
775 um
Sophie–010706–pen2–2441um–chan14–model1
891 um
Nell–012108–pen1–2150um–chan2–model3
1025 um
Sophie–010706–pen2–2441um–chan11–model4
1091 um
Nell–012108–pen1–2150um–chan16–model4
1125 um
Sophie–010706–pen2–2441um–chan6–model2
1191 um
Nell–012108–pen1–2150um–chan1–model5
1225 um
Sophie–010706–pen2–2441um–chan6–model7
1191 um
Nell–012108–pen1–2150um–chan3–model1
1425 um
Sophie–010706–pen2–2441um–chan6–model6
1191 um
Nell–012108–pen1–2150um–chan6–model0
1625 um

Figure 11. Temporal response profiles are similar along electrode penetration. A., B. Cumulative PSTH's for single AI neurons recorded simultaneously from different channels of a 16-channel linear array. PSTH's are arranged according to the depth of the channel. Neurons at the top were closest to the surface of the cortex. The neurons in column A had onset responses to tones while the neurons in column B had more sustained responses to tones. C. Histogram of Cluster Index values for each of 27 penetrations from which multiple neurons were recorded simultaneously. Values of +1 indicate all neurons in a penetration were Sustained. Values of -1 indicate all neurons in a penetration were Onset.

Discussion

Multiple response types and stimulus encoding in AI

What is the function of the variety of pure tone response types observed in AI of awake mammals? Our data have demonstrated at least one functional difference: sustained and onset neurons create a dual population code for spectral modulation rate, an important parameter of animal vocalizations and music. The difference in the preferred range of spectral modulation rate between Sustained and Onset populations produced opposing functions of response magnitude and modulation speed. These opposing functions may allow for the unambiguous representation of multiple stimulus parameters using different populations of neurons. For example, a dual representation may aid in the discrimination of changes in the speed of frequency modulation from changes in the length of a static tones within local regions of cortex. For sustained neurons, response magnitude will increase as tone length increases or as sweep speed decreases. In contrast, the response magnitude of neurons with onset responses will not change as tone length varies but will increase as the sweep speed increases. Encoding of stimuli with dual populations of neurons with opposing response functions has been demonstrated for repetition rate encoding and may be a general feature of AI (T. Lu et al., 2001a; T. Lu and X. Wang, 2004; D. Bendor and X. Wang, 2007).

Our data also suggests that neurons with different tone response types represent different aspects of acoustic stimuli in general. Neurons with onset tone responses are sensitive to rapid modulations of stimulus energy as demonstrated by their response to the onset of pure tones and their preference for the fastest sweep speeds in our stimulus set. Studies in anesthetized cats AI also demonstrated the sensitivity of onset responses to rapid changes in stimulus energy (P. Heil, 1997a, b). In these studies, the strength and timing of onset responses depended on integration of the rate of change of the sound pressure level of tones. In general, slower rates of change produced higher thresholds. The rate of change of sound pressure level is analogous to the speed of frequency sweeps because both variables measure the rate of change of energy within a receptive field. In the case of frequency sweeps, slower speeds are equivalent to longer rise times and will evoke fewer spikes than faster speeds.

The firing rate of neurons with sustained responses to pure tones may continuously represent the energy of stimuli within the tonal receptive field. This notion is also supported by a study in the awake macaque which demonstrated that the firing rate of AI neurons encodes the envelope shape of amplitude modulated tones (B. J. Malone et al., 2007). In our study, the responses of sustained neurons matched the length of time that the instantaneous sweep frequency was within the tonal receptive field. Neurons with sustained tone responses often also had sustained responses to continuous broadband noise.

Together, onset and sustained neurons represent the wide range of energy modulations and static aspects of acoustic stimuli. Our data thus complement a recent study in the awake cat examining responses to vocalizations which showed that phasic neurons respond to amplitude modulations at the beginning and end of stimuli while tonic neurons responded during the static portions of stimuli (L. Qin et al., 2008).

Mechanisms generating variation in temporal response patterns

Studies using *in vivo* voltage clamp in AI of anesthetized rat have demonstrated that cortical inhibition quickly overcomes excitation and limits spiking responses to the onset of stimuli (M. Wehr and A. M. Zador, 2003; A. Y. Tan et al., 2004). While we did not directly measure the timing and strength of synaptic inhibition, we have shown that neurons with onset tone responses have higher thresholds, sharper frequency tuning, and lower spontaneous activity, than neurons with sustained responses. This suggests that onset neurons have greater inhibitory tone than sustained neurons and therefore may not be capable of sustained responses in general. Rapid inhibitory input could also explain the preference of onset neurons for rapid frequency sweeps. Faster sweeps would produce more synchronous responses across input to an AI neuron which, in turn, would produce a large depolarization before the onset of inhibition. Sweeps that move slowly through the receptive field produce less synchronized excitation that is vulnerable to co-tuned inhibition. Variations in time constants of adaptation or synaptic release probability may also account for some of the differences between onset and sustained responses (M. Atzori et al., 2001) though such a mechanism is less likely to account for the observed differences in frequency tuning bandwidth and threshold.

The generality of differences between responses types was shown in our study by the fact that multiple stimuli elicit similar response types from the same neurons. Other studies in awake auditory cortex have demonstrated congruence between tone response types and frequency sweep response types (I. C. Whitfield and E. F. Evans, 1965; H. Schulze et al., 1997) and between tone responses and responses to broadband noise (S. A. Shamma and D. Symmes, 1985; G. H. Recanzone, 2000). Together, this data suggests that the sustained or onset nature of the pure tone response in AI is a general property of the neuron and not a stimulus specific effect (X. Wang, 2007).

Local clustering of response profile type

We found that response types of nearby neurons along the depth of an electrode penetration tended to be the same. This clustering of response type suggests that the mechanisms underlying them are generated by local columnar microcircuitry. Previous work in the awake and ketamine anesthetized cat demonstrated more sustained responses in lower cortical layers V and VI (I. O. Volkov and A. V. Galaziuk, 1985; I. O. Volkov and A. V. Galazjuk, 1991; I. O. Volkov and A. V. Galazyuk, 1992). While our data suggest that in the awake monkey, tone response types are similar within a column or local region, preliminary data suggests that neurons in the infragranular layers (V and VI) had greater TRR's (more sustained responses) than neurons in granular and supragranular layers. Differences in temporal response patterns across cortical lamina are the subject of ongoing studies in our laboratory.

References:

Abeles M, Goldstein MH, Jr. (1972) Responses of single units in the primary auditory cortex of the cat to tones and to tone pairs. Brain Res 42:337-352.

Atzori M, Lei S, Evans DI, Kanold PO, Phillips-Tansey E, McIntyre O, McBain CJ (2001) Differential synaptic processing separates stationary from transient inputs to the auditory cortex. Nat Neurosci 4:1230-1237.

Bendor D, Wang X (2005) The neuronal representation of pitch in primate auditory cortex. Nature 436:1161-1165.

Bendor D, Wang X (2007) Differential neural coding of acoustic flutter within primate auditory cortex. Nat Neurosci 10:763-771.

Brugge JF, Merzenich MM (1973) Responses of neurons in auditory cortex of the macaque monkey to monaural and binaural stimulation. J Neurophysiol 36:1138-1158.

Cheung SW, Bedenbaugh PH, Nagarajan SS, Schreiner CE (2001) Functional organization of squirrel monkey primary auditory cortex: responses to pure tones. J Neurophysiol 85:1732-1749.

Chimoto S, Kitama T, Qin L, Sakayori S, Sato Y (2002) Tonal response patterns of primary auditory cortex neurons in alert cats. Brain Res 934:34-42.

Gerstein GL, Kiang NY (1964) Responses of Single Units in the Auditory Cortex. Exp Neurol 10:1-18.

Godey B, Atencio CA, Bonham BH, Schreiner CE, Cheung SW (2005) Functional organization of squirrel monkey primary auditory cortex: responses to frequency-modulation sweeps. J Neurophysiol 94:1299-1311.

Heil P (1997a) Auditory cortical onset responses revisited. II. Response strength. J Neurophysiol 77:2642-2660.

Heil P (1997b) Auditory cortical onset responses revisited. I. First-spike timing. J Neurophysiol 77:2616-2641.

Heil P, Irvine DR (1998) Functional specialization in auditory cortex: responses to frequency-modulated stimuli in the cat's posterior auditory field. J Neurophysiol 79:3041-3059.

Heil P, Rajan R, Irvine DR (1992) Sensitivity of neurons in cat primary auditory cortex to tones and frequency-modulated stimuli. I: Effects of variation of stimulus parameters. Hear Res 63:108-134.

Hromadka T, Deweese MR, Zador AM (2008) Sparse representation of sounds in the unanesthetized auditory cortex. PLoS Biol 6:e16.

Lewicki MS (1994) Bayesian modeling and classification of neural signals. Neural Comput 6:1005-1030.

Lu T, Wang X (2004) Information content of auditory cortical responses to time-varying acoustic stimuli. J Neurophysiol 91:301-313.

Lu T, Liang L, Wang X (2001a) Temporal and rate representations of time-varying signals in the auditory cortex of awake primates. Nat Neurosci 4:1131-1138.

Lu T, Liang L, Wang X (2001b) Neural representations of temporally asymmetric stimuli in the auditory cortex of awake primates. J Neurophysiol 85:2364-2380.

Malone BJ, Scott BH, Semple MN (2007) Dynamic amplitude coding in the auditory cortex of awake rhesus macaques. J Neurophysiol 98:1451-1474.

Miller JM, Beaton RD, O'Connor T, Pfingst BE (1974) Response pattern complexity of auditory cells in the cortex of unanesthetized monkeys. Brain Res 69:101-113.

Nuding SC, Chen GD, Sinex DG (1999) Monaural response properties of single neurons in the chinchilla inferior colliculus. Hear Res 131:89-106.

Qin L, Wang J, Sato Y (2008) Representations of cat meows and human vowels in the primary auditory cortex of awake cats. J Neurophysiol.

Recanzone GH (2000) Response profiles of auditory cortical neurons to tones and noise in behaving macaque monkeys. Hear Res 150:104-118.

Schreiner CE, Mendelson JR (1990) Functional topography of cat primary auditory cortex: distribution of integrated excitation. J Neurophysiol 64:1442-1459.

Schreiner CE, Winer JA (2007) Auditory cortex mapmaking: principles, projections, and plasticity. Neuron 56:356-365.

Schulze H, Ohl FW, Heil P, Scheich H (1997) Field-specific responses in the auditory cortex of the unanaesthetized Mongolian gerbil to tones and slow frequency modulations. J Comp Physiol [A] 181:573-589.

Shamma SA, Symmes D (1985) Patterns of inhibition in auditory cortical cells in awake squirrel monkeys. Hear Res 19:1-13.

Shapley R, Hawken M, Xing D (2007) The dynamics of visual responses in the primary visual cortex. Prog Brain Res 165:21-32.

Tan AY, Zhang LI, Merzenich MM, Schreiner CE (2004) Tone-evoked excitatory and inhibitory synaptic conductances of primary auditory cortex neurons. J Neurophysiol 92:630-643.

Volkov IO, Galaziuk AV (1985) [Reactions of neurons of the auditory cortex of unanesthetized cats to tones of a characteristic frequency]. Neirofiziologiia 17:500-508.

Volkov IO, Galazjuk AV (1991) Formation of spike response to sound tones in cat auditory cortex neurons: interaction of excitatory and inhibitory effects. Neuroscience 43:307-321.

Volkov IO, Galazyuk AV (1992) Peculiarities of inhibition in cat auditory cortex neurons evoked by tonal stimuli of various durations. Exp Brain Res 91:115-120.

Wang X (2007) Neural coding strategies in auditory cortex. Hear Res 229:81-93.

Wehr M, Zador AM (2003) Balanced inhibition underlies tuning and sharpens spike timing in auditory cortex. Nature 426:442-446.

Whitfield IC, Evans EF (1965) Responses of Auditory Cortical Neurons to Stimuli of Changing Frequency. J Neurophysiol 28:655-672.

Young ED (1984) Response characteristics of neurons of the cochlear nuclei. In: Hearing Science Recent Advances (Berlin CI, ed), pp 423-460. San Diego: College-Hill Press.

Zhang LI, Tan AY, Schreiner CE, Merzenich MM (2003) Topography and synaptic shaping of direction selectivity in primary auditory cortex. Nature 424:201-205.

Chapter 3

Tradeoff Between Information From Spike Timing and Spike Counts in Primary Auditory Cortex of Awake Squirrel Monkeys

Abstract:

Sounds carry information over a wide range of timescales. In human speech, for example, rapid frequency modulations are essential for consonant-vowel identification whereas slower modulations carry prosodic information. Multiple coding regimes may be required to efficiently encode the range of informative timescales. For identification of rapid stimuli there may not be enough time to use a rate code. By contrast, the detection of slower frequency modulations may require monitoring of neurons that respond continuously to sounds. Here, we show that in primary auditory cortex (AI) of awake squirrel monkeys (*Saimiri sciureus*) both spike timing and spike rate carry information about the speed and direction of frequency sweep stimuli. For individual neurons, there is an inverse relation between information carried by spike count and spike timing. This tradeoff suggests that neurons in AI are optimized either for sustained responses or for temporally precise responses. Thus, information in AI responses lies on a continuum between rate and temporal codes resulting in multiple representations of sounds.

Introduction:

The exact parameters of neuronal responses in sensory cortex that form the basis of perception remain unknown (S. Panzeri and S. R. Schultz, 2001). However, individual or joint temporal patterns of action potential occurrences likely play a major role. In the primary auditory cortex of awake animals, neurons fire in response to acoustic stimuli either predominantely at stimulus onset (onset response), throughout stimuli (sustained response), or in some combination of the two (onset-sustained response) (I. C. Whitfield and E. F. Evans, 1965; I. O. Volkov and A. V. Galaziuk, 1985; G. H. Recanzone, 2000; X. Wang et al., 2005). Because of the diversity of response types, there are a number of proposed neural codes for sounds in auditory cortex (AC). These include temporal codes that rely on the precise timing of spikes, such as first-spike latency, phase-locking, and temporal correlations between neuronal responses (R. C. deCharms and M. M. Merzenich, 1996; J. J. Eggermont, 1997; S. Furukawa et al., 2000; P. Heil, 2004). In contrast to these temporal codes, several recent publications have focused on the firing rate of neurons with sustained responses, suggesting that there is a transformation from codes that are temporally isomorphic to stimuli into a more abstract non-isomorphic rate code (X. Wang et al., 2005; X. Wang, 2007). According to this hypothesis, a small subset of preferred stimuli evokes sustained responses, while non-preferred stimuli evoke onset-only responses. In this model, onset responses are less stimulus-specific and mark the occurrence of events, while sustained responses code a specific stimulus feature. Yet, few studies in the auditory system have compared the information contained in onset responses to that available from sustained responses. Furthermore, several experiments have demonstrated that even in neurons with sustained responses, the latency to the first spike contains significant stimulus information (S. Furukawa and J. C. Middlebrooks, 2002; B. J. Mickey and J. C. Middlebrooks, 2003).

A more general alternative to the rate-based feature coding hypothesis is that the auditory system employs not a single code but, rather, uses different codes in parallel depending on the timescale of analysis and the features of sounds that are relevant to the behavioral context. Evidence for the rate-based feature coding hypothesis comes from the examination of single neuron responses to static stimuli, such as pure tones, and to prolonged repetitive stimuli, such as clicks and amplitude-modulated tones. However, many important features of sounds are neither prolonged nor repetitive and can occur over a range of time scales. For example, in some bats, FM sweeps in the biosonar vocalizations of some bats provide crucial information about target distance (N. Suga, 1989). Many primate vocalizations consist of frequency sweeps, or changes in formant frequency over time (P. Winter et al., 1966; J. D. Newman, 1978; T. Riede and K. Zuberbuhler, 2003). In speech, differences in parameters of frequency modulations occur within 10s of milliseconds and differentiate some consonant-vowel syllables (A. M. Liberman et al., 1967). In music, melodic information is carried by frequency modulations over 100s of milliseconds or longer, as is prosodic and syllabic information in speech (S. Rosen, 1992; D. Poeppel, 2003).

Cortical responses to FM sweeps have been studied in many species with particular focus on the sensitivity or tuning of neurons to sweep direction and velocity (J. R. Mendelson and M. S. Cynader, 1985; D. P. Phillips et al., 1985; P. Heil et al., 1992b; P. Heil et al., 1992a; J. R. Mendelson and K. L. Grasse, 1992; J. R. Mendelson et al., 1993; B. Tian and J. P. Rauschecker, 1994; J. P. Rauschecker et al., 1995; B. Tian and J. P. Rauschecker, 1998; I. Nelken and H. Versnel, 2000; B. Tian and J. P. Rauschecker, 2004; B. Godey et al., 2005). Our goal was to compare the information contained in the temporal response pattern and the spike count of single AI neurons in response to frequency sweeps. We used information theory to quantify stimulus encoding using spike counts or temporal patterns and found that, in AI, neurons transmit stimulus information in different ways. Neurons with high spike count and accompanying high rate information have low temporal information whereas neurons with high temporal information have low spike count information. To determine whether rate coding was specific to the spectrotemporal properties in one stimulus as suggested by the rate-based feature coding hypothesis mentioned above, we used a wide range of FM sweep speeds and durations. High rate-information neurons had sustained responses to all sweep speeds and the response followed the stimulus duration. In contrast, neurons with high temporal information had onset-dominated responses to both dynamic sweeps. Our data suggest that neurons in AI encode FM information with different emphasis on rate and time codes

Methods:

Animal Preparation

All procedures related to the maintenance and use of animals in this study were approved by the Institutional Animal Care and Use Committee at the University of California, San Francisco, and were consistent with national and state animal welfare guidelines.

The preparation for awake recording procedures were adapted for the squirrel monkey from those used in the awake marmoset monkey (T. Lu et al., 2001a). Two adult female squirrel monkeys (*Saimiri sciureus*) were trained to sit quietly in a restraint chair over several weeks. Animals were then implanted with a head post to allow for head fixation during physiological recording. After using ketamine (25mg/kg) and midazolam (0.1mg/kg) for induction, the animals were maintained in a steady plane of anesthesia using isoflurane gas (0.5-5%). Implants were secured to the skull using bone screws and dental acrylic. Animals were then trained based on positive reinforcement methods to sit in the primate chair with their head fixed to a frame over the course of several weeks after which they underwent a second surgery to implant a recording chamber of auditory cortex. During this procedure, animals were anesthetized using the protocol above. The bone overlying auditory cortex was exposed and a 8-10mm diameter ring was secured using bone screws and dental acrylic. To expose the auditory cortex, a 1-3mm burr hole was placed under magnification with a surgical microscope. A small slit was made in the dura using microsurgical instruments after application of 1%

lidocaine. Under sterile conditions, 5-10 electrode penetrations were made in each burr hole after which another region of cortex was exposed and the recording process repeated.

Electrophysiology

All recordings were made in a soundproof chamber (Industrial Acoustics Company, Bronx, New York). During each recording session, the animal was seated comfortably in a custom-built primate chair with its head fixed to a frame. Animals were not required to perform tasks but had to remain awake and received randomly-timed juice rewards during the recording sessions. Data were obtained using 16-channel linear electrodes (177μm^2 contact size, 100 or 150μm spacing; 1-3MOhm impedance) from NeuroNexus Technologies (Ann Arbor, MI). An electrode was advanced into cortex using a microdrive (David Kopf Instruments, Tujunga, CA) to the depth at which most channels were active (tip depth of ~1-2mm from the depth of first spontaneous activity identified audio-visually). Penetrations were made perpendicular to the surface of AI when possible, though it was often impossible to see the surface through such the small craniotomy and dural incision. Electrical signals from the brain were amplified using a 16-channel pre-amplifier (RA16 Medusa; Tucker-Davis Technologies, Alachua, FL), filtered (600-7000Hz band-pass) and recorded using an RX-5 amplifier and Brainware software (Tucker-Davis Technologies, Alachua, FL) on a personal computer. Brainware was used for online estimation of neural responsiveness and tuning, and the raw waveform was recorded (25 kHz sampling rate). Single neurons were sorted offline using Spikesort (written by Mark Kvale) which uses a Bayesian algorithm (M. S. Lewicki, 1994) to derive spike templates. In the squirrel monkey, AI is located on the surfaces of the temporal gyrus and in the supratemporal plane of the lateral sulcus. The precise location of our recordings were determined physiologically by the characteristics of AI neurons including vigorous pure tone responses, latency, and tonotopic gradient in the rostrocaudal dimension (S. W. Cheung et al., 2001). A terminal mapping experiment in the anesthetized animal confirmed the location and extent of AI.

Acoustic Stimulation

All sounds were presented using a Sony XXX free field speaker positioned 50cm in front of the animal. The sound delivery system was calibrated using a sound-level meter (Model2209, Brüel & Kjær, Norcross, GA) and SigCal software (Tucker-Davis Technologies, Alachua, FL). Logarithmic frequency sweeps were created in Matlab (The MathWorks, Natick, MA) and written as .wav files for delivery using SigGen and Brainware (Tucker-Davis Technologies, Alachua, FL). The sweep frequency ranged from 50 to 21,000 Hz in upward and downward directions with rates of frequency change of 5, 10, 20, 35, 60, 85, and 110 octaves/s (Fig. 1). Thus, there were a total of 14 frequency sweep direction-speed combinations. Because the sweep frequency range was held constant, the length of the stimuli changed as sweep speed was varied. Corresponding sweep lengths were the following: 1743, 871, 436, 249, 145, 103, and 79 ms. Each sweep also contained a 100 ms constant tone at the start and end frequencies. These constant frequency portions had a 5 ms cosine ramp up and ramp down at the beginning and end of the stimulus. Sweeps were played at 60 dB sound-pressure level (SPL). Each sweep was repeated 20 times in a random order with a minimum of 500 ms inter-trial interval. Tone bursts (50-500 ms duration, 5 ms on/off cosine gate, 500 ms inter-stimulus interval) were generated using SigGen software (Tucker-Davis Technologies, Alachua, FL). For measurement of frequency response areas (FRA), randomized tone bursts were played while frequency and intensity were varied. The range of frequencies used varied from 1-4 octaves (semitone or tone spacing) centered on the estimated center frequency of the neurons. Tone intensities spanned 0-70 dB in 10 dB steps. 5 repetitions were presented for each frequency-level combination.

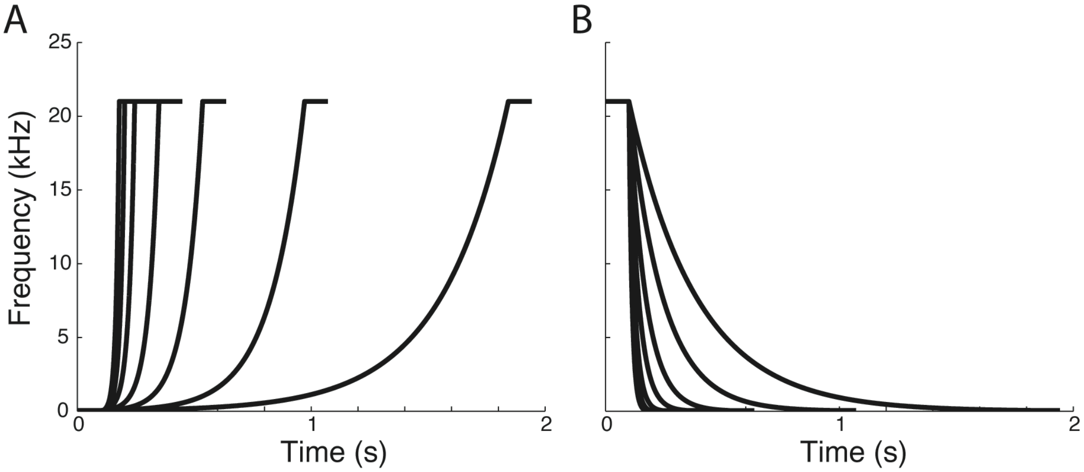

Figure 1.

Frequency sweep stimuli. A: curves depict the frequency of the stimuli as a function of time for sweeps with increasing frequency (Up direction) ranging from 50-21000 Hz. Each curve

represents one of the 7 different speeds used: 5, 10, 20, 35, 60, 85, and 110 octaves/second. The flat portion at the beginning and end of each stimulus is the 100 ms constant frequency portion. B: same as A except for decreasing frequency sweeps (Down sweeps).

Data Analysis

Information theoretic analysis of spike trains in response to frequency sweeps

Shannon's mutual information (abbreviated as MI) was used to quantify the amount of information that a neuronal response transmits about a stimulus set (C. Shannon, 1948; T. M. Cover and J. A. Thomas, 2006). Mutual information is defined as,

$$MI = \sum_{s} P(s) \sum_{r} P(r \mid s) \log_2 \left[\frac{P(r \mid s)}{P(r)} \right]$$

where $P(s)$ is the probability of a single sweep stimulus s, $P(r|s)$ is the probability of a response, r, given s, and $P(r)$ is the unconditional probability of response r. Mutual information can be interpreted as the average reduction in uncertainty about which stimulus, s, occurred given observation of r (F. Rieke et al., 1997; I. Nelken and G. Chechik, 2007). MI is also interpreted as the average reduction in the number of binary digits required to encode the set of stimuli once the set of responses is known (E. E. Thomson and W. B. Kristan, 2005).

To determine mutual information, one must make assumptions about what parameter of the neural response is used or read out downstream. Because we were interested in comparing rate and temporal codes, we first used the cumulative spike count as a measure of rate information. The cumulative spike count was determined by counting the number of spikes during a 1743 ms widow beginning 5ms after stimulus onset. This window corresponded to the length of the longest sweep stimulus (5 oct/s). Because the window length was constant and the stimulus length varied, this method may add noise from spontaneous activity for shorter stimuli (faster speeds) while the stimulus is off and the window continues. Thus, we also computed the rate information using the following method: for each stimulus presentation, the spike train was convolved with a Gaussian function (5ms standard deviation) to produce a smoothed firing rate as a function of time. The mean and standard deviation of the spontaneous activity was determined. We then found the times during the stimulus presentation when the firing rate function was three standard deviations above the mean spontaneous rate. The sum of the firing rate function during this time was used as the response magnitude. This method postulates that the readout begins counting the response only when the firing rate exceeds the spontaneous activity. Results using this method were quantitatively similar to the cumulative spike counting method and thus only the cumulative spike counting method is presented.

Information in the temporal spike pattern was calculated by constructing cumulative peri-stimulus time histograms (PSTH) for all repetitions of each stimulus. Each PSTH was normalized by the total number of spikes to create a probability distribution of spike times. MI was then calculated using the spike time distributions. This method assumes that the spike counts in each bin are independent of all other bins. Thus more information may be transmitted by stimulus independent correlations in the timing of spikes (S. Panzeri et al., 2001). It was necessary to make this assumption because of limitations in our data set size and the high firing rate of some neurons which prevented us from calculating the full spike pattern information.

All information analyses followed the method of Strong et. al. (1998) to correct for an upward bias in the estimate of MI from limited sampling of response distributions. We randomly drew samples of proportion N (0.98, 0.9, 0.8, 0.7, 0.6, 0.5, 0.4) from our data set and recalculated MI 100 times. We could then estimate the true MI by extrapolating to infinite sample size from the following quadratic function:

$$MI_{Estimate} = MI_{Inf} + \frac{a}{N} + \frac{b}{N^2}$$

where $MI_{Estimate}$ is the mutual information estimated from a proportion N of the full data, and MI_{Inf} is the true mutual information with infinite sample size. The MI was considered significant in neurons that were well fit (r-value > 0.95) by the above equation. Finally, we used Monte Carlo simulation to confirm that the MI calculated with trials randomized with respect to stimulus identity was significantly lower (5000 simulations, $p < 0.001$) than the estimated information.

To quantify the degree to which a neuron coded stimuli with firing rate or temporal patterns, we used a *Mutual Information Index* (MII) defined as

$\text{MII} = \frac{MI(temp) - MI(rate)}{MI(temp) + MI(rate)}$ where *MI(temp)* was the temporal information and *MI(rate)* was the rate information. This index ranged from −1 for neurons with only rate information to +1 for neurons with only temporal information.

Analysis of cumulative PSTH

To compare the specificity of sustained or onset response types between dynamic frequency sweeps and static pure tone stimuli, we classified the PSTH of responses to frequency sweeps as sustained or onset. We classified responses as sustained if there was at least one sweep stimulus for which the response had 5 or more spikes/trial on average (one-sided t-test, $p < 0.05$). Onset neurons were those neurons which had less than 5 spikes per trial but significantly more than 0 (one-sided t-test, $p < 0.05$). For other comparisons, the FM sweep response magnitude, response length, and response latency for each frequency sweep was determined by finding consecutive times during which the firing rate in the cumulative PSTH (10 ms bins) was 3 standard deviations above the mean spontaneous rate. Response magnitude was defined as the number of spikes during this time.

Analysis of pure tone responses

To quantify the sustained/onset nature of the response to characteristic frequency (CF) pure tones, we used a *Tone Response Ratio* (TRR) defined as:

$\frac{\text{Response}_{\text{Onset}}}{\text{Response}_{\text{Sustained}}}$ where $\text{Response}_{\text{Onset}}$ was the firing rate of the neuronal response to the tone during the first 100 ms of the stimulus and $\text{Response}_{\text{Sustained}}$ was the firing rate during the remainder of the stimulus. The spontaneous rate was subtracted from both response measures. A higher TRR indicated a more sustained tone response. This ratio could then be compared with rate and temporal MI.

Results:

Responses to frequency sweeps

The response patterns of neurons in the awake squirrel monkey typically fell into one of two categories: onset-dominated (phasic) or sustained (Figures 2 and 3). Raster plots are organized according to the speed and direction of the sweep stimuli (indicated by the red lines). By appearance, neurons in Figure 2 responded to each sweep by emitting only a few spikes per stimulus repetition during a short - phasic - time period, presuambly when the FM sweep enters the frequency receptive field of the neuron. We quantified responses to each sweep direction/speed combination by determining the times in the cumulative peri-stimulus time histogram (PSTH) during which the firing rate was 2 standard deviations above the mean spontaneous rate. This time was used as the window during which spikes were counted on each trial for each sweep speed/direction combination. Figures 2B, F, and J plot this data and show that the mean number of spikes in response to each stimulus varies from 0-2. These neurons are direction and speed selective; the neurons in 2A and E responded more reliably to fast up sweeps whereas the neuron in 2I responds best to fast down sweeps. Because of the small number of spikes emitted per trial, the length of the response to each sweep did not vary by more than a few milliseconds with changes in stimulus length (Fig 2D, H, L). While the spike count and response length did not vary much as a function of sweep speed or direction, each response occurs at a precise time, and there was a systematic relationship between response latency and sweep velocity as described in previous studies caused by the frequency selectivity of AI neurons (Fig 2C, G, K) (D. P. Phillips et al., 1985; P. Heil et al., 1992b; P. Heil et al., 1992a; I. Nelken and H. Versnel, 2000; B. Godey et al., 2005; C. A. Atencio et al., 2007).

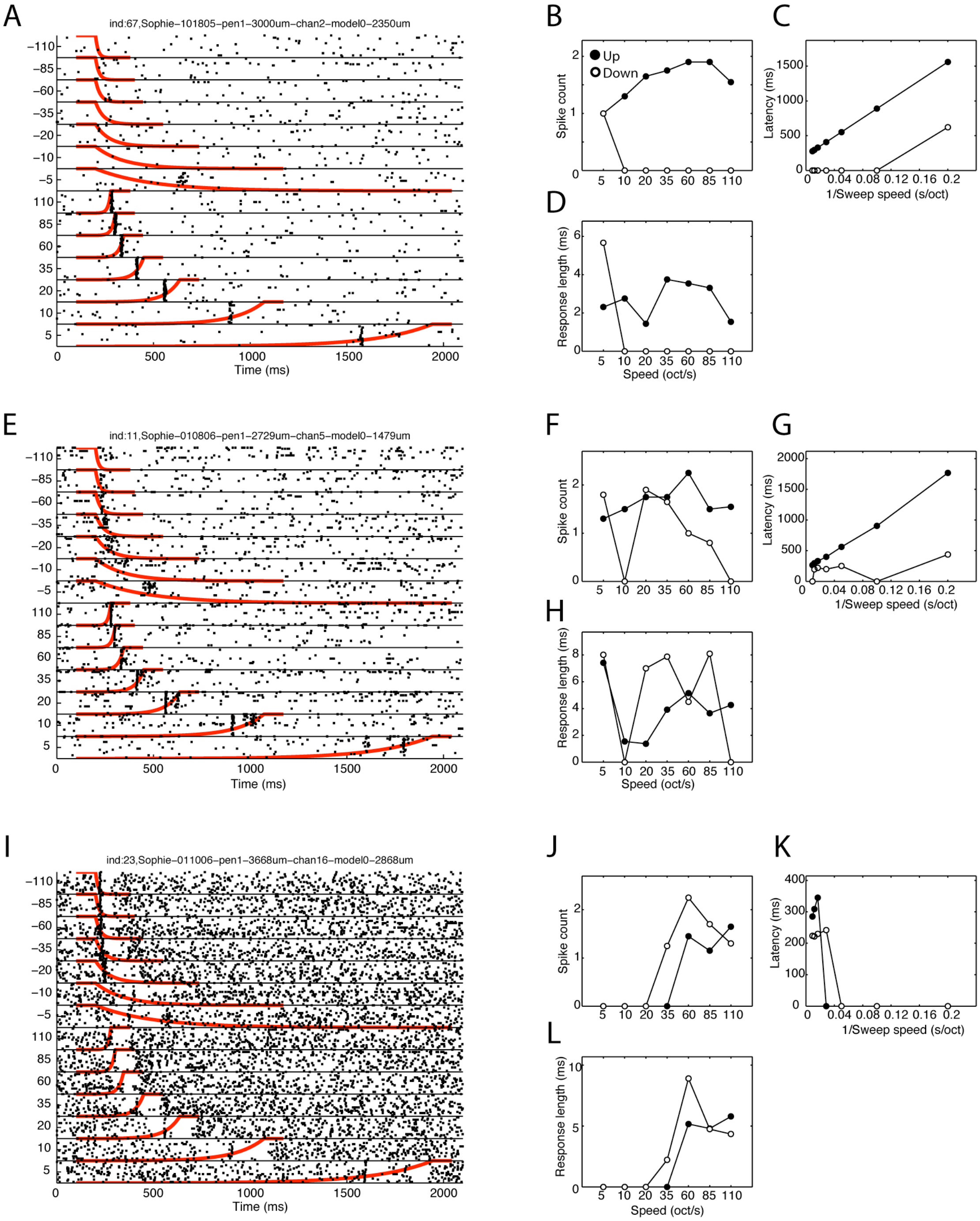
A
ind:67,Sophie–101805–pen1–3000um–chan2–model0–2350um
–110
–85
–60
–35
–20
–10
–5
110
85
60
35
20
10
5
0
500
1000
1500
2000
Time (ms)
B
Up
Down
Spike count
C
Latency (ms)
1/Sweep speed (s/oct)
D
Response length (ms)
Speed (oct/s)
5
10
20
35
60
85
110
0
0.04
0.08
0.12
0.16
0.2
E
ind:11,Sophie–010806–pen1–2729um–chan5–model0–1479um
F
G
H
I
ind:23,Sophie–011006–pen1–3668um–chan16–model0–2868um
J
K
L

Figure 2.

Three example neurons exhibiting onset responses to sweep stimuli. A: raster plots for three single neurons. The x-axis is time (ms). Sweep speed increases from lowest to highest moving up the y-axis. Up and down directions are indicated by positive or negative speeds respectively. B: Mean spike count during response (defined in Methods section) as a function of sweep speed for up and down directions for the neuron shown in the first group of raster plots in column A. Up responses are indicated by filled circles. Down responses are indicated by open circles. C: Response latency as a function of sweep speed for up and down sweeps (indicated as in B). D: Response length versus sweep speed for up and down directions. E, F, and G: same functions as in B, C, and D, for raster plots in row two of column A. H, I, J: same functions as in B, C, and D, for raster plots in row three of column A.

In contrast to Figure 2, neurons in Figure 3 followed the envelope of each sweep stimulus with a sustained increase in firing rate. The average spike count decreased as sweep speed increased suggesting that these neurons fired as long as the sweep was within their receptive field. Longer stimuli elicited more spikes and longer responses while shorter stimuli elicited fewer spikes and shorter responses (Fig 3B, F, J and 3D, H, L). All of these neurons responded best (defined by highest spike count) to the slowest sweep speed which has the longest duration. Some Sustained neurons exhibited direction sensitivity (Fig 3I). The latency to the beginning of the response varied with sweep speed in a similar fashion as Onset neurons (Fig 3C, G, K).

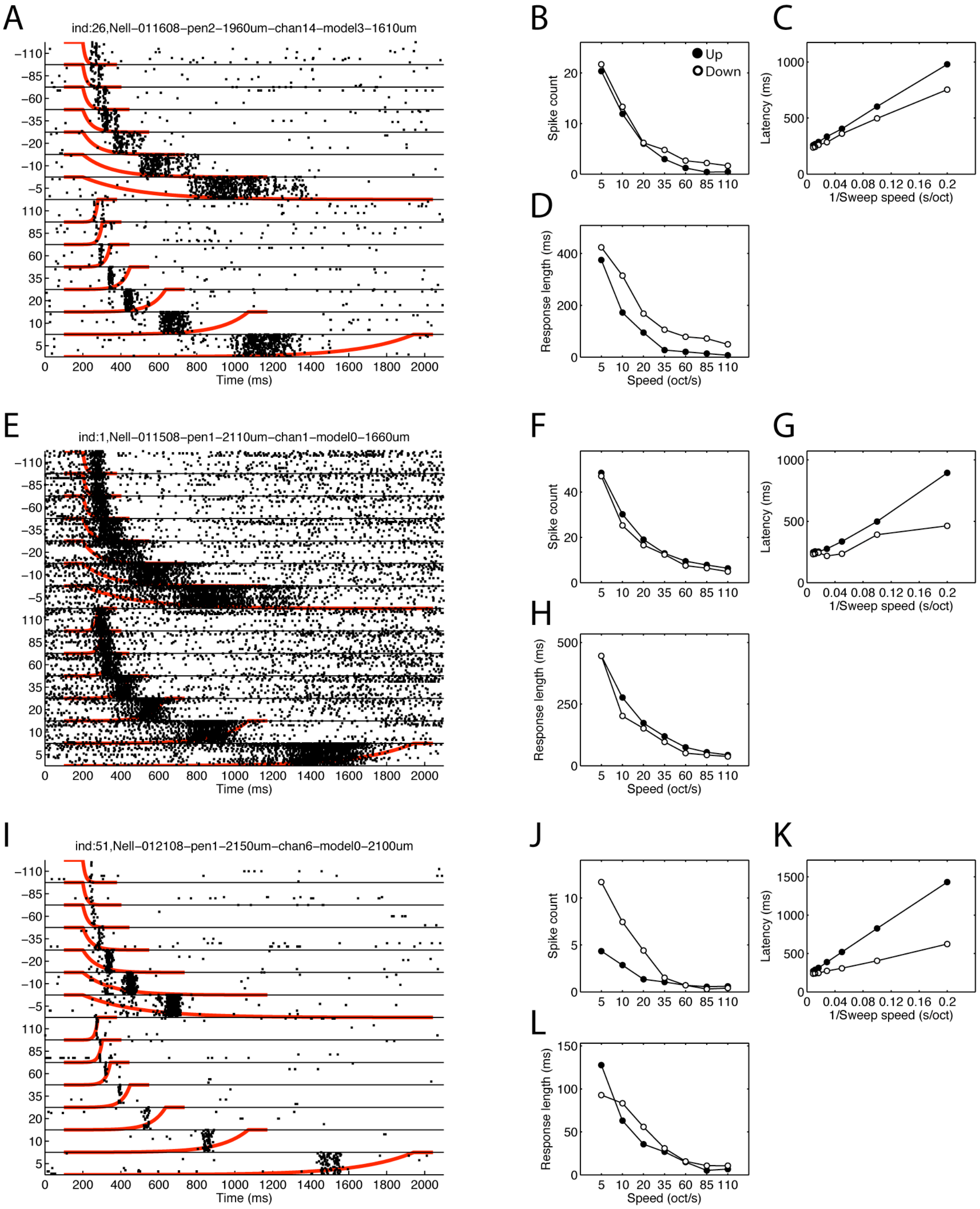

Figure 3.

Three examples of neurons exhibiting sustained responses to sweep stimuli. The organization of this figure is identical to Figure 2.

In most studies of the auditory cortex, a sustained (or tonic) neural response is one for which the response duration is approximately equal to the duration of the stimulus (I. O. Volkov and A. V. Galaziuk, 1985; G. H. Recanzone, 2000; X. Wang et al., 2005; B. J. Malone et al., 2007). Because the frequency extent of our sweep stimuli always exceeded the frequency tuning bandwidth of AI neurons, we never encountered a neuron that responded throughout the whole duration of our longest stimuli (1.7 s). Figure 3, however, suggests that the responses of some AI neurons are prolonged and/or track the duration of dynamic stimuli. In order to compare the encoding of frequency sweeps between response types, we classified frequency sweep responses as *Sustained* or *Onset*. *Sustained* responses were those for which at least one sweep stimulus evoked a mean response that was significantly greater than 5 spikes/trial (One-sided t-test, $p<0.05$). *Onset* responses were those with at least one FM response that was significantly greater than 0 spikes/trial (One-sided t-test, $p<0.05$) but less than 5 spikes/trial. Thus, by our classification, all of the neurons in Figure 2 had Onset sweep responses while all of the neurons in Figure 3 had Sustained sweep responses. The proportion of neurons with Sustained responses was 21% (32/147) and the proportion of neurons with Onset responses was 78% (115/147).

The dramatically different responses of neurons in Figures 2 and 3 suggest that these neurons encode information about the frequency sweeps differently. Because our goal was to determine how well sweep stimuli are encoded in AI of the awake primate, we needed to quantify how well aspects of the neural response discriminate between variations in stimulus parameters. Previous studies of auditory cortical responses to frequency sweeps have used the spike count in the cumulative PSTH to determine selectivity to sweep parameters such as speed and direction (J. R. Mendelson and M. S. Cynader, 1985; D. P. Phillips et al., 1985; P. Heil et al., 1992b; P. Heil et al., 1992a; J. R. Mendelson and K. L. Grasse, 1992; J. R. Mendelson et al., 1993; B. Tian and J. P. Rauschecker, 1994; J. P. Rauschecker et al., 1995; B. Tian and J. P. Rauschecker, 1998; I. Nelken and H. Versnel, 2000; B. Tian and J. P. Rauschecker, 2004; B. Godey et al., 2005). While this approach is valuable, it does not take into account the trial-to-trial variability of neural responses which sets limits on the ability of downstream areas to decode the stimulus given a response. Sensory stimulus discriminations and identifications must be made based on a single presentation, and thus the variability of neural responses is critical. Figure 4B illustrates this point; it plots the probability distributions of spike counts in response to the 14 sweep stimuli from a Sustained neuron. If one were to observe 40 spikes from this neuron, one could say with a high degree of certainty that the stimulus was a 5 oct/s down sweep because this spike count does not frequently occur in response to other sweep stimuli. If, however, one were to observe 10 spikes, one could not differentiate between stimuli of 35, 60, or 80 oct/s.

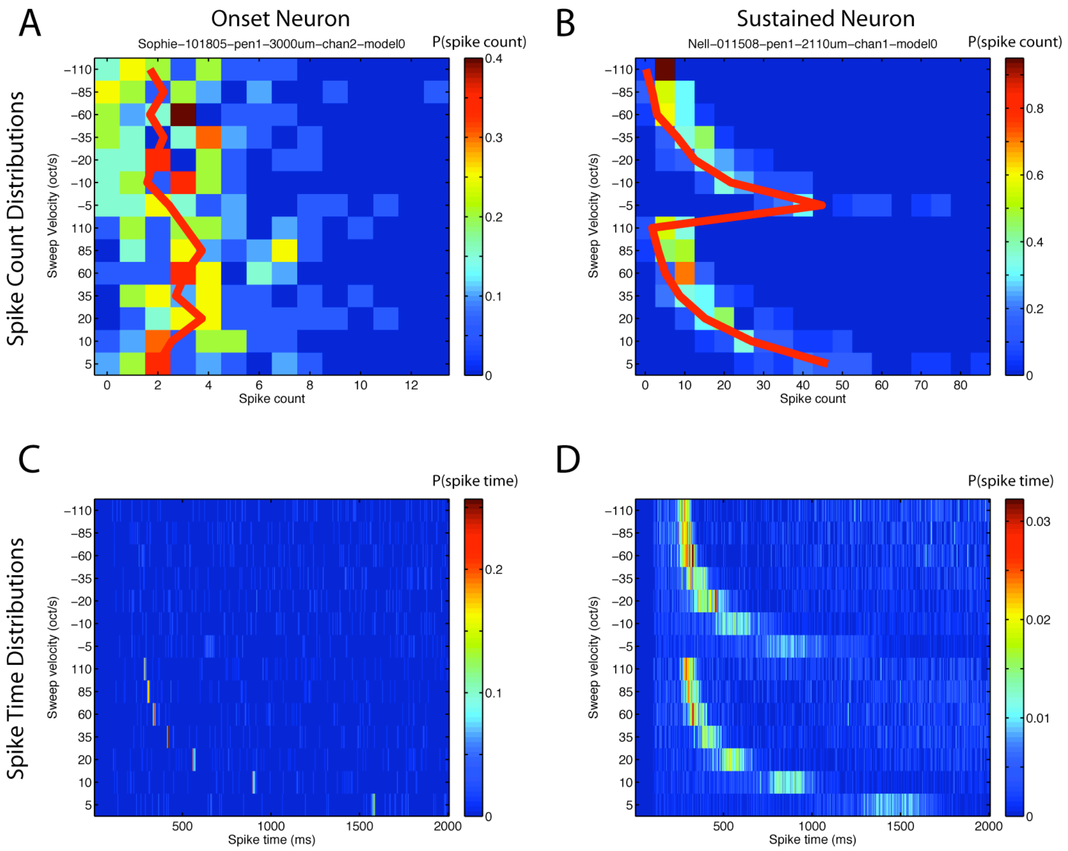

Figure 4.

Spike count and spike time probability distributions for sustained and onset neurons. A: probability of a spike count occurring for each sweep speed/direction combination for the onset neuron from Fig 2A. Brighter colors indicate greater probability of the occurrence of the spike count indicated on the x-axis. Mean spike count for each stimulus is shown by red line. B: same as A, but for the sustained neuron from Fig. 3E. C: probability of a spike occurring at a specific time bin indicated by the x-axis for the sustained neuron in A. Bin lengths were 10 milliseconds in this figure. Brighter colors indicate greater probability of a spike occurring in that time bin. D: same as C, but for the onset neuron from B.

A further limitation of using the mean spike count as the only measure of stimulus encoding is that it leaves out the temporal pattern of the neural response which may be highly informative. Consider a neuron for which the response to two different stimuli has the same spike count but the firing rate as a function of time (or the shape of PSTH) is consistently different. Such is the case with the Onset neuron shown in Figure 4A. The variations in the spike count distributions between stimuli are not greater than the variations among stimulus repetitions. Thus the spike count alone does not significantly co-vary with the stimulus identity. The spike time probability distributions, shown in 4D, are different for each of the seven up sweeps with almost no overlap. Thus a readout mechanism that keeps track of the spike times of this neuron could be used to identify the stimulus. For the Sustained neuron in 4D, the spike time distributions have more overlap between speeds of the same direction and between directions because the responses of this neuron are more prolonged and the neuron is less direction selective than the Onset neuron. Because both spike timing and spike count could be used to discriminate between stimuli, a measure that can take into account both of these aspects of responses is necessary.

Information theoretic analysis of sweep responses

Shannon's mutual information has been used in a number of sensory systems to quantify the stimulus encoding (L. M. Optican and B. J. Richmond, 1987; B. J. Richmond and L. M. Optican, 1990; S. Panzeri et al., 2001; T. Lu and X. Wang, 2004).

This quantity takes into account the full distribution of a response measure and quantifies the maximum number of stimuli that can be discriminated by an observer who reads out the responses of a neuron (F. Rieke et al., 1997; I. Nelken and G. Chechik, 2007). To quantify how spike rate and spike timing could support the discrimination of dynamic stimuli, we applied an information analysis to responses of AI neurons to frequency sweeps.

The mutual information from the cumulative spike counts (abbreviated MI(rate)) of AI neurons was determined by counting the number of spikes over a 1943 ms time widow (corresponding to the length of the longest sweep). The dotted lines in Figure 5 plot the mutual information from the total spike counts of the Sustained and Onset neurons from Figure 4. The MI(rate) for the Sustained neuron was 1.99 ± 0.06 bits ($p<0.0005$, Monte Carlo simulations, $n = 2000$). The maximum information in this experiment is limited by the entropy of our stimulus set which was 3.81 bits ($\log_2 14$). Therefore, this Sustained neuron encoded 40% of the maximum information. The spike count information for the Onset neuron was 0.46 ± 0.08 bits but was not significantly different from the information calculated from randomized trials in our Monte Carlo simulations ($p = 0.3925$, Monte Carlo simulations, $n = 2000$). Consistent with our intuitions from Figure 4, we cannot say that the Onset neuron carries information in its cumulative spike count.

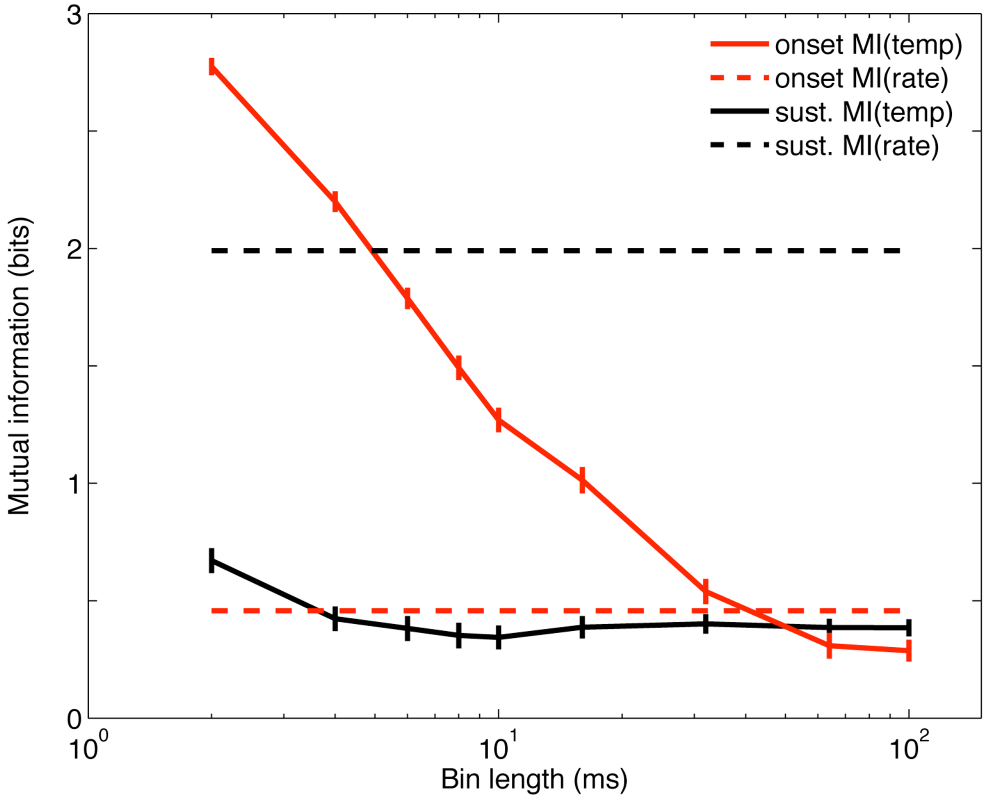

Figure 5.

Two examples of mutual information determined from firing rate and spike timing. The mutual information from the cumulative spike counts (MI(rate)) for the sustained neuron from Fig. 4B is shown by the dashed black line. MI(rate) was calculated using one bin size, not for different bin lengths and is therefore a flat line. The temporal information, MI(temp), for this neuron is shown by the solid black line as a function of the bin width used to determine the information. Both MI(rate) and MI(temp) were significant for this neuron ($p < 0.0002$). MI(rate) and MI(temp) from the onset neuron in figure 4A are shown by the dashed red line and the solid red line, respectively. Only the temporal information was significant ($p < 0.0002$).

To determine if a spike timing code in AI could support stimulus discrimination, we calculated the mutual information between the distribution of spike times and the sweep stimuli. The mutual information from the spike time distributions of the neurons in Figure 4 are plotted as solid lines in Figure 5 as functions of the PSTH bin length. By varying the bin length, one can determine the degree of temporal precision of the neural responses. If the information increases as bin size decreases, then spike timing must be precise at a scale of at least the smaller bin size. For the Onset neuron, the mutual information increases as the bin length becomes shorter (Fig. 5). This neuron has spike timing precision on the order of 2 ms which can support discrimination of the different sweep stimuli. Forth the two longest bin lengths, the Sustained neuron (shown in red) had slightly more information than the Onset neuron (shown in black). Because the Onset neuron fires only a few spikes per stimulus, counting spikes over longer bins adds spontaneous spikes to the evoked response which flattens the distribution of spikes as a function of time. This makes the response conditional and response unconditioned distributions more similar. Because the mutual information measures the difference between the response conditional and unconditional distributions, lengthening the bins decreases mutual information for the Onset neuron. The Sustained neuron retains more information at longer bin lengths because each response has more spikes so that adding spontaneous spikes has less effect on the response signal-to-noise level. For bin lengths shorter than 64 ms, the Onset neuron has greater information than the Sustained neuron. The responses of the Onset neuron are highly localized in time which results in very little overlap in the response conditional distributions (Fig. 4C) and makes each spike time informative about which stimulus occurred. The responses of the Sustained neuron are more dispersed in time and have slightly more overlap with each other which decreases mutual information (note the difference in the scales between the two neurons in Fig 4C and D).

Both spike timing and spike rate carry information about frequency sweeps

We now consider the full set of 482 recorded neurons in AI. The distribution of spike count information values from all neurons with statistically significant values is shown in Figure 6A. The mean, median and range of mutual information were 0.51, 0.33, and 0.04-2.92 bits respectively. Only 82/482 neurons had significant rate information. This indicates that only 17% of AI neurons had reliable covariations of firing rate with this set of frequency sweep parameters. Coding efficiency is the ratio of the measured mutual information to the entropy of the stimulus set (3.81 bits) (E. Arabzadeh et al., 2004, 2006). The mean coding efficiency based on spike counts was 13% (range = 1-77%). This suggests that pure rate information provides only a small proportion of the possible information carried about FM stimuli.

While the mutual information is the average of information transmitted over the entire stimulus set, it is possible to quantify how well individual speeds are represented by determining what is called the stimulus-specific information (M. R. DeWeese and M. Meister, 1999; S. Panzeri et al., 2001). The stimulus specific information measures the difference between the response to a single stimulus and the mean response to all stimuli. Figure 6B plots the mean specific information for each sweep speed/direction combination for neurons with significant mutual information. The mean specific information (0.37 bits, SD = 0.32 bits) was failry low, in accordance with the low overall MI. The specific information was significantly greater at the slowest speed for both up and down directions (One-way ANOVA, $p < 0.01$, Tukey's honest significant difference test, $p < 0.05$). Thus, the slowest speeds used in this study were strongly represented by firing rates in AI.

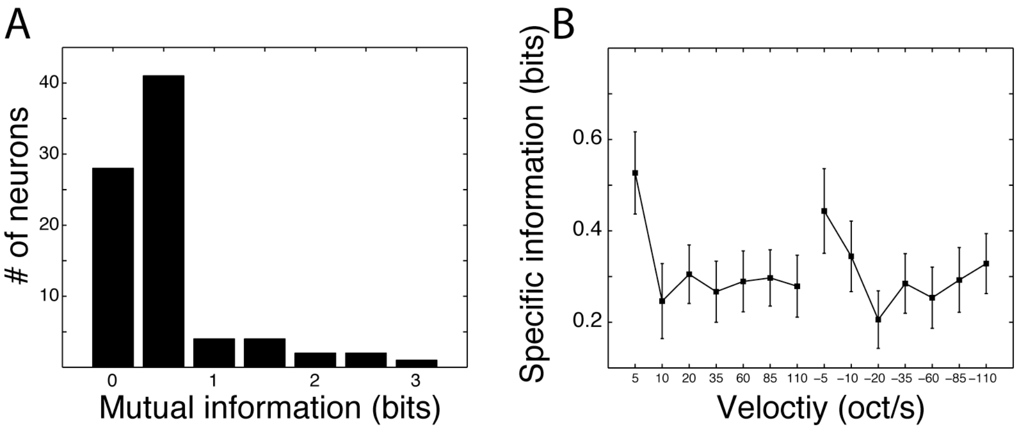

Figure 6.

Population distribution of rate information. *A:* Histogram of mutual information values for neuron with significant rate information. *B:* Population mean specific information for each sweep speed/direction combination. Error bars indicate standard error of the mean.

To compare the information available from a rate code with that from a temporal code, we quantified the temporal information for all neurons in our data set. The distribution of mutual information values for all neurons is plotted in histogram form as a function of bin length in Figure 7A. The MI distribution in AI shifts toward higher values as the bin length decreases (Fig. 7B). The median temporal information increases from 0.08 to 1.43 bits as the bin length becomes shorter. The median coding efficiency also increases from 2% to 38%. This suggests that increasing the sampling rate (smaller bin widths) of a hypothetical cortical readout increases the ability to identify frequency sweep speed and direction from firing rate modulation. For bin lengths less than 10 ms, both the median temporal mutual information and coding efficiency is greater than the mean rate information in AI (dotted line in Fig. 7B). Figure 7C plots the proportion of neurons with significant information values as a function of bin length. As bin length decreases from 100 ms, the number of neurons with significant information first increases to a maximum of 54% at 64 ms. At bin lengths shorter than 32 ms, the proportion decreases, reaching a minimum at the shortest bin length used, 2 ms. Over all neurons, the median mutual information grows with decreasing bin lengths. However, the population of neurons that have spike timing precision at short bin lengths decreases. At 2 ms bin length, still more than 30% of the population had significant information which is three times the proportion of neurons with significant rate information (~17%; dotted line Fig. 7C).

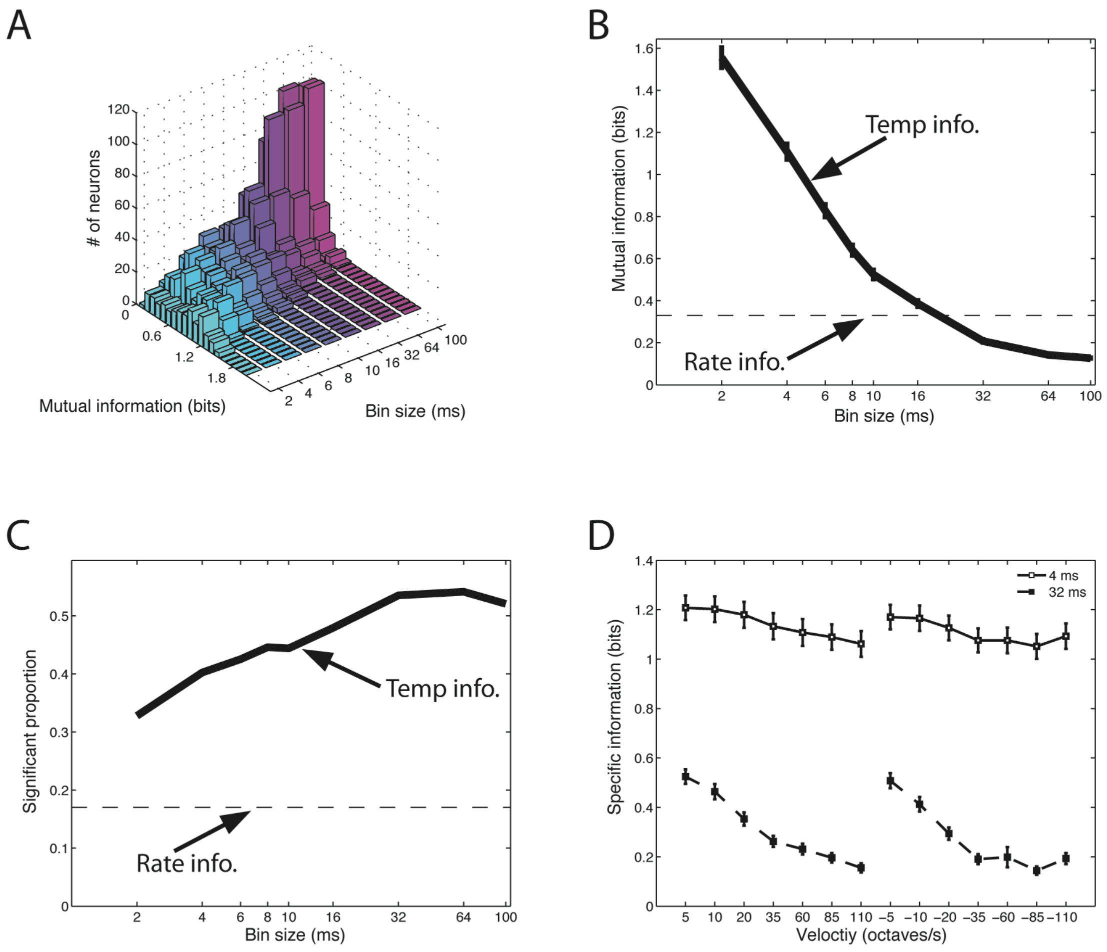

Figure 7.

Population distribution of temporal information. *A:* Histogram of mutual information values for neurons with significant temporal information. Mutual information was calculated using different bin lengths ranging from 2-100 milliseconds. *B:* Median temporal information as a function of bin length. The median rate information is represented by the dashed black line for comparison. *C:* Proportion of neurons with significant temporal information as function of bin length. The proportion of neurons with significant rate information is shown by the black dashed line for comparison. *D, E:* Specific information for each stimulus for 100 and 4 millisecond bin lengths.

To determine how well particular speeds/direction combinations were represented by the timing of action potentials, we calculated the specific information for each stimulus. For longer bin lengths, the slower speeds had more information (Fig. 7D, filled squares, dashed line; Table 1). This result is similar to the spike count specific information which was also greatest at the slowest speeds (Fig 6B). For shorter bin lengths, the specific information values were evenly distributed (Fig. 7D, solid line; Table 1). As expected, the specific information was also greater on average for the shorter bin lengths. The greatest increase in specific information came from the fastest speeds. Thus, the increased information for shorter bin lengths resulted from greater specific information for fast sweep speeds. The greater specific information for slower speeds at long bin lengths is likely due to the longer response latencies as seen in Figures 2 and 3. This separates the responses to these sweeps from all other speeds. For faster speeds, the latencies are much closer to one another in time. It is therefore likely that the greater specific information for slower speeds is caused by our choice of stimuli rather than a cortical preference for slow modulation rates. For example, one could imagine choosing a set of sweep rates that elicited response latencies that were of equal distance from each other. This would likely produce a more even distribution of specific information values as a function of sweep speed.

Rate and temporal information are inversely related in single AI neurons

It has been shown that the responses of neurons in AI of the awake Marmoset monkey respond to repetitive stimuli are either synchronized to the period of the stimulus or non-synchronized (T. Lu and X. Wang, 2000; T. Lu et al., 2001b; T. Lu and X. Wang, 2004; D. Bendor and X. Wang, 2007). These studies suggest that neurons in AI of the awake primate may be segregated into two populations: one for which the firing rate alone encodes repetitive stimuli and one for which the timing of responses may encode repetitive stimuli. Our results also demonstrate that information about the parameters of non-repetitive frequency sweeps is contained in both the rate and timing of neural responses in AI. However, the two example neurons in Figure 5 differed in amount of rate and temporal information contained in their responses. For the Sustained neuron, the rate information was greater than that in the Onset neuron while the temporal information was lower. Thus, neurons in AI may encode sweep stimuli with either firing rate or temporally precise responses. To determine whether there is a relationship between temporal and rate representations of non-repetitive stimuli in individual AI neurons, we compared the rate and temporal information of each neuron (Fig. 8). For short bin lengths, there was an inverse relation between the amount of information in the spike counts of responses and the information in the temporal modulation of the response. Neurons with high rate information had lower temporal information while neurons with high temporal information had lower rate information. For longer bin lengths, the correlation decreased until neurons had low temporal information and a range of rate information values. Thus, the relation between rate and temporal coding of frequency sweeps within single neurons depended on the sampling rate used to measure temporal modulations of the firing rate. In general, there is a tradeoff between rate and temporal information in single AI neurons. Rather than being divided into two distinct populations, there is a continuum between rate and temporal codes across the neural population.

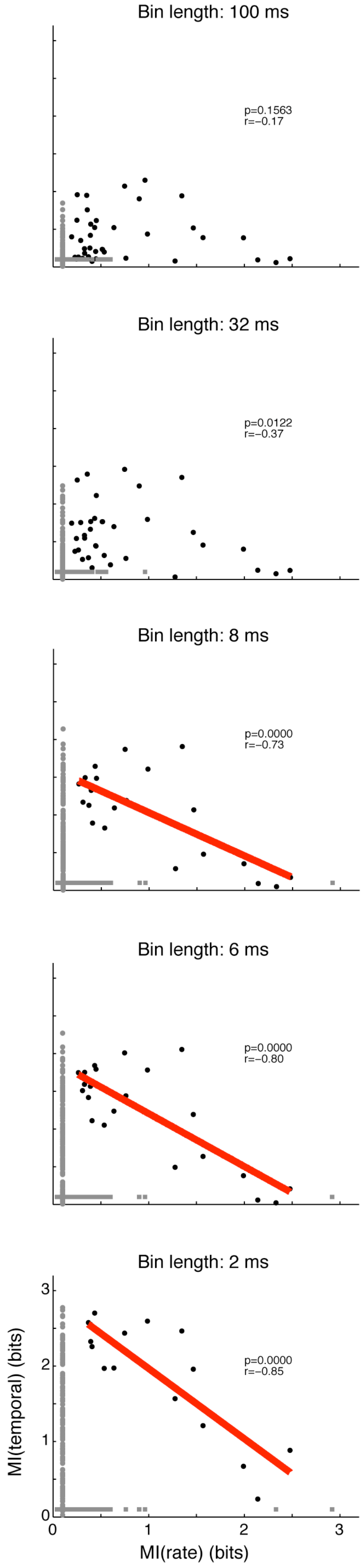
Bin length: 100 ms
p=0.1563
r=−0.17
Bin length: 32 ms
p=0.0122
r=−0.37
Bin length: 8 ms
p=0.0000
r=−0.73
Bin length: 6 ms
p=0.0000
r=−0.80
Bin length: 2 ms
p=0.0000
r=−0.85
MI(temporal) (bits)
0
1
2
3
MI(rate) (bits)
0
1
2
3

Figure 8.

Rate and temporal information are inversely correlated. Plots of mutual information calculated from spike time distributions, MI(temporal), as a function of mutual information calculated from the spike count, MI(rate). Only neurons with significant values for both MI(rate) and MI(temporal) are shown. Functions are plotted for different bin lengths. Red lines indicate least square best fit. All best fit lines are significant ($p < 0.001$).

Mutual information differs between onset and sustained response types

Cortical neurons can have either sustained or onset responses to frequency sweeps (Fig. 2 and 3). To determine whether these response types encode dynamic sounds differently, we compared the rate and temporal information between these two classes (Fig. 9). Sustained neurons had significantly greater MI(rate) than Onset neurons (Fig. 9A, first two columns; Wilcoxon rank sum test, $p < 0.05$, Sustained mean = 1.20 bits, S.E.M. = 0.17 bits, Onset mean = 0.37, S.E.M. = 0.04 bits). By contrast, MI(temporal) in Onset neurons was greater than that in Sustained neurons for bin lengths of 16 ms or less (Fig. 9A; Wilcoxon rank sum test, $p < 0.05$). For bin lengths longer than 16 ms, temporal information was the same for Onset and Sustained neurons. Consequently, if FM decoding is restricted to sustained neurons using rate code, fewer neurons would be required to discriminate between these stimuli than for Onset neurons. For a high resolution temporal code (≤16ms bin length), pooling the responses of Onset neurons would enable better stimulus discrimination than for Sustained neurons.

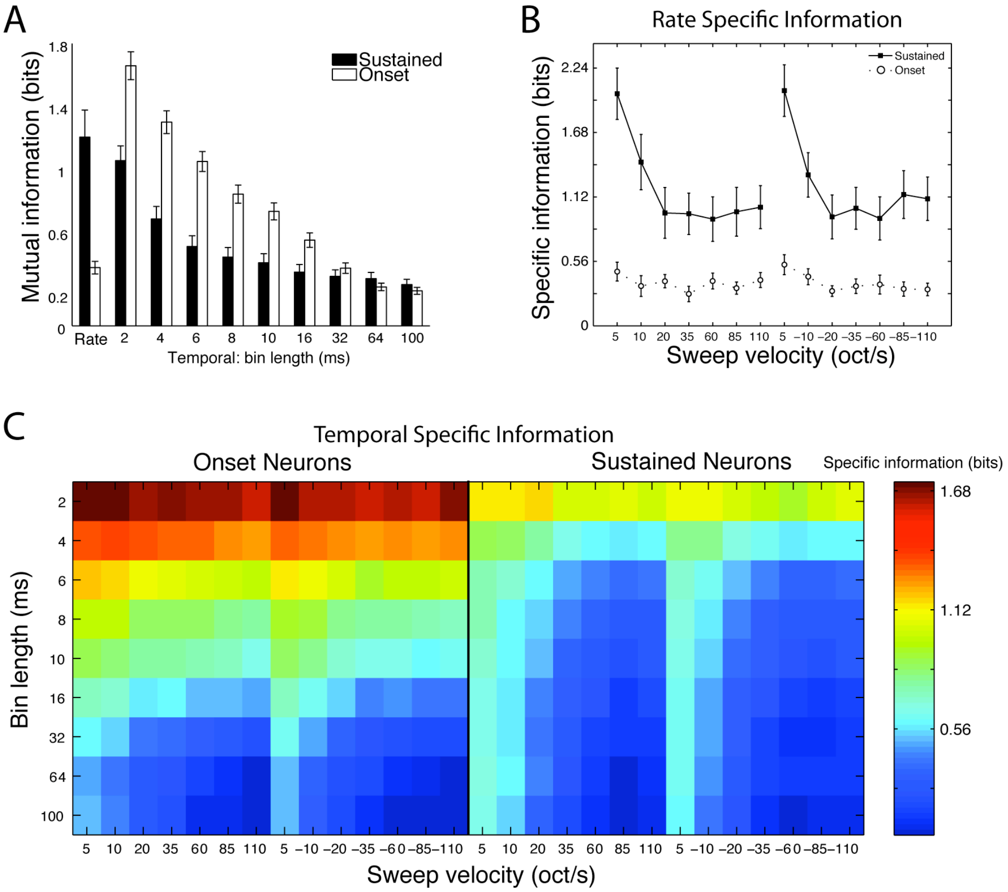

Figure 9.

Comparison of rate and temporal information in sustained and onset responses. *A*: Mean mutual information values for neurons with sustained or onset responses (see Methods section for definition) shown in black and white, respectively. Only neurons with significant information are plotted. Column one is the rate information. All following columns are temporal information. Error bars represent the S.E.M. *B*: Mean specific information from the spike counts of sustained and onset neurons. The specific information from sustained neurons is shown by solid black circles. The specific information for onset neurons is shown by the unfilled circles. *C*: Mean specific information calculated from the spike time distributions for sustained and onset neurons. Onset neurons are shown in the left half of the figure while sustained neurons are shown in the right half.

Neurons with sustained and onset responses in the awake squirrel monkey prefer different sweep speeds (Thesis Chapter 1). To determine if frequency modulation rate is represented differently between neurons with sustained and onset sweep responses, we compared the stimulus specific information between these response types (Fig 9B, C). In sustained neurons, the specific rate information differed among speeds (Fig. 9B solid lines; One-way ANOVA, $p < 0.05$, $F = 3.49$). The specific information for slowest sweep speeds was much greater than that for speeds greater than 10 oct/s (Tukey's honest significant difference test, $p < 0.05$). The firing rate of these neurons clearly reported whether the stimulus was or was not 5 oct/s up or down. This coincides with data from a previous study demonstrating that these neurons respond best to slow modulation rates that evoke longer responses (Thesis Chapter 1). The specific information for neurons with onset sweep responses did not differ significantly between sweep speeds.

The pattern of specific temporal information for both response types depended on the bin length (Fig. 9C). For 100 ms bin length, both sustained and onset neurons had greatest specific information at 5 oct/s. As the bin length decreased, the specific information increased in the faster speeds until there was no difference. Therefore, the firing rates of AI sustained neurons emphasize slow modulation rates whereas the temporal response patterns encode all rates.

Information in first-spike timing

Studies in several sensory systems of anesthetized animals have demonstrated that the first spike in a response carries the majority of information about a stimulus (S. Panzeri et al., 2001; S. Furukawa and J. C. Middlebrooks, 2002). However, a recent study showed that the first-spike timing precision of AI neurons in awake gerbils is less precise than in anesthetized gerbils. We have shown that spike timing is precise in some AI neurons of the awake primate as demonstrated by the larger amount of temporal information at short bin lengths. To determine the contribution of first-spike timing to stimulus encoding in AI of the awake primate, we calculated the mutual information for each neuron from the PSTH of responses for which only the timing of the first-spike of the response was preserved. The timing of all other spikes in the response was randomly shuffled. The same bias correction and significance tests were used in this analysis as in the calculation of the full PSTH information above. The fraction of total temporal information carried by the timing of the first spike is shown in Figure 10A for each bin length. For the mutual information calculated using a 2 ms bin length, 92% of the information is carried by the timing of the first spike. The ratio decreases as the bin length increases. Thus, as the temporal precision of a hypothetical downstream readout increases, the timing of the first spike of the neural response to a frequency sweep becomes more informative relative to other spikes in the response.

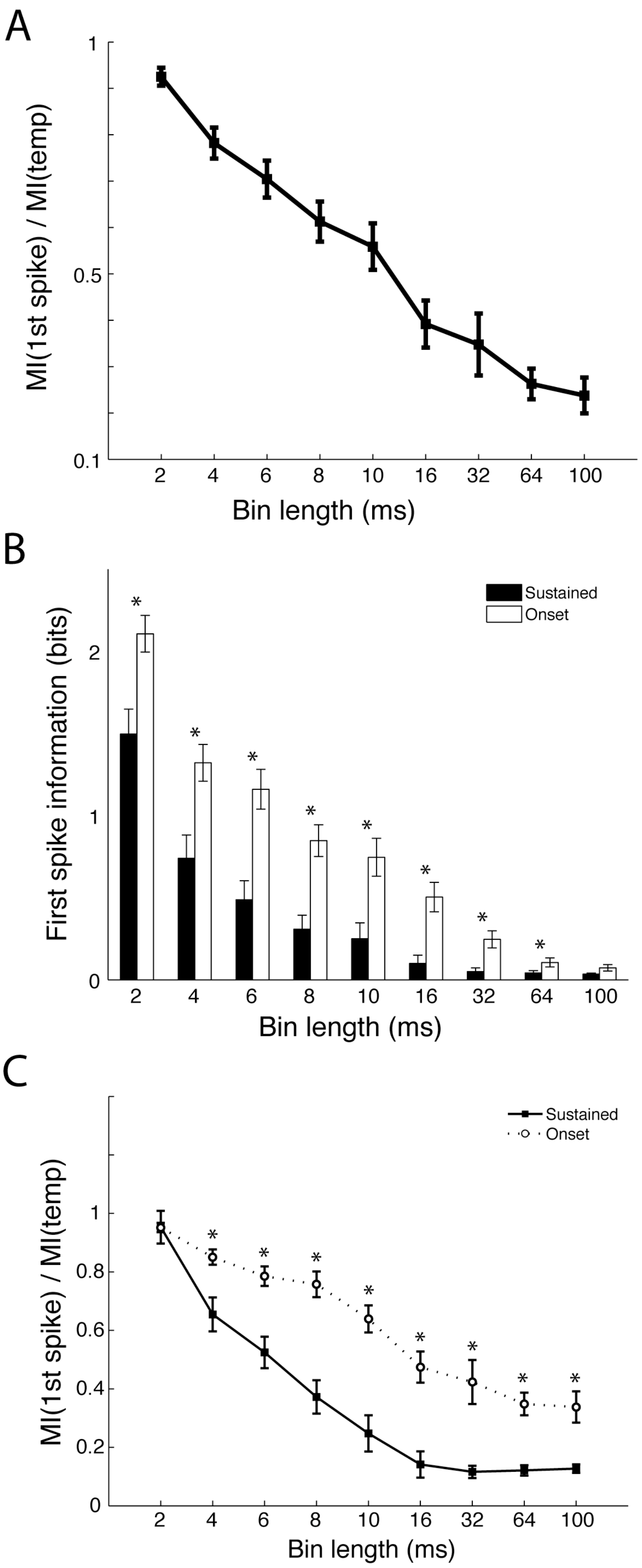
A
MI(1st spike) / MI(temp)
1
0.5
0.1
2
4
6
8
10
16
32
64
100
Bin length (ms)
B
First spike information (bits)
■ Sustained
□ Onset
*
2
1
0
2
4
6
8
10
16
32
64
100
Bin length (ms)
C
MI(1st spike) / MI(temp)
■ Sustained
○ Onset
*
1
0.8
0.6
0.4
0.2
0
2
4
6
8
10
16
32
64
100
Bin length (ms)

Figure 10.

Comparison of first spike information with temporal and rate information. *A:* Mean of the proportion of temporal information contained in the timing of the first spike in a response for each bin length. Mean proportions were calculated from neurons with significant first spike and temporal information. Error bars represent S.E.M. *B:* Mean first spike information for sustained and onset neurons for each bin length. *C:* Mean proportion of temporal information carried by the first spike for sustained and onset neurons. Error bars represent S.E.M.

The first-spike timing information may differ between Onset and Sustained populations. For Onset neurons, the first spike of the response often constitutes the entire response. The response latency shifts systematically depending on the sweep speed while the shape of the response itself does not change. In contrast, in Sustained neurons, other parameters of the response, such as the length, vary along with the latency. Thus, the temporal information in Sustained neurons likely comes from a combination of first-spike latency and the presence (or absence) of spikes later in the response. Figure 10B demonstrates that neurons with onset responses had greater first-spike timing information than neurons with Sustained responses for bin lengths less than 100 ms (Wilcoxon rank-sum test, $p < 0.05$). Furthermore, the proportion of information carried by the timing of the first spike was greater for Onset neurons for bin lengths greater than 2 ms (Fig 10C, Wilcoxon rank-sum test, $p < 0.05$). As expected, the first spike timing of neurons with onset responses accounts for more of the total temporal information available for stimulus identification. However, as the temporal precision increased, the first spike timing of sustained neurons becomes relatively more informative as well.

Neurons with sustained and onset tone responses encode frequency sweeps differently

A previous study demonstrated that neurons with sustained tone responses also have sustained frequency sweep responses (Thesis Chapter 1). Conversely, neurons with onset tone responses usually have onset sweep responses. Because of this relation, neurons with onset and sustained tone responses likely also encode sweeps differently. To compare pure tone and sweep responses, we used the same tone response ratio (TRR) that was used in the previous study (see Methods). Neurons with tone response ratios greater than 0.9 were classified as Sustained tone responses while neurons with TRR's less than 0.5 were classified as Onset tone responses. We then quantified the encoding of frequency sweep using a mutual information index (MII, see Methods). This index ranged from –1 for neurons with only rate information to +1 for neurons with only temporal information. Figure 11 shows the percentage of MII values for neurons with sustained tone responses and onset tone responses (upper half and lower half of figure, respectively) for each bin length. Both tone response types were dominated by neurons with greater temporal information because of the small overall proportion of neurons with significant rate information. For each bin length, the percentage of the population of neurons with pure temporal information (MII = 1) was greater for the onset tone response group than for the sustained tone response group (paired t-test, $p < 0.05$). Conversely, neurons with sustained tone responses had a higher percentage of pure rate information than the onset tone response group (paired t-test, $p < 0.05$). Consequently, the pure tone temporal response pattern does determine the encoding of frequency sweeps.

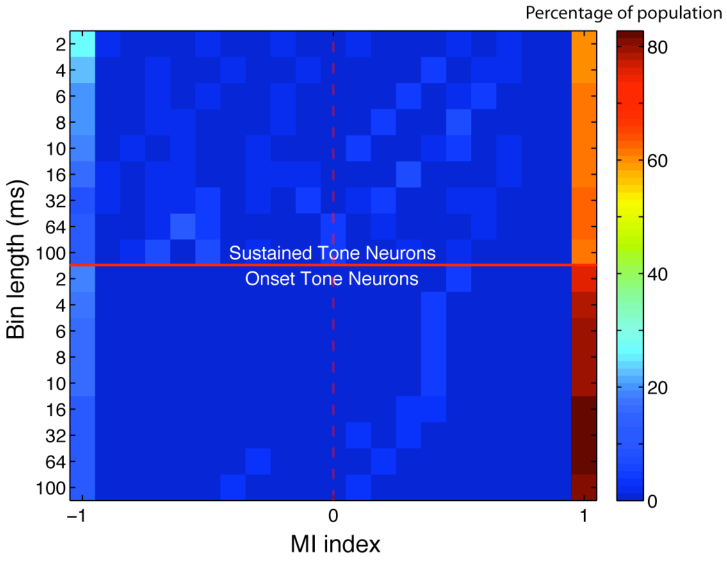

Figure 11.

Comparison of tone response class and frequency sweep encoding. Colorplot of the histograms of the *Mutual Information Index* (MII) for neurons with sustained and onset tone responses. Neurons with positive MII values had more temporal information than rate information. Neurons with negative MII values had greater rate information than temporal information.

Discussion:

Spike rate and spike timing of AI neurons encode frequency sweeps

Our results demonstrate that the parameters of frequency sweeps are encoded by a combination of the timing of spikes and number of spikes in responses of AI neurons. In particular, the amount of rate and temporal information is weighted differently in individual neurons depending on the response dynamics of the neuron. For some neurons, sweeps elicit a sustained response and substantial stimulus information is encoded in the firing rate over a long time window while the timing of spikes is not informative. For other neurons the distribution of spike times during the stimulus is highly informative whereas the spike count is not. Between these extremes, the responses of neurons lie on a continuum, having both rate and temporal information with inversely related amounts of each.

Studies in a number of sensory systems have demonstrated the importance of the timing and number of action potentials in a response for stimulus encoding (S. Furukawa et al., 2000; T. Lu et al., 2001b; S. Panzeri et al., 2001; S. Furukawa and J. C. Middlebrooks, 2002; I. Nelken et al., 2005). In the auditory cortex, the timing of spikes and the spike count carry information about sound source location (S. Furukawa and J. C. Middlebrooks, 2002; B. J. Mickey and J. C. Middlebrooks, 2003). For the encoding of complex sounds, Nelken et al. (2005) demonstrated that a combination of spike count and the mean response latency of AI neurons accounted for the majority of information available from neural responses in AI of the anesthetized cat and ferret. However, because most neurons in anesthetized animals have transient responses (generally <4 spikes/response for Nelken et al. (2005)) the amount of rate information may be more prevalent in awake animals where neurons often have more sustained responses. While both spike count and spike timing contain information in our dataset, these two codes are not equally weighted across the neuronal population with an inverse relation between temporal and rate information.

Our results most closely resemble those of Lu et al. (1999) who demonstrated that the encoding of the repetition rate of click trains in AI of the awake marmoset is divided into stimulus synchronized and non-synchronized populations. These two populations encoded different ranges of temporal modulation rates. In a related study, Lu and Wang (2004) measured the mutual information available from spike counts and inter-spike interval distributions in AI responses to the same click stimuli. They demonstrated that the spike counts of non-synchronized neurons have significant mutual information while the inter-spike interval distributions do not. They concluded that non-synchronized neurons encode click trains using a rate code. Our results are also consistent with the existence of a population of neurons with high rate/low temporal information similar to the non-synchronizing population in those studies. Additionally, Lu and Wang showed that both inter-spike intervals and spike counts of synchronized neurons encoded click rate. Thus, in both theirs and our study, there is a second population of AI neurons with temporally precise responses. Both temporally modulated sounds and frequency modulated sweeps may be encoded in parallel by the firing rate and temporally pattern of spikes in different populations of neurons in AI.

There are, however, several important differences between results from Lu et al. (1999, 2005) and this study. First, measuring the mutual information from the ISI distribution assumes that the relevant temporal information comes either from a response synchronized to the stimulus period or that particular spike intervals will occur for different click repetition rates. While such a code may work for repetitive stimuli, it may not be useful for neuron with brief onset responses to non-repetitive frequency sweeps. For example, in our dataset, many neurons with onset responses had the same number of spikes per stimulus but the latency depended on the sweep parameters. Such responses will not differ in their ISI distributions and would thus carry no mutual information calculated in this manner. Our PSTH analysis makes no assumptions about synchronization to stimuli. Rather, it assumes that the distribution of spike times (reflected in the shape of the PSTH) is relevant to the downstream decoder. A second important difference is that, in the study by Lu and Wang (2004), there was no significant trade-off between temporal and rate information whereas there was a clear inverse correlation in our study. This difference could be due to the fact that the spike count of synchronized neurons may also co-vary with repetition rate (or number of events) and so for the stimuli used in Lu and Wang (2005), synchronized neurons had significant spike count information as well as information computed from ISI distributions.

First spike timing carries most of the temporal information in AI

First spike timing has been shown to be informative in a number of sensory systems including the somatosensory, visual, and auditory systems (P. Heil, 1997; R. Van Rullen et al., 1998; J. F. Brugge et al., 2001; S. Panzeri et al., 2001; S. Thorpe et al., 2001; S. Furukawa and J. C. Middlebrooks, 2002; B. J. Mickey and J. C. Middlebrooks, 2003; R. S. Johansson and I. Birznieks, 2004; T. Gollisch and M. Meister, 2008). With the exception of Mickey and Middlebrooks (2003), most studies that examined the role of fist spike timing for stimulus encoding in the auditory cortex were performed in anesthetized animals. In the un-anesthetized cat, Mickey and Middlebrooks demonstrated that the latency to the first spike carried less information about sound source location than spike count. Overall, however, first spike timing was highly informative about stimulus location in that study. Our results from un-anesthetized squirrel monkeys demonstrate that the timing of the first spike contains most of the information present in the temporal pattern of the response to frequency sweeps and are thus consistent with the notion that first spike timing is highly informative. In contrast to Mickey and Middlebrooks, first spike latency contained more information on average than spike counts. This difference in results could be due to species or stimulus differences, or the manner in which mutual information was computed.

In our study the information contained in the first spike timing depended upon whether or not the neuron had a sustained or an onset response; first spike timing was more informative in neurons with onset responses than in neurons with more sustained responses. For the majority of bin lengths, the proportion of information that could be accounted for by the first spike timing was greater in onset neurons than in sustained neurons. These data suggest that a population of neurons encodes spectrotemporally complex stimuli with highly precise onset responses. Such precise responses have been reported in the auditory cortex of anesthetized and awake animals (P. Heil, 1997; P. Heil and D. R. Irvine, 1997; M. R. DeWeese et al., 2003; M. Elhilali et al., 2004). Our results emphasize the importance of these responses for encoding frequency sweeps in the awake primate.

Relation to previous studies of FM encoding in AI

Studies in a number of species have examined the responses of AI neurons to frequency sweeps. In anesthetized animals, neurons have been shown to be direction selective and some studies have demonstrated a relation between the pure tone best frequency (BF) of the neuron and the preference for up or down modulation such that neurons with lower BFs prefer up sweeps while neurons with higher BFs prefer down sweeps (D. P. Phillips and M. S. Cynader, 1985; P. Heil et al., 1992b; P. Heil et al., 1992a; S. A. Shamma et al., 1993; B. Tian and J. P. Rauschecker, 1994; I. Nelken and H. Versnel, 2000; P. W. Poon and P. P. Yu, 2000; L. I. Zhang et al., 2003; B. Godey et al., 2005). In addition, many of these studies have demonstrated that AI neurons are sensitive to the rate of change of frequency, or sweep speed.

Fewer studies have examined the frequency sweep responses of AI neurons in un-anesthetized. In the awake state, AI neurons show similar ranges of direction selectivity and speed tuning as in the anesthetized preparation (I. C. Whitfield and E. F. Evans, 1965; C. A. Atencio et al., 2007).

The relation between the selectivity of neurons in AI for frequency sweep parameters and the ability of animals to detect and discriminate between these parameters is unclear (though see Klump (1991)). In the studies of FM responses discussed above, both direction selectivity and speed tuning were calculated from the average spike count of AI neurons. These analyses assume that average firing rate is the response parameter that is read out by downstream areas. In the visual and somatosensory systems, thresholds calculated from the spike counts of single neurons often match behavioral thresholds and covary with decisions during a task suggesting that spike count may be the relevant response parameter from single neurons for downstream decision areas (A. J. Parker and W. T. Newsome, 1998; R. Romo and E. Salinas, 2003). However, several recent studies in the auditory system have shown that temporal pattern of neural responses may convey behaviorally relevant information (J. W. Schnupp et al., 2006; R. Narayan et al., 2007). It is thus necessary to analyze the temporal modulations of firing rate in the responses of AI neurons to frequency sweeps in addition to cumulative spike count. Such an analysis was the focus of this study.

Relation between tone response and sweep coding

Our results indicate that neurons that respond continuously to static also more frequently encode dynamic sweeps purely with firing rate. In AI of awake primates, neurons respond to unmodulated pure tones with onset, sustained, or onset-sustained responses (Thesis Chapter 2) (G. H. Recanzone, 2000). A relationship between the temporal characteristics of sweep responses and static tone responses has also been shown in the awake cat and gerbil (I. C. Whitfield and E. F. Evans, 1965; H. Schulze et al., 1997). In agreement with our data, neurons with sustained or tonic tone discharges also had sustained discharges for frequency sweeps. In Schulze et al. (1997) tonic and phasic response types were segregated among cortical fields: AI and the anterior auditory field (AAF) contained neurons with phasic responses to FM and pure tones while the ventral and dorsal posterior fields (VP and DP, respectively) contained neurons with tonic responses. All of our recordings were from neurons in AI where we found both tonic and phasic (onset) responses to tones and sweeps. Comparisons between FM responses in different fields and among the different layers of auditory cortex of the awake squirrel monkey are the subject of ongoing investigations in our laboratory.

The different FM response types and codes seen in all of these studies raise the question of whether these response types are actually different neuronal types. That neurons have similar static and dynamic tone response properties suggests that there may be different neuronal types. Differences in response dynamics could be conferred by differences in adaptation properties of synaptic inputs or by difference in feedforward inhibition (M. Atzori et al., 2001). However, many neurons with sustained tone responses had purely temporal information. Furthermore, because our stimulus set was limited to two classes (tones and sweep) we cannot say for certain whether some stimuli would elicit a change in the encoding regime. Furthermore, some neurons in our study had intermediate response properties and had both significant rate and temporal codes, suggesting that there is a continuum of response types in AI. Undoubtedly, a very brief stimulus will only evoke brief onset responses for all neurons simply due to its length. Thus, classifying response types in such cases is not useful. The relevant question is whether or not a neuron will change from having temporal information to having only rate information or vice versa.

References:

Arabzadeh E, Panzeri S, Diamond ME (2004) Whisker vibration information carried by rat barrel cortex neurons. J Neurosci 24:6011-6020.

Arabzadeh E, Panzeri S, Diamond ME (2006) Deciphering the spike train of a sensory neuron: counts and temporal patterns in the rat whisker pathway. J Neurosci 26:9216-9226.

Atencio CA, Blake DT, Strata F, Cheung SW, Merzenich MM, Schreiner CE (2007) Frequency-modulation encoding in the primary auditory cortex of the awake owl monkey. J Neurophysiol 98:2182-2195.

Atzori M, Lei S, Evans DI, Kanold PO, Phillips-Tansey E, McIntyre O, McBain CJ (2001) Differential synaptic processing separates stationary from transient inputs to the auditory cortex. Nat Neurosci 4:1230-1237.

Bendor D, Wang X (2007) Differential neural coding of acoustic flutter within primate auditory cortex. Nat Neurosci 10:763-771.

Brugge JF, Reale RA, Jenison RL, Schnupp J (2001) Auditory cortical spatial receptive fields. Audiol Neurootol 6:173-177.

Cheung SW, Bedenbaugh PH, Nagarajan SS, Schreiner CE (2001) Functional organization of squirrel monkey primary auditory cortex: responses to pure tones. J Neurophysiol 85:1732-1749.

Cover TM, Thomas JA (2006) Elements of information theory, 2nd Edition. Hoboken, N.J.: Wiley-Interscience.

deCharms RC, Merzenich MM (1996) Primary cortical representation of sounds by the coordination of action-potential timing. Nature 381:610-613.

DeWeese MR, Meister M (1999) How to measure the information gained from one symbol. Network 10:325-340.

DeWeese MR, Wehr M, Zador AM (2003) Binary spiking in auditory cortex. J Neurosci 23:7940-7949.

Eggermont JJ (1997) Firing rate and firing synchrony distinguish dynamic from steady state sound. Neuroreport 8:2709-2713.

Elhilali M, Fritz JB, Klein DJ, Simon JZ, Shamma SA (2004) Dynamics of precise spike timing in primary auditory cortex. J Neurosci 24:1159-1172.

Furukawa S, Middlebrooks JC (2002) Cortical representation of auditory space: information-bearing features of spike patterns. J Neurophysiol 87:1749-1762.

Furukawa S, Xu L, Middlebrooks JC (2000) Coding of sound-source location by ensembles of cortical neurons. J Neurosci 20:1216-1228.

Godey B, Atencio CA, Bonham BH, Schreiner CE, Cheung SW (2005) Functional organization of squirrel monkey primary auditory cortex: responses to frequency-modulation sweeps. J Neurophysiol 94:1299-1311.

Gollisch T, Meister M (2008) Rapid neural coding in the retina with relative spike latencies. Science 319:1108-1111.

Heil P (1997) Auditory cortical onset responses revisited. II. Response strength. J Neurophysiol 77:2642-2660.

Heil P (2004) First-spike latency of auditory neurons revisited. Curr Opin Neurobiol 14:461-467.

Heil P, Irvine DR (1997) First-spike timing of auditory-nerve fibers and comparison with auditory cortex. J Neurophysiol 78:2438-2454.

Heil P, Rajan R, Irvine DR (1992a) Sensitivity of neurons in cat primary auditory cortex to tones and frequency-modulated stimuli. I: Effects of variation of stimulus parameters. Hear Res 63:108-134.

Heil P, Langner G, Scheich H (1992b) Processing of frequency-modulated stimuli in the chick auditory cortex analogue: evidence for topographic representations and possible mechanisms of rate and directional sensitivity. J Comp Physiol [A] 171:583-600.

Johansson RS, Birznieks I (2004) First spikes in ensembles of human tactile afferents code complex spatial fingertip events. Nat Neurosci 7:170-177.

Lewicki MS (1994) Bayesian modeling and classification of neural signals. Neural Comput 6:1005-1030.

Liberman AM, Cooper FS, Shankweiler DP, Studdert-Kennedy M (1967) Perception of the speech code. Psychol Rev 74:431-461.

Lu T, Wang X (2000) Temporal discharge patterns evoked by rapid sequences of wide- and narrowband clicks in the primary auditory cortex of cat. J Neurophysiol 84:236-246.

Lu T, Wang X (2004) Information content of auditory cortical responses to time-varying acoustic stimuli. J Neurophysiol 91:301-313.

Lu T, Liang L, Wang X (2001a) Neural representations of temporally asymmetric stimuli in the auditory cortex of awake primates. J Neurophysiol 85:2364-2380.

Lu T, Liang L, Wang X (2001b) Temporal and rate representations of time-varying signals in the auditory cortex of awake primates. Nat Neurosci 4:1131-1138.

Malone BJ, Scott BH, Semple MN (2007) Dynamic amplitude coding in the auditory cortex of awake rhesus macaques. J Neurophysiol 98:1451-1474.

Mendelson JR, Cynader MS (1985) Sensitivity of cat primary auditory cortex (AI) neurons to the direction and rate of frequency modulation. Brain Res 327:331-335.

Mendelson JR, Grasse KL (1992) A comparison of monaural and binaural responses to frequency modulated (FM) sweeps in cat primary auditory cortex. Exp Brain Res 91:435-454.

Mendelson JR, Schreiner CE, Sutter ML, Grasse KL (1993) Functional topography of cat primary auditory cortex: responses to frequency-modulated sweeps. Exp Brain Res 94:65-87.

Mickey BJ, Middlebrooks JC (2003) Representation of auditory space by cortical neurons in awake cats. J Neurosci 23:8649-8663.

Narayan R, Best V, Ozmeral E, McClaine E, Dent M, Shinn-Cunningham B, Sen K (2007) Cortical interference effects in the cocktail party problem. Nat Neurosci.

Nelken I, Versnel H (2000) Responses to linear and logarithmic frequency-modulated sweeps in ferret primary auditory cortex. Eur J Neurosci 12:549-562.

Nelken I, Chechik G (2007) Information theory in auditory research. Hear Res 229:94-105.

Nelken I, Chechik G, Mrsic-Flogel TD, King AJ, Schnupp JW (2005) Encoding stimulus information by spike numbers and mean response time in primary auditory cortex. J Comput Neurosci 19:199-221.

Newman JD (1978) Perception of sounds used in species-specific communication: the auditory cortex and beyond. J Med Primatol 7:98-105.

Optican LM, Richmond BJ (1987) Temporal encoding of two-dimensional patterns by single units in primate inferior temporal cortex. III. Information theoretic analysis. J Neurophysiol 57:162-178.

Panzeri S, Schultz SR (2001) A unified approach to the study of temporal, correlational, and rate coding. Neural Comput 13:1311-1349.

Panzeri S, Petersen RS, Schultz SR, Lebedev M, Diamond ME (2001) The role of spike timing in the coding of stimulus location in rat somatosensory cortex. Neuron 29:769-777.

Parker AJ, Newsome WT (1998) Sense and the single neuron: probing the physiology of perception. Annu Rev Neurosci 21:227-277.

Phillips DP, Cynader MS (1985) Some neural mechanisms in the cat's auditory cortex underlying sensitivity to combined tone and wide-spectrum noise stimuli. Hear Res 18:87-102.

Phillips DP, Mendelson JR, Cynader MS, Douglas RM (1985) Responses of single neurones in cat auditory cortex to time-varying stimuli: frequency-modulated tones of narrow excursion. Exp Brain Res 58:443-454.

Poeppel D (2003) The analysis of speech in different temporal integration windows: cerebral lateralization as 'asymmetric sampling in time'. Speech Communication 41:245-255.

Poon PW, Yu PP (2000) Spectro-temporal receptive fields of midbrain auditory neurons in the rat obtained with frequency modulated stimulation. Neurosci Lett 289:9-12.

Rauschecker JP, Tian B, Hauser M (1995) Processing of complex sounds in the macaque nonprimary auditory cortex. Science 268:111-114.

Recanzone GH (2000) Response profiles of auditory cortical neurons to tones and noise in behaving macaque monkeys. Hear Res 150:104-118.

Richmond BJ, Optican LM (1990) Temporal encoding of two-dimensional patterns by single units in primate primary visual cortex. II. Information transmission. J Neurophysiol 64:370-380.

Riede T, Zuberbuhler K (2003) The relationship between acoustic structure and semantic information in Diana monkey alarm vocalization. J Acoust Soc Am 114:1132-1142.

Rieke F, Warland D, Ruyter van Stevenick R, Bialek W (1997) Spikes: exploring the neural code. Cambridge, MA.

Romo R, Salinas E (2003) Flutter discrimination: neural codes, perception, memory and decision making. Nat Rev Neurosci 4:203-218.

Rosen S (1992) Temporal information in speech: acoustic, auditory and linguistic aspects. Philos Trans R Soc Lond B Biol Sci 336:367-373.

Schnupp JW, Hall TM, Kokelaar RF, Ahmed B (2006) Plasticity of temporal pattern codes for vocalization stimuli in primary auditory cortex. J Neurosci 26:4785-4795.

Schulze H, Ohl FW, Heil P, Scheich H (1997) Field-specific responses in the auditory cortex of the unanaesthetized Mongolian gerbil to tones and slow frequency modulations. J Comp Physiol [A] 181:573-589.

Shamma SA, Fleshman JW, Wiser PR, Versnel H (1993) Organization of response areas in ferret primary auditory cortex. J Neurophysiol 69:367-383.

Shannon C (1948) A mathematical theory of communication. Bell Syst Tech J 27:379-423.

Strong SP, Koberle R, de Ruyter van Stevenick RR, Bialek W (1998) Entropy and information in neural spike trains. Phys Rev Lett 80:197-200.

Suga N (1989) Principles of auditory information-processing derived from neuroethology. J Exp Biol 146:277-286.

Thomson EE, Kristan WB (2005) Quantifying stimulus discriminability: a comparison of information theory and ideal observer analysis. Neural Comput 17:741-778.

Thorpe S, Delorme A, Van Rullen R (2001) Spike-based strategies for rapid processing. Neural Netw 14:715-725.

Tian B, Rauschecker JP (1994) Processing of frequency-modulated sounds in the cat's anterior auditory field. J Neurophysiol 71:1959-1975.

Tian B, Rauschecker JP (1998) Processing of frequency-modulated sounds in the cat's posterior auditory field. J Neurophysiol 79:2629-2642.

Tian B, Rauschecker JP (2004) Processing of frequency-modulated sounds in the lateral auditory belt cortex of the rhesus monkey. J Neurophysiol 92:2993-3013.

Van Rullen R, Gautrais J, Delorme A, Thorpe S (1998) Face processing using one spike per neurone. Biosystems 48:229-239.

Volkov IO, Galaziuk AV (1985) [Reactions of neurons of the auditory cortex of unanesthetized cats to tones of a characteristic frequency]. Neirofiziologiia 17:500-508.

Wang X (2007) Neural coding strategies in auditory cortex. Hear Res 229:81-93.

Wang X, Lu T, Snider RK, Liang L (2005) Sustained firing in auditory cortex evoked by preferred stimuli. Nature 435:341-346.

Whitfield IC, Evans EF (1965) Responses of Auditory Cortical Neurons to Stimuli of Changing Frequency. J Neurophysiol 28:655-672.

Winter P, Ploog D, Latta J (1966) Vocal repertoire of the squirrel monkey (Saimiri sciureus), its analysis and significance. Exp Brain Res 1:359-384.

Zhang LI, Tan AY, Schreiner CE, Merzenich MM (2003) Topography and synaptic shaping of direction selectivity in primary auditory cortex. Nature 424:201-205.

Table 1

Bin Length	*p-value*	*F*	(* indicates *p* < 0.05, Tukey's honest sig. difference test)														
100	< 0.001	51.48	Velocity	5	10	20	35	60	85	110	-5	-10	-20	-35	-60	-85	-110
			5			*	*	*	*	*		*	*	*	*	*	*
			10				*	*	*	*			*	*	*	*	*
			20					*	*	*			*	*	*	*	*
			35						*	*						*	
			-5			*	*	*	*	*		*	*	*	*	*	*
			-10				*	*	*	*			*	*	*	*	*
64	< 0.001	38.81		5	10	20	35	60	85	110	-5	-10	-20	-35	-60	-85	-110
			5			*	*	*	*	*		*	*	*	*	*	*
			10			*	*	*	*	*			*	*	*	*	*
			20					*	*	*				*	*	*	*
			-5			*	*	*	*	*		*	*	*	*	*	*
			-10				*	*	*	*			*	*	*	*	*
			-20							*						*	*
32	< 0.001	26.06		5	10	20	35	60	85	110	-5	-10	-20	-35	-60	-85	-110
			5			*	*	*	*	*			*	*	*	*	*
			10				*	*	*	*			*	*	*	*	*
			20						*	*				*	*	*	*
			-5			*	*	*	*	*			*	*	*	*	*
			-10				*	*	*	*				*	*	*	*
			-20							*						*	
16	< 0.001	13.01		5	10	20	35	60	85	110	-5	-10	-20	-35	-60	-85	-110
			5				*	*	*	*			*	*	*	*	*
			10				*	*	*	*				*	*	*	*
			20											*	*	*	*
			-5				*	*	*	*			*	*	*	*	*
			-10						*	*				*	*	*	*
10	< 0.001	7.03		5	10	20	35	60	85	110	-5	-10	-20	-35	-60	-85	-110
			10							*				*	*	*	*
			20							*						*	
			-5						*	*				*	*	*	*
			-10							*				*	*	*	*
8	< 0.001	4.81		5	10	20	35	60	85	110	-5	-10	-20	-35	-60	-85	-110
			5						*	*				*	*	*	*
			10							*					*	*	*
			-5							*					*	*	*
			-10													*	
6	< 0.001	2.91		5	10	20	35	60	85	110	-5	-10	-20	-35	-60	-85	-110
			5													*	
4	0.3858	1.06															
2	0.9574	0.44															

Chapter 4

Background Noise Can Improve Stimulus Representations in Auditory Cortex

Abstract:

Most sounds must be detected and identified in the context of background noise. Traditionally, noise is thought to degrade the cortical representation of sounds by suppressing responses and increasing response variability. However, recent studies of neural network models and brain slices have shown that background synaptic noise can improve the detection of signals through stochastic resonance. Because acoustic noise affects the synaptic background activity of cortical networks, it may actually improve the cortical responses to signals. We determined the functional effects of white noise on the responses of neurons in primary auditory cortex (AI) to a class of sounds called frequency modulated sweeps. While the addition of noise suppressed the responses of some AI neurons, the stimulus representation was enhanced at specific signal-to-noise ratios (SNRs) in many neurons. These enhancements included stronger stimulus responses, increased selectivity, and greater temporal precision. This tuning of neurons to SNR produced a robust population representation that maintained discrimination between acoustic contexts and was not linearly related to SNR as expected.

Introduction

The central auditory system must process behaviorally relevant sounds in the presence of background noises ranging from broadband sounds, such as water rushing down a river, to highly structured sounds, such as multiple speakers or music. In general, the addition of noise has deleterious effects on the ability of humans and other animals to discriminate between sounds (G. A. Miller, Heise, G. A., and Lichtan, W., 1951; J. D. Miller, 1974; S. H. Hulse et al., 1997; R. Narayan et al., 2007). The brain mechanisms that underlie the affects of noise remain unclear. Patients with lesions in temporal cortex are especially susceptible to the effects of noise on auditory perceptual performance (W. O. Olsen et al., 1975) suggesting that the cortex plays a central role in the processing of sounds in noise. Investigations of single neuron responses in anesthetized primates revealed that background noise produces a marked reduction in synchronization of AI neurons with phrases of primate vocalizations (S. S. Nagarajan et al., 2002). Furthermore, a recent study in the avian homolog of primary auditory cortex (AI) demonstrated that the addition of background sounds degraded neuronal responses to bird songs in a manner that matched decrements in behavioral discrimination performance (R. Narayan et al., 2007).

While high levels of background noise affect hearing, humans and animals effortlessly classify and react appropriately to sounds across conditions. A number of experiments have demonstrated that AI neurons adapt to background noise conditions (D. P. Phillips and M. S. Cynader, 1985; D. P. Phillips et al., 1985; D. P.

Phillips, 1990; G. Ehret and C. E. Schreiner, 2000; S. Sadagopan and X. Wang, 2008). In these studies, the threshold and latency for tone responses increased linearly with the noise masker level, and neuronal rate-level functions shifted towards higher sound levels. The response to noise itself also varied, and no neurons responded continuously to noise. Together, this data showed that cortical neurons shift their operating characteristics to match the background context in which signals occur.

In addition to these adaptive changes, more recent studies suggest that external noise may actually enhance stimulus representations in cortex by altering basal network activity. Theoretical and brain slice experiments in single neurons and networks in which noise was added to simulate different levels of synaptic background activity have demonstrated that the basal level of synaptic activity modulates the responsiveness of neurons (N. Ho and A. Destexhe, 2000; F. S. Chance et al., 2002; J. Wolfart et al., 2005; A. Destexhe and D. Contreras, 2006). These studies have demonstrated an increased responsiveness to stimuli during noisy states compared with quiescent states. The increased responsiveness in the presence of noise may be related to *stochastic resonance*, a phenomenon in which non-linear systems carry increased signal information in the presence of noise (K. Wiesenfeld and F. Moss, 1995; F. Moss et al., 2004). Because background acoustic noise likely alters background synaptic activity, it may actually improve cortical responses to signals. These improvements could be crucial for the establishment cortical representations of sounds that are tolerate changes in background noise conditions.

To determine the effects of external noise on cortical sound processing, we quantified the representation of a class of dynamic sounds, called frequency modulated (FM) sweeps, in the presence of different levels of acoustic white noise in single neurons in AI of awake squirrel monkeys. We demonstrate that AI neurons are tuned to the background context in which signals are presented. Many neurons are more responsive and carry more information about signals in the presence of specific levels of background noise. The preference of neurons for different signal-to-noise ratios produces a population representation that tolerates changes in background acoustic conditions. Because speech signals commonly occur in background noise, the data presented here have significant implications for understanding the cortical mechanisms of speech processing in normal acoustic environments.

Methods

All procedures related to the maintenance and use of animals in this study were approved by the Institutional Animal Care and Use Committee at the University of California, San Francisco, and were consistent with national and state animal welfare guidelines.

Animal Preparation

The preparation for awake recording procedures was described in Chapter 2.

Electrophysiology

Electrophysiological methods were described in Chapter 2.

Acoustic Stimulation

All sounds were presented using a Sony SS-MB150H free field speaker positioned 50cm in front of the animal. The sound delivery system was calibrated using a sound-level meter (Model 2209, Brüel & Kjær, Norcross, GA) and SigCal software (Tucker-Davis Technologies, Alachua, FL).

Logarithmic FM sweeps were created in Matlab (The MathWorks, Natick, MA) and delivered via an RP2.1 (Tucker-Davis Technologies, Alachua, FL). FM sweep frequency ranged from 50 to 21,000 Hz in upward and downward directions with rates of frequency change of 5, 10, 20, 35, 60, 85, and 110 octaves/s. For some recording sessions, 5 oct/s was omitted. Because the sweep frequency range was held constant, the length of the stimuli changed as sweep speed was varied. Corresponding sweep lengths were the following: 1743, 871, 436, 249, 145, 103, and 79 ms. Each FM sweep contained a 100 ms constant tone at the start and end frequencies. These constant frequency portions had a 5 ms cosine ramp up and ramp down at the beginning and end of the stimulus. FM sweep stimuli were played at 60 dB sound-pressure level (SPL). Each stimiulus was repeated 20 times in a random order with a minimum of 500 ms inter-trial interval. The FM sweeps were presented in silence and in the presence of continuous white noise at 0, -5, -10, -15, and –20 dB signal-to-noise ratio (SNR) in random order (Fig. 1). These SNRs corresponded to noise levels of 60, 65, 70, 75 and 80 dB SPL. For several recording sessions, -25 and –30 dB SNRs were also used.

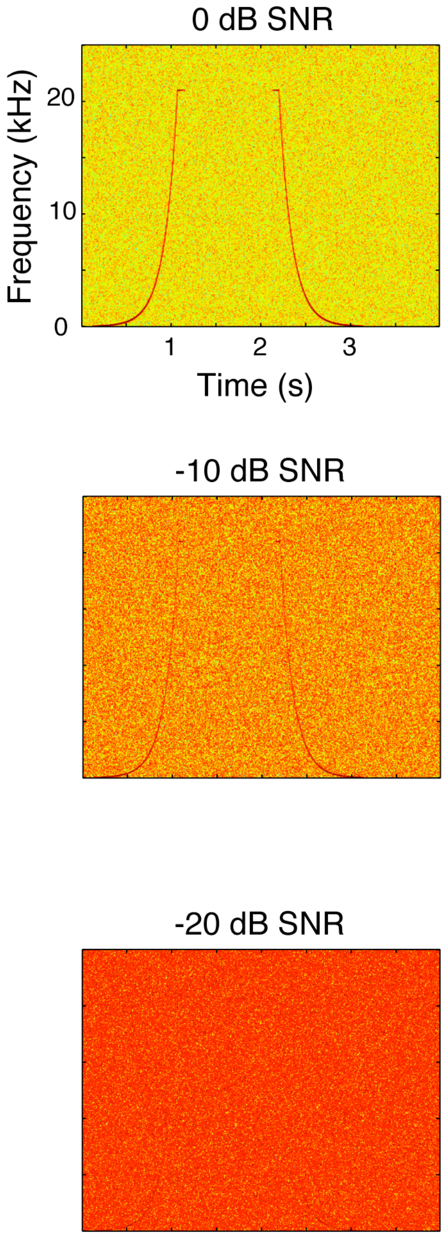

Figure 1. Example spectrograms of FM sweep stimuli presented in white noise. Two FM sweeps with 30 oct/s with upward and downward directions are shown with signal-to-noise ratios of 0, -10, and –20 dB.

To determine the frequency response areas (FRA) of AI neurons, tone bursts of varying frequency and intensity were generated using SigGen software (Tucker-Davis Technologies, Alachua, FL) and played in random order. Tone frequencies ranged from 1-4 octaves (semitone or tone spacing) centered on the estimated center frequency of the neuron under study. Tone had 5 ms on- and off- cosine-squared ramps.

Data Analysis

Response to noise

The response to noise alone was quantified by determining the firing rate during the 100 ms silent period before the presentation of every repetition each sweep stimulus resulting in a total of 280 repetitions for each noise level. For each neuron, the mean, median, and standard error of the firing rate were determined.

Response to sweeps

The response to FM sweeps was determined by finding the times during which the firing rate was 2 standard deviations above the background firing rate and with at least 5 spikes. The background firing rate (as determined above) was subtracted from the firing rate during the sweep response to determine the driven rate. The driven rate was used for the analysis of FM sweep responses.

To determine the effects of background noise on the selectivity of neuronal responses, we calculated the selectivity of AI neurons for the speed and direction of FM sweeps. Speed selectivity was quantified using a value called, *Speed Tuning* (ST) defined as $\frac{n}{n-1}\left[1-\frac{\text{mean}(r)}{\max(r)}\right]$, where r is the driven FM sweep response and n is the number of sweep speeds presented that were in the best direction of the neuron (B. Godey et al., 2005; C. A. Atencio et al., 2007). ST values ranged from 0, for neurons that respond equally to all speeds, to 1, for neurons that responded only to a single speed. The selectivity for the direction of frequency sweeps was quantified using the *Direction Selectivity Index* (DSI) defined as $\frac{\sum_{i=1}^{n} r_{up} - \sum_{i=1}^{n} r_{dn}}{\sum_{i=1}^{n} r_{up} + \sum_{i=1}^{n} r_{dn}}$, where r_{up} is the driven response to *upward* sweeps, r_{dn} is the driven response to *downward* sweeps, and n is the number of frequency sweep speeds. DSI values range from −1, for neurons that respond only to down sweeps, to +1, for neurons that responded only to up sweeps.

Information analysis

We used Shannon's mutual information (abbreviated as MI) to quantify how well AI neurons encoded FM sweeps (C. Shannon, 1948; T. M. Cover and J. A. Thomas, 2006). MI is defined as,

$$MI = \sum_s P(s) \sum_r P(r \mid s) \log_2 \left[\frac{P(r \mid s)}{P(r)} \right]$$

where $P(s)$ is the probability of one of the 14 FM sweep stimuli, s, $P(r|s)$ is the probability of a response r given s, and $P(r)$ is the unconditional probability of response r. MI can be interpreted $\log_2$ of the number of stimuli that can be identified using the responses of a neuron (I. Nelken and G. Chechik, 2007).

The MI between the spike counts or spike timing of AI neurons and the FM sweep stimuli was determined in the same manner as in Thesis Chapter 2. Briefly, the cumulative spike count distributions were determined by counting the number of spikes during a widow length corresponding to the length of the longest FM sweep stimulus beginning 5ms after stimulus onset for each repetition of each stimulus. Each different spike count was a possible response, r, and was used to determine the MI between the spike count and FM sweep stimuli. Information from the temporal response pattern was determined from the normalized cumulative peri-stimulus time histograms from each stimulus (2 ms bins). Each normalized PSTH is a distribution of spike times and the information was determined by considering each time bin as a possible response, r. The MI between the spike time distribution and the FM sweep stimuli could then be determined from the normalized PSTH. We used the method of Strong et. al. (1998) to correct for bias due to limited sample sizes. Monte Carlo simulations confirmed that the MI calculated with trials randomized with respect to stimulus identity was significantly lower (5000 simulations, $p < 0.001$) than the information estimated from the empirical distributions.

The MI between the spike count of AI neurons and the background noise level was calculated using the spike count during the 100 ms period before each sweep presentation. This quantified how the firing rate of AI neurons represented the noise level itself.

Measurement of intensity tuning of tone responses

To compare the tuning of neurons for sound intensity with the effects of noise on cortical responses, we calculated a *Monotonicity Index* from the responses to CF tones played at different intensities (0-70 dB, 10 dB steps, 2-5 repetitions). The *Monotonicity Index* was defined as $\textit{Monotonicity Index} = \frac{R(I_{70}) - R(I_{\max})}{R(I_{70}) + R(I_{\max})}$ where $R(I_{70})$ was the response to a CF tone at 70 dB SPL (the highest intensity used) and $R(I_{max})$ was the response at the intensity that evoked the largest response. The Monotonicity Index ranged from 0 for neurons responded best to tones at 70 db SPL to –1 for neurons that did responded at another sound level and had no response at 70 dB SPL.

Results

Cortical Responses to Continuous Noise

While neurons in anesthetized animals do not respond continuously to noise, neurons in AI of awake squirrel monkeys often responded in a sustained steady-state manner. The neurons in Figure 2B, C, and D all responded continuously to noise and had maximal firing rates at different noise intensities (Fig. 2, right column). In contrast, the spontaneous activity of some neurons was inhibited by noise (Fig. 2A). The noise level that evoked maximal background activity for each neuron (best noise level) is shown in Figure 3A. The background firing rate of most neurons was greatest when the noise level was 60 dB, though there were neurons with maximal firing rates at each of the noise levels tested and in silence. Figure 3B shows the mean normalized firing rate of AI neurons as a function of the noise level. The mean firing rate varied significantly across noise conditions (one-way ANOVA, $F(5, 966) = 4.32$, $p < 0.001$) and was significantly greater at 60 dB than at 0 dB (Tukey's honest significant difference, $p < 0.01$). By shifting the level of activity in cortex, noise may alter the state and excitability of neurons in a manner similar to that observed when injecting random currents into brain slices or network models. Furthermore, because neurons are affected at different noise levels, this affect will vary between neurons and cortical regions.

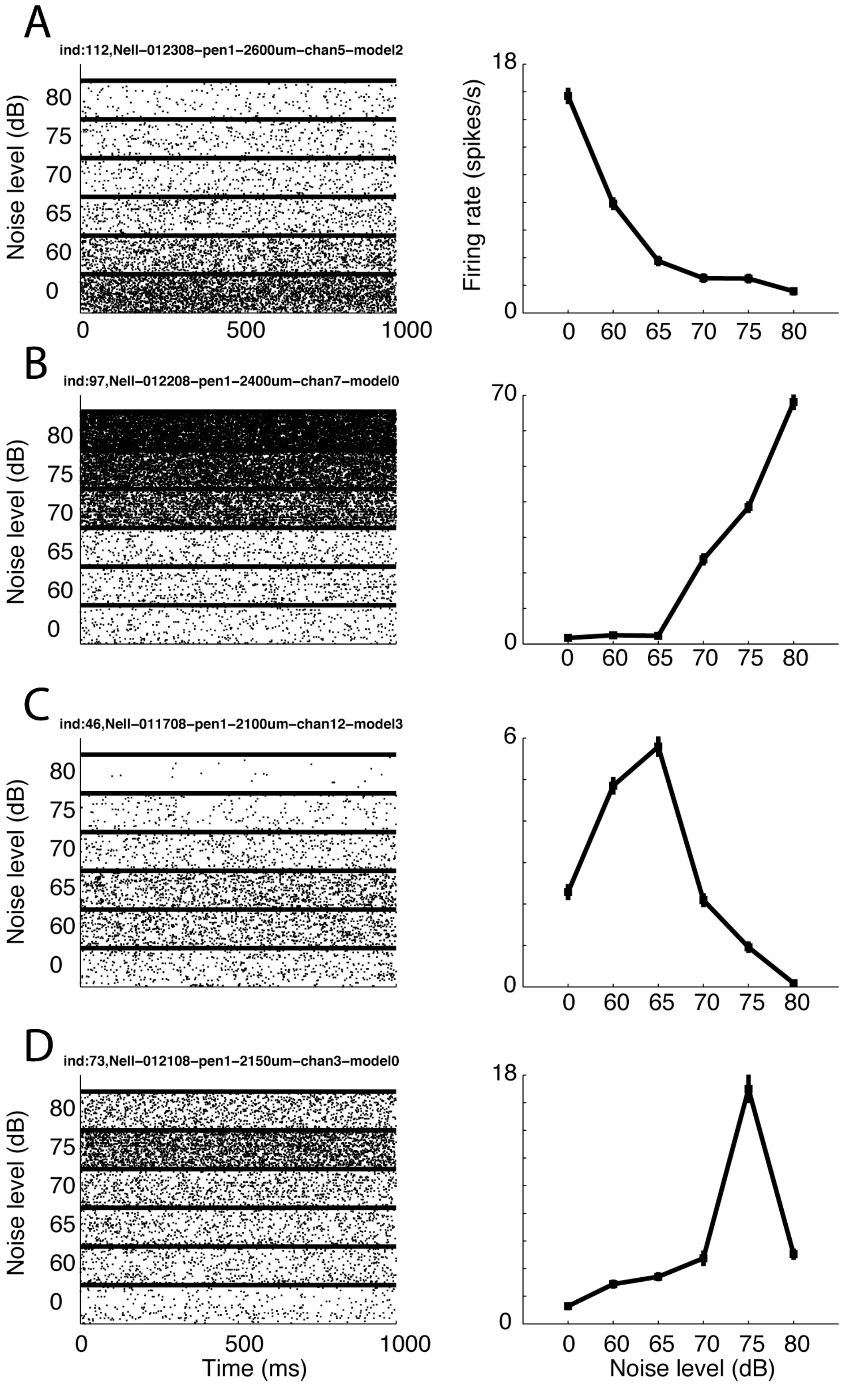
A
ind:112,Nell–012308–pen1–2600um–chan5–model2
B
ind:97,Nell–012208–pen1–2400um–chan7–model0
C
ind:46,Nell–011708–pen1–2100um–chan12–model3
D
ind:73,Nell–012108–pen1–2150um–chan3–model0
Noise level (dB)
80
75
70
65
60
0
Time (ms)
0
500
1000
Firing rate (spikes/s)
18
70
6
0
Noise level (dB)
0
60
65
70
75
80

Figure 2. Responses of AI neurons to continuous white noise A. *Left:* Example AI neuron with spontaneous activity that was inhibited by noise. *Right:* The firing rate of the neuron in the left column is plotted as a function of the level of the continuous white noise stimulus. B, C, D. The format is identical to A. The activity of the neuron in B increased as the noise level increased. The neurons in C and D had non-monotonic firing rate-noise level functions.

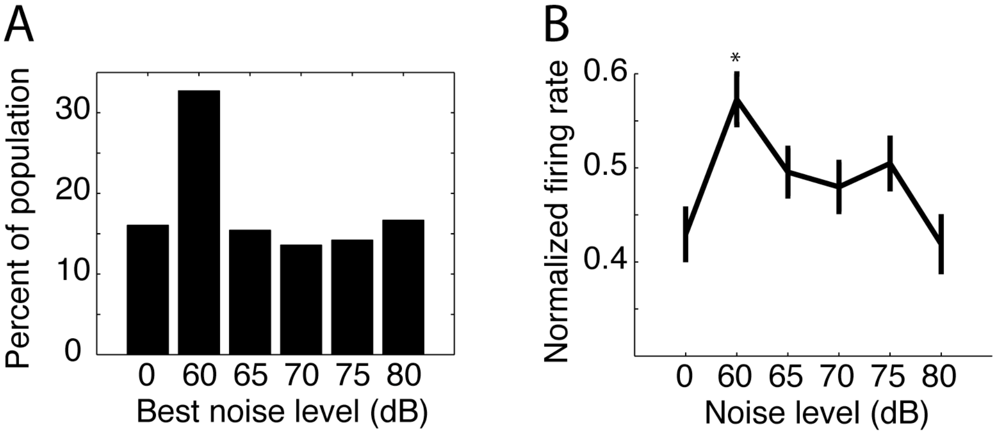

Figure 3. Summary of noise response in AI. A. Histogram of the best noise level for all AI neurons. The best noise level of a neuron was defined as the noise level that evokes the maximum response. B. Mean normalized response to noise for all AI neurons. Error bars represent the standard error of the mean (S.E.M.).

Background noise can enhance cortical responsiveness to signals

To determine the effects of different levels of background noise on cortical responses to signals, we played FM sweeps with varying directions and modulation velocities in silence and in the presence of different levels of background noise. We used FM sweeps because of the prevalence of spectral modulations in communication sounds and because AI neurons in primates are selective for the parameters of these sounds (B. Godey et al., 2005; C. A. Atencio et al., 2007) which enabled us to determine the effects of noise on parameter selectivity.

The addition of noise produced a range of effects on the FM sweep responses of AI neurons. PSTH's of responses to FM sweeps of varying velocity and direction in silence and in the presence of different levels of noise are shown in Figure 4A, D, G and J. Noise suppressed the FM sweep responses of some AI neurons (Fig 4A, **Inf** = infinite SNR, or silent background). Figure 4B plots the response magnitude (with the background firing rate subtracted) of the neuron in Figure 4A for each sweep stimulus and shows that the responses to each sweep stimulus decayed monotonically as the SNR decreased. By contrast, other AI neurons became more responsive to FM sweeps when they were presented in the presence of background noise as exemplified by the neurons in Figure 4A, D, G, and J. The response magnitudes of these neurons were non-monotonic functions of SNR (Fig. 4E, H, and K). In fact, the neuron in Figure 4K only had significant FM responses at −10 dB SNR. These data suggest that the SNR is a critical sound parameter to which AI neurons are tuned, and that AI neurons can actually become more responsive at poor SNRs.

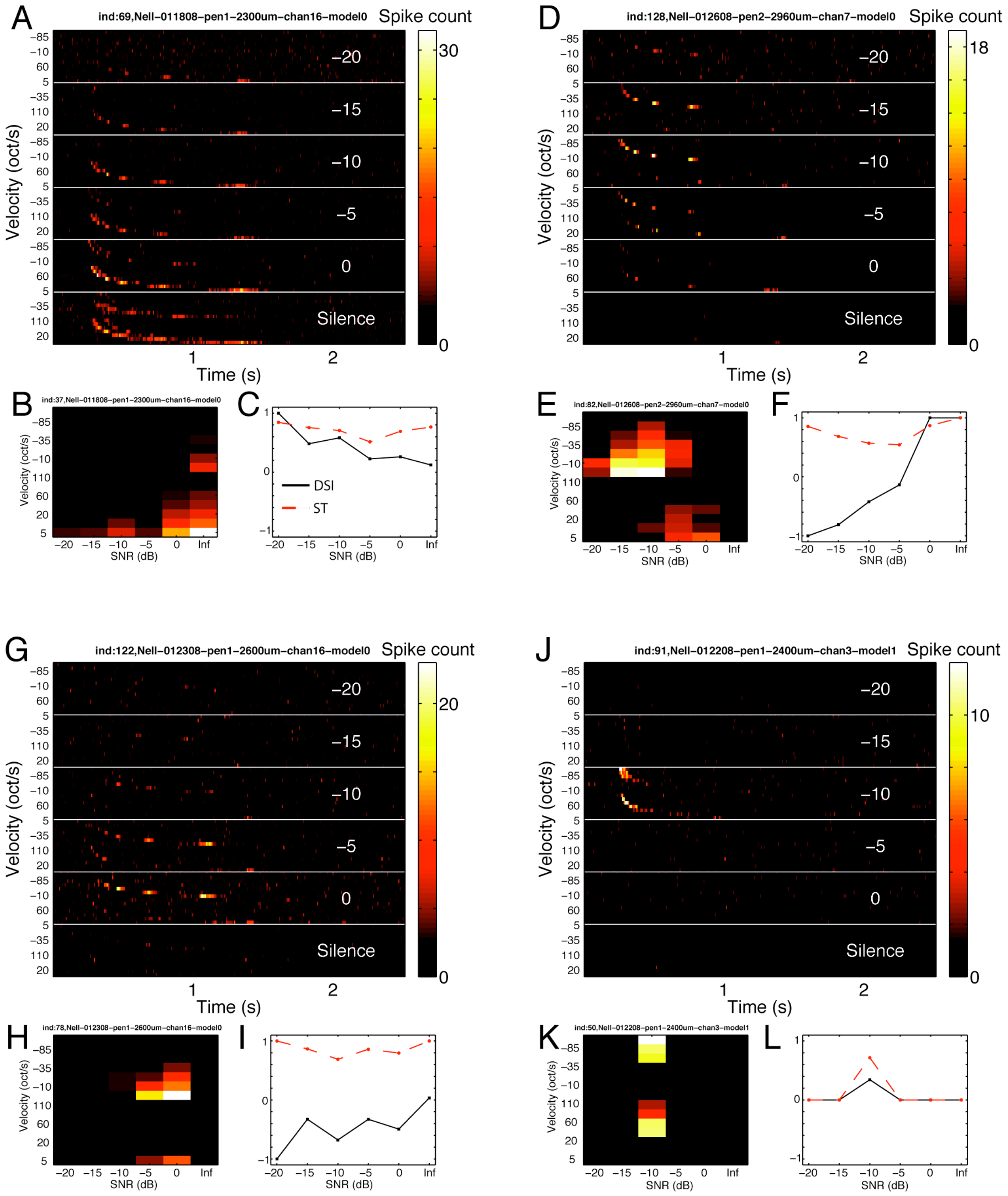

Figure 4. Responses to FM sweeps in background noise. A, D, G, J. The responses of example neurons to frequency sweeps with varying velocity and direction presented with different levels of a continuous white noise masker are shown as cumulative PSTHs. B, E, H, K. Summary for each neuron in A, D, G, J of the response magnitude for each combination of SNR, FM sweep velocity, and direction. C, F, I, L. Direction selectivity index (DSI, solid black line)

and speed tuning (ST, dashed red line) are plotted as a function of SNR for each respective example neuron.

The normalized mean response of AI neurons to each sweep stimulus are shown in Figure 5A. The addition of noise significantly affected the mean response of AI neurons (One-way ANOVA, $F(6, 1342) = 15.68$, $p < 1x10^{-5}$). The mean cortical response to all stimuli at SNRs greater than –15 dB was significantly greater than the response at –20 dB SNR (Tukey's honest significant difference, $p < 0.0005$, stars in Fig. 5A). The distribution of SNRs that evoke the maximum FM response from AI neurons is shown in Figure 5B. Most neurons respond best to FM sweeps presented in silence. However, significant proportions of neurons responded best while continuous noise was played. This proportion decreased as the SNR decreased, and none of the neurons tested showed significant responses to FM sweeps at SNRs less than –20 dB.

To summarize, AI neurons are tuned to different background noise conditions, and many neurons become more responsive to signals in the presence of noise. In spite of the existence of neurons tuned to low SNRs, the mean cortical response decreases as the SNR decreases. Furthermore, while some neurons respond better to signals in noise, the number of neurons tuned to a SNR decreases as the SNR decreases.

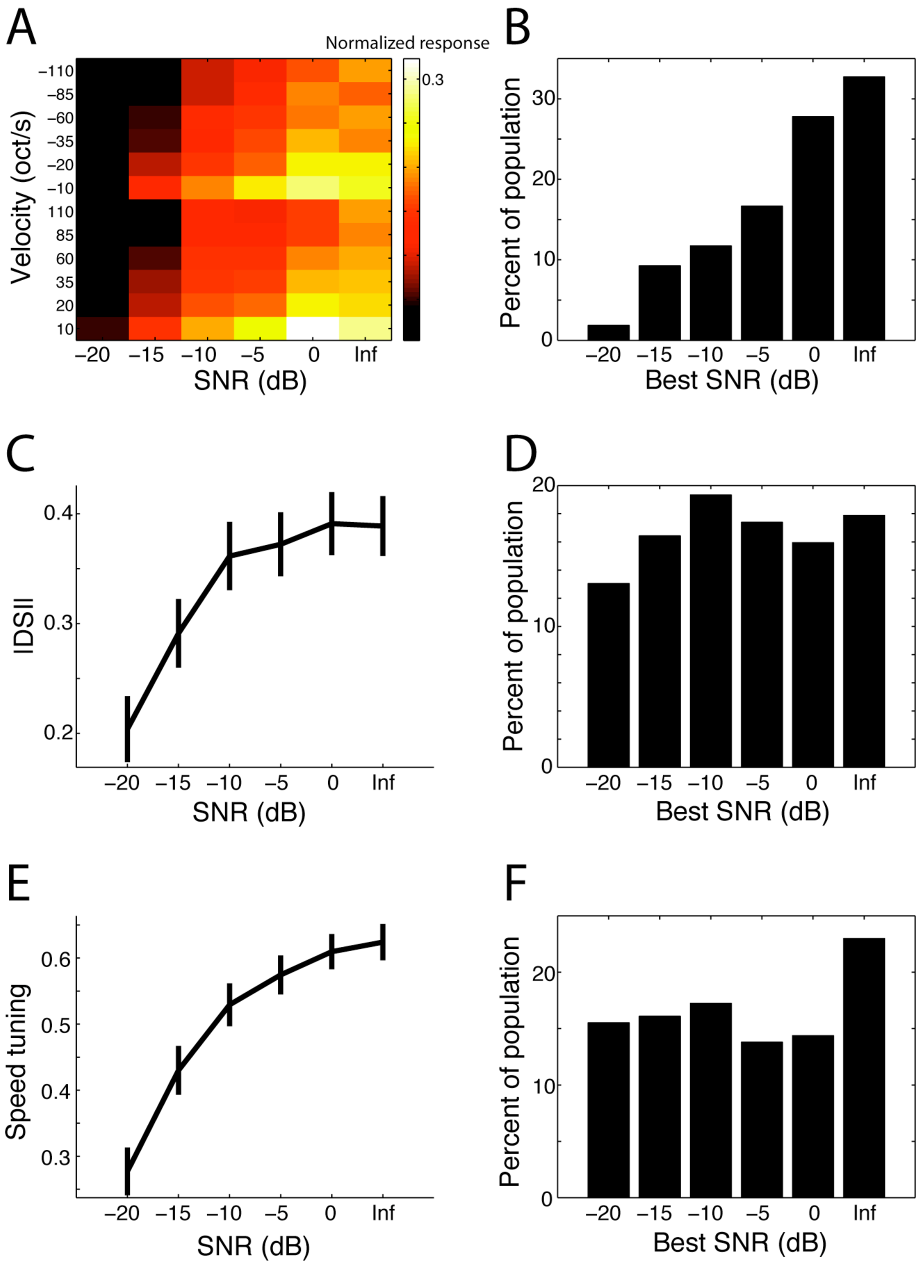

Figure 5. Summary of response magnitude and selectivity for FM sweeps as a function of SNR. A. Mean normalized response magnitude of AI neurons for each FM sweep stimulus for each SNR. B. Histogram of SNR levels that evoked the maximum FM sweep response for each AI neuron. C. Population mean absolute value of the DSI for AI neurons plotted as a function of the SNR. Error bars represent the S.E.M. D. Histogram of SNR values in which neurons were most direction selective. E. Population mean speed tuning as a function of SNR. Error bars

represent the S.E.M. F. Histogram of SNR values in which neurons had the greatest speed tuning values.

Neuronal selectivity is altered by background noise

The effects of the addition of white noise on neuronal selectivity for parameters of FM sweeps were determined by comparing the *Speed Tuning* (ST) and *Direction Selectivity Index* (DSI) of AI neurons across SNRs (see Methods, Fig 4C, F, I, L). The addition of noise produced variable effects on the selectivity of single AI neurons for the directions and speed of FM sweeps. In silence, the neuron in Figure 4A responded well to both up and down sweep directions. However at –20 dB SNR, the neuron only responded to upward FM sweeps. Thus, the DSI of this neuron increased as the SNR decreased (black line, Fig. 4C). The ST of this neuron remained relatively constant (red line, Fig. 4C). The best direction of the neuron in Figure 4D was reversed by at low SNRs. In silence and at 0 dB SNR, the neuron preferred upward sweeps (DSI > 0), while in SNRs below –5 dB, the neuron responded more strongly to downwards sweeps (DSI < 0). The ST of this neuron was lower at –5 through –15 dB (Fig. 4F, red line). This decline in ST occurred as the response magnitude increased (Fig. 4E) suggesting that moderate noise levels effectively decreased the threshold of this neuron and made it less selective for FM sweep velocity. Similarly, a decrease in overall responsiveness may have caused the neuron in Figure 4A to become more sensitive to the direction of FM stimuli.

The effect of SNR on the responses of AI neurons is summarized in Figure 5C-F. On average, direction selectivity and speed selectivity decreased as the SNR decreased. Figure 5C plots the mean of absolute value of the DSI for all neurons with significant FM responses. The absolute value of the DSI measures direction selectivity without regard to whether the preferred direction was up or down. Direction selectivity was affected by the SNR (One-way ANOVA, $F(5,966) = 7.31$, $p < 1x10^{-6}$). At –20 dB SNR, the |DSI| was significantly lower than the |DSI| at –10 dB, -5 dB, 0 dB, and in silence (Tukey's honest significant difference, $p < 0.001$). Direction selectivity values at SNRs greater than –15 dB were not significantly different from each other (Tukey's honest significant difference, $p > 0.05$) suggesting that selectivity is maintained at moderate noise levels. The percentage of neurons with maximum direction selectivity at each SNR is shown in Figure 5D. There is a fairly even distribution of neurons with maximal selectivity at each SNR. Thus, while the |DSI| of some neurons was degraded by noise, it was increased for others. However, average selectivity decreased as the noise level increased.

A similar trend was observed for the speed selectivity of AI neurons (Fig 5E, F). ST values at SNRs greater than –15 dB were greater than those at –20 dB (One-way ANOVA, $F(5, 966) = 22.61$, $p < 1x10^{-6}$; Tukey's honest significant difference, $p < 0.001$). The largest proportion of AI neurons had maximal speed selectivity in silence and roughly even numbers of neurons had the greatest ST at other SNRs.

Stimulus information across noise conditions

In AI, both the firing rate and the precise timing of action potentials can encode sounds (X. Wang, 2007). To quantify how neuronal encoding of stimuli by these two response parameters is affected by background noise, we determined the mutual information (MI) between the firing rate and the temporal pattern of responses and the FM sweep stimuli (Methods). Figure 6 shows the PSTH's in response to FM sweeps presented in different levels of noise. The responses of the neuron in Figure 6A were suppressed by high intensity noise. Because of this suppression, the mutual information between the spike count of the response and the FM sweep stimuli decreased when the SNR was less than 0 dB (Fig 6A, right column, dashed line). The length of FM sweep responses became shorter at high noise levels. This temporal sparseness increased decreased the overlap between the PSTHs of responses to different FM sweep stimuli and produced greater mutual information between the temporal response pattern and the FM sweep stimuli at low SNRs (Figure 6A, right column, solid line). The opposite effect was observed in the neuron in Figure 6B. This neuron was more responsive to FM sweeps presented in noise and had greater spike count mutual information. As the firing rate to both sweeps and noise increased, the temporal information decreased. The temporal and rate information both increased at moderate SNRs for the neuron in Figure 6C. In general, higher firing rates increase the number of potential responses that can be used to encode stimuli and therefore increase the potential information between spike counts and stimuli (L. C. Osborne et al., 2004). Thus, in examples where noise increased responsiveness, the rate information increased. Temporal information depends upon differences in the timing of action potential between responses to stimuli and may decrease if increased firing rates lead to greater overlap between stimulus evoked spike timing distributions.

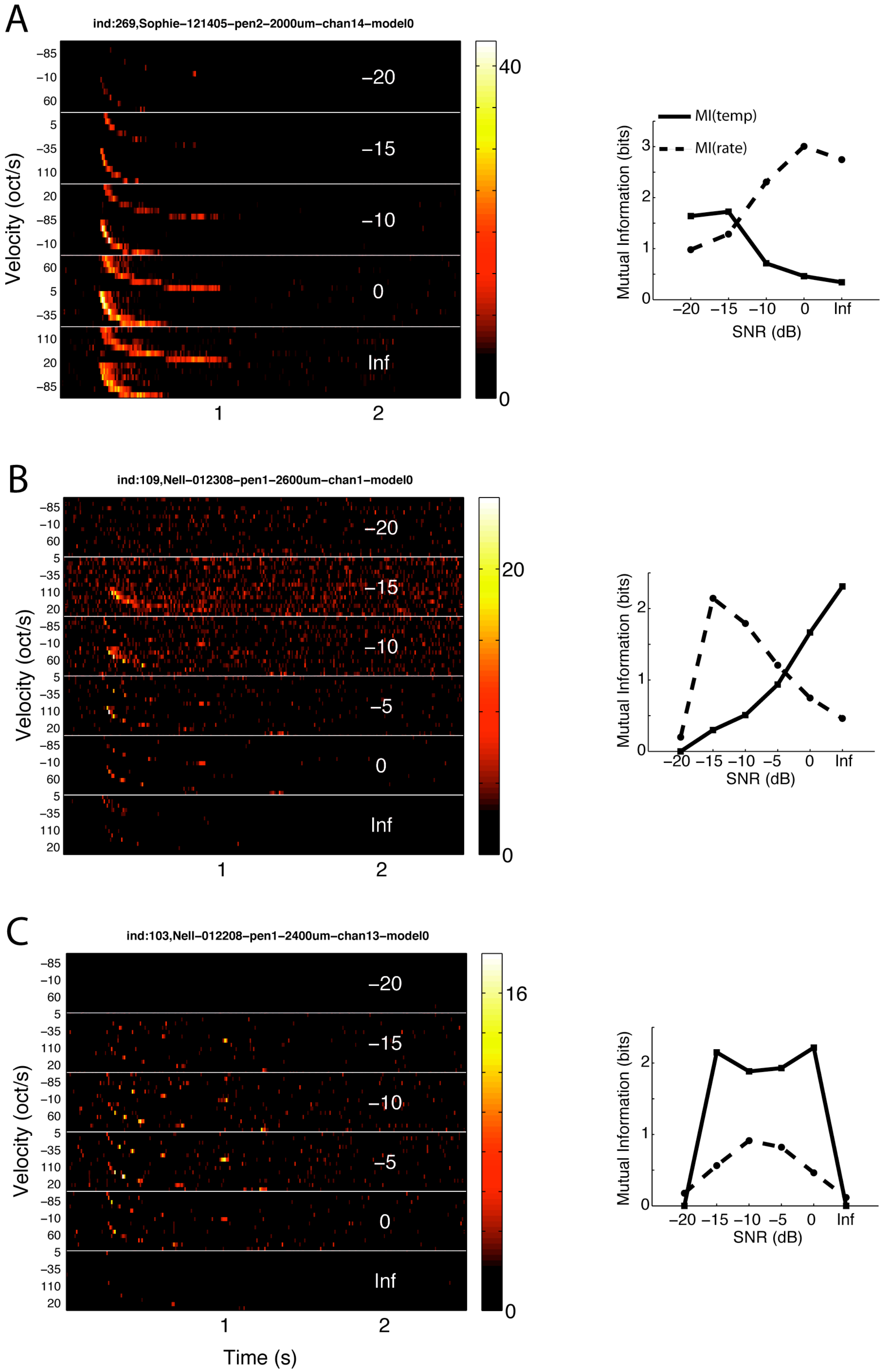
A
ind:269,Sophie−121405−pen2−2000um−chan14−model0
Velocity (oct/s)
−85
−10
60
5
−35
110
20
−20
−15
−10
0
Inf
1
2
40
0
MI(temp)
MI(rate)
Mutual Information (bits)
SNR (dB)
−20 −15 −10 0 Inf
B
ind:109,Nell−012308−pen1−2600um−chan1−model0
−20
−15
−10
−5
0
Inf
20
−20 −15 −10 −5 0 Inf
C
ind:103,Nell−012208−pen1−2400um−chan13−model0
16
Time (s)

Figure 6. Effects of background noise on mutual information. A, B, C. *Left* PSTHs for responses to FM sweep in noise for three example neurons. *Right* The mutual information between firing rate and FM sweep stimuli is plotted as a function of the SNR by the dashed line for each exemplar. *Left* Mutual information between the temporal pattern of FM sweep responses and the FM sweep stimuli for each example neuron is plotted as a function of SNR by the solid line for each exemplar.

Figure 7A summarizes the effects of SNR on the MI in AI. The proportion of neurons with significant mutual information between spike counts and FM sweep stimuli is shown by the solid line in Figure 7A (Methods). As the SNR decreased, fewer neurons carried significant information with spike counts, and at SNRs less than –20 dB, no neurons had significant MI. The proportion of neurons with significant mutual information between the timing of spikes and FM sweep stimuli first increased with the addition of noise and then decreased as the SNR decreased. Again, no neurons had significant MI at SNRs below –20 dB. Figure 7B plots the mean temporal MI, the mean rate MI, and the MI between the spike counts and noise level itself for neurons with significant information. The mean temporal MI and rate MI did not vary significantly between SNRs (Fig. 7B dashed black line and solid black line respectively; Temporal MI: One-way ANOVA, $F(5, 387) = 0.8$, $p > 0.5$; Rate MI: One-way ANOVA, $F(5, 128) = 0.56$, $p > 0.5$). This figure demonstrates that while the fewer neurons contained significant information at low SNRs, the MI carried by neurons that had significant information was the same as the mutual information in silence.

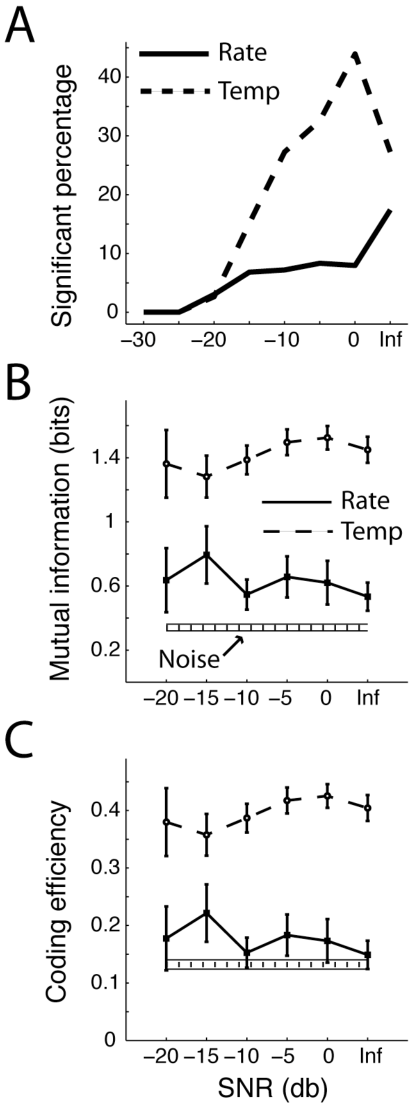

Figure 7. Effects of SNR on the mutual information in AI. A. Proportion of neurons with significant rate information (solid line) and temporal information (dashed line) is plotted as a function of the SNR. B. The mean rate information (solid line) and temporal information (dashed line) for neurons with significant information are plotted as functions of SNR. Error bars represent the S.E.M. The mean rate information for the noise level is plotted by the dotted line ± S.E.M. (solid lines). C. Mean coding efficiency for the rate information and temporal information for FM sweeps are plotted in the same format as B. The coding efficiency for the noise level is also shown in the same format as C.

In addition, the MI between spike counts and the noise level itself is shown (Fig. 7B, dotted line, black lines represent +/- standard error). 87% of neurons had significant MI between the firing rate and the noise level. Therefore, the spike counts of AI neurons represented both FM sweeps and the background noise level. To compare rate information for FM sweeps with the rate information for the noise level, we calculated the coding efficiency of each significant MI value. The coding efficiency is defined as $\frac{\mathrm{MI}}{\log_2(\text{number of stimuli})}$. This quantity represents the MI normalized by the maximum MI possible from the stimulus set and thus allows one to compare information values between stimulus sets. While the temporal coding efficiency for FM sweeps was greater than the coding efficiency for noise level (Wilcoxon rank-sum test, $p < 0.001$ for each SNR greater than –25 dB), there was no significant difference between rate coding efficiency for FM sweeps and coding efficiency for noise level (Wilcoxon rank-sum test, $p > 0.05$ for each SNR). This suggests that the spike counts of AI neurons are no more or less informative about FM sweeps than they are about the background noise level in which they occur.

Relation between responses in noise and tonal receptive fields

How general are the effects of noise on the encoding of stimuli? While we did not record responses to other stimuli in each noise condition because of experimental time constraints, we measured the frequency response area (FRA) for each neuron in silence. We then compared the percentage of neurons in which we were able to obtain an FRA between groups with strongest FM sweep responses in silence and those with strongest FM sweep responses in noise. Thus, we could determine if there was a relationship between the optimal SNR for FM sweep responses and the responsiveness to tones in silence. Figure 8A shows that a greater percentage of neurons with maximum FM sweep responses in silence had significant tonal receptive fields than neurons that had maximum FM sweep responses in the presence of noise. Therefore, it is likely that neurons with low best SNRs would also respond better to tones in noise and that noise affects responsiveness in general.

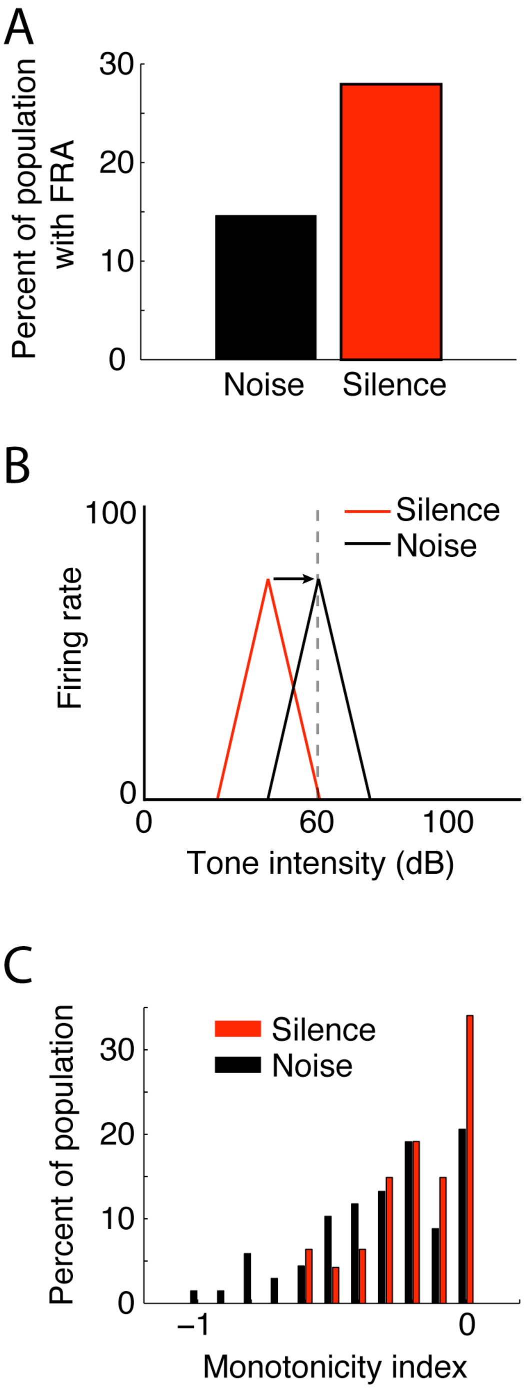

Previous experiments demonstrated that the rate-level functions of AI neurons are altered by the presence of background noise. Specifically, the best-level of neurons that have non-monotonic rate-level functions is increased when white noise is present (D. P. Phillips, 1990; G. Ehret and C. E. Schreiner, 2000; S. Sadagopan and X. Wang, 2008). The best level for FM sweep responses is highly correlated with the best level for tone responses, and rate-level functions derived from FM sweeps undergo similar changes in intensity tuning as rate-level functions derived from tones (S. Sadagopan and X. Wang, 2008). Thus, in our experiment, the addition of noise may have shifted the rate-level functions of non-monotonic neurons towards the intensity at which the FM sweep stimuli were played and increased the responsiveness of these neurons to FM sweeps. This possibility is schematized in Figure 8B which shows the rate-level function of a hypothetical neuron in silence (solid black line) and the rate-level function in noise (red line). In the presence of noise, the neuron is more responsive to tones at 60 dB (dashed gray line), which corresponds the sound level of the FM sweep stimuli in our experiment. Thus, this neuron may also become more responsive to FM sweeps at 60 dB in the presence of noise. We therefore hypothesized that non-monotonic neurons would be more likely to respond better to FM sweeps in noise than neurons with monotonic rate-level functions. To test this hypothesis we compared the distribution of *Monotonicity Index* values (Methods) for neurons that responded best to FM sweeps in silence with the values for neurons that responded best to FM sweeps in noise (Fig. 8C). Neurons that were most responsive to FM sweeps in noise were less monotonic than neurons that were most responsive in silence (Wilcoxon rank-sum test, p = 0.013). This means that neurons with strongest FM responses in noise were often non-monotonic. Therefore, it is likely that the increased responsiveness in the presence of noise for AI neurons was, in part, caused by non-monotonic rate-level functions and adaptation that shifted the best levels toward the level of the FM sweep stimuli.

Discussion

Consistent with previous studies (D. P. Phillips and M. S. Cynader, 1985; D. P. Phillips et al., 1985; D. P. Phillips, 1990; G. Ehret and C. E. Schreiner, 2000; S. S. Nagarajan et al., 2002; R. Narayan et al., 2007; S. Sadagopan and X. Wang, 2008), our data demonstrates that background noise significantly alters cortical responses to sounds. At the population level, noise ultimately degraded the cortical representation of FM sweeps. The response strength at SNRs below –10 dB, the population response, direction selectivity, and speed tuning of AI neurons decreased. Furthermore, the proportion of neurons with informative responses declined as the SNR declined. These effects are consistent psychophysical data demonstrating decrements in discrimination between sounds as the level of noise maskers increase (G. A. Miller, Heise, G. A., and Lichtan, W., 1951; J. D. Miller, 1974; R. Narayan et al., 2007).

While the average response and average selectivity of the population of AI neurons decreased as the level of a noise masker increased, the effect on single neurons was more variable. We demonstrated that many neurons become more responsive in the presence of noise than in silence. These neurons were tuned to SNRs and in some cases only responded to FM sweeps presented in a specific noise level. That some neurons become more responsive to signals in the presence of noise has been previously observed in anesthetized preparations (D. P. Phillips, 1990; S. S. Nagarajan et al., 2002). Phillips et al*.* (1990) reported that the responses of some AI neurons in anesthetized cats to tones increased in when presented with noise, and Nagarajan et al. (2002) showed a similar effect on responses to vocalizations in anesthetized marmoset monkeys. This data suggests that increased responsiveness of populations of neurons in the presence of noise is a general feature of stimulus encoding in AI.

The ability of noise to increase responsiveness has not been previously reported to the degree observed in our study. It is possible that neurons that did not respond to signals in silence but were responsive in noise were not studied due to a bias towards neurons that were responsive in silence. Because we recorded data and sorted neurons off-line, there is no bias towards recording from neurons that respond to signals in silence. A recent experiment in the awake rat demonstrated a high prevalence of neurons that were not responsive to stimuli (T. Hromadka et al., 2008). Some of these neurons may have become responsive in the presence of background noise.

The tuning of neurons to different SNRs produced a population response that was tolerant to some changes background noise conditions. For example, the mean temporal information and rate information were preserved across conditions by neurons that were informative in different SNRs. Furthermore, pooling over neurons that are tuned to different SNRs would produce a representation of signals that is invariant to changes in acoustic background. Because, however, fewer neurons have significant information in increased noise levels, there are fewer neurons from which responses can be pooled, and ultimately, noise eliminated information about the stimuli, as one would expect.

We demonstrated that the noise level significantly affects the background firing rate many of AI neurons. A continuous representation of the ambient noise level itself is critical because changes in background conditions may signify a behaviorally relevant event. These changes in background activity may also be partially responsible for enhancing responses to FM sweeps. Increased levels of background synaptic activity have been shown to shift neurons into a high conductance state that increases sensitivity to low level inputs and increases the temporal resolution (A. Destexhe et al., 2003; M. Rudolph and A. Destexhe, 2003; A. Destexhe and D. Contreras, 2006). While these experiments addressed the issue of internal states of synaptic activity, it is possible that stochastic driven activity produces similar affects and is responsible for the enhanced responsiveness of auditory cortical neurons in the present study.

The dependence of neuronal responses on SNR is another example of the sensitivity of central auditory neurons to the acoustic context in which sounds occur. AI neurons in the awake marmoset are tuned to the spectral contrast of broadband sounds (D. L. Barbour and X. Wang, 2003), and the sensitivity of macaque AI neurons to intra-aural phase disparity also depends upon the preceding stimulus history (B. J. Malone et al., 2002). Neurons in the inferior colliculus (IC) are sensitive to the frequency and amplitude context of sounds (B. J. Malone and M. N. Semple, 2001; I. Dean et al., 2005) and a recent study demonstrated that the temporal filters of IC neurons adapt to the presence of background noise in a manner that maintains stimulus information (N. A. Lesica and B. Grothe, 2008). While all of these studies and data from this experiment have demonstrated that the context in which signals occur has importance consequences for auditory encoding, the relation between the changes in neuronal responsiveness resulting from changes in context and psychophysical performance remains an important question for future investigations.

References

Atencio CA, Blake DT, Strata F, Cheung SW, Merzenich MM, Schreiner CE (2007) Frequency-modulation encoding in the primary auditory cortex of the awake owl monkey. J Neurophysiol 98:2182-2195.

Barbour DL, Wang X (2003) Contrast tuning in auditory cortex. Science 299:1073-1075.

Chance FS, Abbott LF, Reyes AD (2002) Gain modulation from background synaptic input. Neuron 35:773-782.

Cover TM, Thomas JA (2006) Elements of information theory, 2nd Edition. Hoboken, N.J.: Wiley-Interscience.

Dean I, Harper NS, McAlpine D (2005) Neural population coding of sound level adapts to stimulus statistics. Nat Neurosci 8:1684-1689.

Destexhe A, Contreras D (2006) Neuronal computations with stochastic network states. Science 314:85-90.

Destexhe A, Rudolph M, Pare D (2003) The high-conductance state of neocortical neurons in vivo. Nat Rev Neurosci 4:739-751.

Ehret G, Schreiner CE (2000) Regional variations of noise-induced changes in operating range in cat AI. Hear Res 141:107-116.

Godey B, Atencio CA, Bonham BH, Schreiner CE, Cheung SW (2005) Functional organization of squirrel monkey primary auditory cortex: responses to frequency-modulation sweeps. J Neurophysiol 94:1299-1311.

Ho N, Destexhe A (2000) Synaptic background activity enhances the responsiveness of neocortical pyramidal neurons. J Neurophysiol 84:1488-1496.

Hromadka T, Deweese MR, Zador AM (2008) Sparse representation of sounds in the unanesthetized auditory cortex. PLoS Biol 6:e16.

Hulse SH, MacDougall-Shackleton SA, Wisniewski AB (1997) Auditory scene analysis by songbirds: stream segregation of birdsong by European starlings (Sturnus vulgaris). J Comp Psychol 111:3-13.

Lesica NA, Grothe B (2008) Efficient temporal processing of naturalistic sounds. PLoS ONE 3:e1655.

Malone BJ, Semple MN (2001) Effects of auditory stimulus context on the representation of frequency in the gerbil inferior colliculus. J Neurophysiol 86:1113-1130.

Malone BJ, Scott BH, Semple MN (2002) Context-dependent adaptive coding of interaural phase disparity in the auditory cortex of awake macaques. J Neurosci 22:4625-4638.

Miller GA, Heise, G. A., and Lichtan, W. (1951) The Intelligibility of Speech as a Function of the Context of the Test Materials. Journal of Experimental Psychology 41:329-335.

Miller JD (1974) Effects of noise on people. J Acoust Soc Am 56:729-764.

Moss F, Ward LM, Sannita WG (2004) Stochastic resonance and sensory information processing: a tutorial and review of application. Clin Neurophysiol 115:267-281.

Nagarajan SS, Cheung SW, Bedenbaugh P, Beitel RE, Schreiner CE, Merzenich MM (2002) Representation of spectral and temporal envelope of twitter vocalizations in common marmoset primary auditory cortex. J Neurophysiol 87:1723-1737.

Narayan R, Best V, Ozmeral E, McClaine E, Dent M, Shinn-Cunningham B, Sen K (2007) Cortical interference effects in the cocktail party problem. Nat Neurosci 10:1601-1607.

Nelken I, Chechik G (2007) Information theory in auditory research. Hear Res 229:94-105.

Olsen WO, Noffsinger D, Kurdziel S (1975) Speech discrimination in quiet and in white noise by patients with peripheral and central lesions. Acta Otolaryngol 80:375-382.

Osborne LC, Bialek W, Lisberger SG (2004) Time course of information about motion direction in visual area MT of macaque monkeys. J Neurosci 24:3210-3222.

Phillips DP (1990) Neural representation of sound amplitude in the auditory cortex: effects of noise masking. Behav Brain Res 37:197-214.

Phillips DP, Cynader MS (1985) Some neural mechanisms in the cat's auditory cortex underlying sensitivity to combined tone and wide-spectrum noise stimuli. Hear Res 18:87-102.

Phillips DP, Orman SS, Musicant AD, Wilson GF (1985) Neurons in the cat's primary auditory cortex distinguished by their responses to tones and wide-spectrum noise. Hear Res 18:73-86.

Rudolph M, Destexhe A (2003) A fast-conducting, stochastic integrative mode for neocortical neurons in vivo. J Neurosci 23:2466-2476.

Sadagopan S, Wang X (2008) Level invariant representation of sounds by populations of neurons in primary auditory cortex. J Neurosci 28:3415-3426.

Shannon C (1948) A mathematical theory of communication. Bell Syst Tech J 27:379-423.

Strong SP, Koberle R, de Ruyter van Stevenick RR, Bialek W (1998) Entropy and information in neural spike trains. Phys Rev Lett 80:197-200.

Wang X (2007) Neural coding strategies in auditory cortex. Hear Res 229:81-93.

Wiesenfeld K, Moss F (1995) Stochastic resonance and the benefits of noise: from ice ages to crayfish and SQUIDs. Nature 373:33-36.

Wolfart J, Debay D, Le Masson G, Destexhe A, Bal T (2005) Synaptic background activity controls spike transfer from thalamus to cortex. Nat Neurosci 8:1760-1767.

Chapter 5

Conclusion

Discussion of Results

The goal of this thesis was to identify strategies that underlie the representation of components of communication sounds in different acoustic conditions in primary auditory cortex of awake primates (AI). While the representation of some elements of communication sounds have been determined in anesthetized animals, a detailed account of the processing of such sounds in auditory cortex of awake animals is still required. In addition, little is known about the encoding principles that underlie cortical sound processing in noisy environments. To address these gaps in our knowledge, we examined the encoding of frequency-modulated (FM) sweeps in silence and in the presence of different levels of background noise in AI of awake squirrel monkeys.

We began, in chapter 2, with an examination of the relation between basic properties of AI neurons with the encoding of FM sweeps. Studies had reported that the responses of AI neurons to pure tones range from onset to sustained (I. O. Volkov and A. V. Galaziuk, 1985; G. H. Recanzone, 2000; X. Wang et al., 2005) suggesting that multiple concurrent response modes exist for a single stimulus. We demonstrated that these different response modes generalize to the encoding of FM sweeps such that neurons with sustained tone responses also have sustained FM sweep responses while neurons with onset tone responses also have onset responses to FM sweeps. The temporal response mode also determined the range of preferred frequency modulation speeds: Neurons with onset responses preferred fast modulation rates while neurons with sustained responses preferred slower modulation rates and faithfully represented the envelope of these stimuli. Additionally, response modes are related to more general features of AI neurons such as the threshold, spectral tuning bandwidth, and spontaneous firing rate. Neurons with high thresholds, low spontaneous activity, and sharp frequency tuning had brief onset responses to tones and FM sweeps, and were primarily unresponsive to broadband noise. In contrast, neurons with high spontaneous activity, low thresholds, and broad frequency tuning had sustained responses to tones, FM sweeps, and broadband noise.

A recent study by Atencio et al. also demonstrated a continuum of interrelated properties of neurons in AI of anesthetized cats (C. A. Atencio and C. E. Schreiner, 2008). In that study, properties such as feature selectivity and phase locking were different between neurons with high firing rates and neurons with low firing rates. Neurons for which the high firing rate regime was dominant had low feature selectivity and weaker phase locking to spectro-temporal ripple stimuli than neurons with lower firing rates. A related study in IC of anesthetized cats also demonstrated that neurons with high firing rates carry less information per spike and were less feature selective than neurons with low firing rates (M. A. Escabi et al., 2005). Data from this thesis demonstrated that neurons with sustained responses and high spontaneous firing rates were less selective for FM rate than neurons with low firing rates when responses were normalized by response length. These neurons essentially responded as long as the instantaneous sweep frequency was within the tonal receptive field. They were also more broadly tuned for tone frequency and frequently had sustained responses to continuous noise. While neurons in anesthetized animals have predominately onset responses, our data suggests that neurons with sustained responses in AI of awake primates may be less selective in general than neurons with low spontaneous rates. Thus our data from awake primate AI match results in the anesthetized cat and suggests that the observed differences in response mode may be a reflection of some fundamental processing features of AI neurons with multiple functional consequences for stimulus encoding.

Escabi et al. (2005) demonstrated that, in the IC, the relation between firing rate, feature selectivity and information transmission could be accounted for by a model in which the membrane potential-based threshold of neurons determined the response mode. High threshold neurons were more feature selective, carried more information per spike than neurons with low thresholds. Our data demonstrated a difference between neurons with sustained and onset responses that suggest that this mechanism could also underlie the difference between these processing regimes in cortex.

The mechanisms that underlie the difference in effective response threshold were not determined in either study. As discussed in chapter 2, our data is consistent with a model in which the temporal dynamics and strength of cortical inhibition differ between neurons with different response modes. We hypothesize that neurons with onset responses in awake AI have strong rapid and early onset inhibition following excitation in a manner similar to that reported in AI of anesthetized rats where onset responses dominate (M. Wehr and A. M. Zador, 2003; A. Y. Tan et al., 2004), whereas neurons in which the sustained response mode dominates have weaker inhibition in general and with a later onset in onset-sustained neurons.

In Atencio et al. (2008), response mode was statistically not related to spectral or temporal modulation preference of neurons, whereas in our study neurons with low spontaneous activity and onset responses preferred faster FM modulation speeds than neurons with sustained responses and high spontaneous activity.

This discrepancy could be due to a difference between awake and anesthetized preparationsbut likely is the consequence of a more detailed parametric analysis that was possible with the FM analysis. As stated previously, neurons in anesthetized animals predominately have onset responses whereas neurons in awake animals have a higher proportion of neurons with sustained responses. This difference in response mode between anesthetic states could change the range of preferred spectral modulation rates as is also the case for temporal modulation rates (T. Lu et al., 2001). Another potential explanation for the difference in results is that very different stimuli were used to characterize the spectral modulation rate preference of AI neurons. Atencio et al. determined the best spectral modulation rate from spectro-temporal receptive fields (STRFs) whereas our study used FM sweeps. Response non-linearities may lead to inconsistencies in the preferred spectral modulation rate determined from different stimuli (C. A. Atencio et al., 2007).

Our results demonstrated that populations of neurons with different response modes produce opposing response functions of FM sweep speed. Other studies in awake primates have also demonstrated that different populations of neurons have anti-correlated response functions. The firing rate of neurons in secondary somatosensory cortex (S2) are either monotonically increasing or decreasing functions of the repetition rate of a finger tap stimulus (A. Hernandez et al., 2000). Similarly, in auditory cortex, the firing rate of neurons can be monotonically increasing or decreasing functions of the temporal modulation rate of amplitude modulated tone or of stimulus azimuth (G. H. Recanzone et al., 2000; G. C. Stecker et al., 2005; D. Bendor and X. Wang, 2007). It has been hypothesized that populations with opposing response functions may increase the number of stimuli that may be encoded with the firing rate of single neurons (G. C. Stecker et al., 2005; D. Bendor and X. Wang, 2007).

In our data, the response mode of AI neurons was constant throughout penetrations that spanned the depth of AI. Using a 16-channel linear array, we showed that simultaneously recorded neurons within a penetration had similar response properties. Single penetrations were dominated either by neurons with onset firing modes or were dominated by neurons with sustained firing modes. A qualitatively similar result was recently obtained in anesthetized guinea pig (M. N. Wallace and A. R. Palmer, 2008). While we could not obtain detailed topographic maps of the response mode, this response parameter may be clustered across the surface of AI and thus be another spatially organized functional parameter akin to bandwidth, CF, latency and FM direction selectivity (C. E. Schreiner and J. R.

Mendelson, 1990; J. R. Mendelson et al., 1997; G. H. Recanzone et al., 1999; S. W. Cheung et al., 2001; B. Godey et al., 2005).

In chapter 3 we determined how well the spike counts and temporal response patterns of AI neurons encode FM sweeps. In AI neurons both spike timing and spike rate carry information about the speed and direction of frequency sweep stimuli. For individual neurons, there is an inverse relation between information carried by spike count and spike timing. This tradeoff suggests that neurons in AI are optimized either for sustained responses or for temporally precise responses. Thus, information in AI responses lies on a continuum between rate and temporal codes resulting in multiple representations of sounds.

The relevance of precise spike timing for behavioral decisions remains unclear. In somatosensory cortex, neurons also carry information in the timing and firing rate (A. Hernandez et al., 2000; S. Panzeri et al., 2001). Yet studies comparing the activity of neurons with behavioral decision demonstrated that for repetition rate encoding, theoretical thresholds based upon spike counts matched psychophysical threshold better than those based upon the temporal pattern of responses. Additionally, the firing rates of neurons co-vary with behavioral decisions during the discrimination of flutter rates (A. Hernandez et al., 2000; R. Luna et al., 2005). Spike timing also carries significant information in the visual cortex (G. T. Buracas et al., 1998; D. S. Reich et al., 2000). Yet, here too, psychophysical thresholds match theoretical thresholds based upon spike counts and behavioral decisions co-vary with neuronal firing rates (K. H. Britten et al., 1992; K. H. Britten et al., 1996). In addition to our study, a number of studies in AI have demonstrated that spike timing carries information about many stimulus classes including the depth and rate of amplitude modulations, click repetition rates, spatial location, and animal vocalizations and human speech (B. J. Mickey and J. C. Middlebrooks, 2003; I. Nelken et al., 2005; B. J. Malone et al., 2007; N. Mesgarani et al., 2008). Liu and Schreiner (2007) demonstrated that an increase of temporal precision in responses to a natural sound - due to an enhanced behavioral significance of that sound - likely contribute to an enhanced detection and discrimination ability of the animal. Studies have also demonstrated that thresholds derived from the temporal pattern of neuronal responses to stimuli match performance of auditory discrimination tasks (R. Narayan et al., 2007; C. T. Engineer et al., 2008). However, the firing rate itself of some neurons in AI and the caudomedial field (CM) match the behavioral thresholds of macaque monkeys performing a spatial localization task (G. H. Recanzone et al., 2000). Taken together, these results indicate that the influence of precise spike timing on behavioral decisions likely depends upon the task being performed and may differ among auditory cortical areas. Our data demonstrates that for FM sweeps different populations encode stimuli with different emphasis on firing rate or spike timing. AI thus maintains a flexible representation of sounds consistent with its role as a general auditory processing center at the interface between processing stages dominated by external, stimulus-based frameworks and internal, object and/or concept-based frameworks. The ability to integrate over different time scales is likely necessary for representation of the wide variety of behaviorally relevant time scales of sounds.

In chapter 4, we examined the effects of background noise on the representation of FM sweeps in AI. Noise affected the responses of AI neurons in dramatically different ways; noise degraded the responses of some neurons and, quite substantially, improved the responses of others. In addition, we demonstrated that some cortical neurons respond continuously to different levels of noise, thus altering the local level of network activity. Therefore, external noise itself can shift the response mode or state of auditory cortical neurons. We hypothesize that this shift in state is similar to shifts in the responsiveness or gain of cortical neurons that occur during different internal states such as different levels of arousal and attention (H. Spitzer et al., 1988; I. Lampl et al., 1999; C. J. McAdams and J. H. Maunsell, 1999b, a; M. Steriade et al., 2001).

A number of studies have modeled the effects of changes in sensory cortical activity produced by shifts in alertness or attention. These changes in internal state alter the baseline level of synaptic bombardment in cortical neurons (N. Ho and A. Destexhe, 2000; A. Destexhe et al., 2003; Y. Shu et al., 2003; A. Destexhe and D. Contreras, 2006; B. Haider et al., 2007). *In vitro* experiments and computational studies have demonstrated that while a pure increase in membrane conductance increases the current required to produce a constant firing rate, depolarization and increased membrane potential variance can dramatically increase the neuronal responsiveness, dynamic range, and temporal precision. Internal states also affect responsiveness to external stimuli *in vivo*. Haider et al. (2007), for example, demonstrated that neurons in visual cortex were more responsive to visual stimuli during *Up states*, during which slow oscillations increase the level of network activity. External acoustic noise, by analogy, may shift the state of some quiescent AI neurons into the equivalent of an Up state. These neurons thus became more responsive to FM sweeps when presented in background noise.

External acoustic stimuli have been shown to alter the state of the auditory system. Miller et al. (2000) demonstrated that spectro-temporally complex broadband ripple stimuli dampen thalamocortical oscillations in anesthetized cats. The ripple stimulus is thought to shift the thalamocortical system into a desynchronized state resembling that of alert animals. Taken together, Miller et al. and our data suggest that multiple broadband stimuli may produce general affects on the auditory system that change the level of synaptic bombardment and alter the responses to signals that occur in their presence.

Improvements in the performance of auditory perceptual tasks have been demonstrated in humans when signals were presented in the presence of noise. The addition of white noise decreased the detection threshold of subjects with normal hearing, cochlear implants, and auditory brainstem implants (F. G. Zeng et al., 2000). Furthermore, the discrimination of the level of a component of a suprathreshold harmonic was improved by the addition of suprathreshold white noise (S. E. Behnam and F. G. Zeng, 2003). These improvements were thought to result from stochastic resonance, a phenomenon in which the addition of noise in a non-linear system decreases the threshold for detection of a stimulus (F. Moss et al., 2004). Effects similar to those observed in our study may contribute to these psychophysical phenomena and be essential for understanding auditory processing in different background noise conditions. Furthermore, stochastic resonance may produce the increased responsiveness of some AI neurons in the presence of noise.

Continuous acoustic white noise may produce alterations in the state of cortex that span beyond the auditory system. A series of studies in the 1970’s revealed that continuous white noise can actually improve performance of non-auditory psychomotor tasks such as the Stroop color-word test (E. C. Poulton, 1979). These affects were thought to be mediated by an increased level of arousal while perform tasks in noise suggesting that acoustic noise may have widespread affects on brain states.

Future Directions

Our results in chapter 2 suggest that different response modes (onset versus sustained) may be produced by differences in the strength and kinetics of cortical inhibition. To elucidate the mechanism that generates these different responses, *in vivo* voltage clamp recordings in awake animals must be performed. By holding the membrane potential of neurons at the equilibrium potential for excitatory currents, one may record the dynamics and size of inhibitory currents. These currents should differ between neurons with sustained responses and neurons with onset responses. In addition, juxtacellular labeling of neurons with different response properties would reveal potential differences anatomy and laminar location of cells with different response modes.

Studies of awake behaving animals would allow experimenters to identify the functional relation between response modes and psychophysical performance of auditory tasks. For example, how do the behavioral decisions of an animal co-vary with the responses of neurons with different response modes? One could imagine that neurons with onset responses may be more informative for a task in which fast FM sweep speeds must be discriminated because these neurons preferentially represented faster speeds. Furthermore, neurons with onset responses carried more temporal information than neurons with sustained responses. The answer to this question would shed light on the behaviorally relevant aspects of neuronal responses.

Representational plasticity in the cortex can significantly alter its functional organization (W. M. Jenkins and M. M. Merzenich, 1987; J. S. Bakin and N. M. Weinberger, 1990; G. H. Recanzone et al., 1993). Studies which compare the responses of neurons in animals that have been trained on a discrimination task with responses of naïve animals have the potential to reveal the role of neurons with different response properties in behavior. Through representational plasticity, the relevant aspects of representations are emphasized in cortex. Behavioral training combined with neurophysiology can therefore be used to examine the functional significance of different response properties. For example, a task that requires the discrimination of the length of tonal stimuli may produce a shift in the population of AI neurons toward sustained responses that faithfully represent the envelope of stimuli which would suggest that these response types are important for this task. Similarly, training may produce changes in the mutual information between either the firing rate of temporal patterns of responses and trained stimuli thereby suggesting that one of these response parameters is important for behavioral decisions.

A number of questions arise from the data presented in chapter 4. First, are similar effects observed in the presence of background sounds with different spectro-temporal characteristics? Many background sounds, such as the vocalizations of conspecifics or music, are highly complex. How do these sounds affect the responses of auditory cortical neurons to FM sweep signals or other elements of communication sounds? Second, what synaptic mechanisms generate the altered responsiveness in noise? This question may be answered by recording the membrane potential of neurons *in vivo*. Such data would reveal whether or not noise produces membrane potential variations similar to those observed cortical Up states (B. Haider et al., 2007). Changes in spiking responses to intracellular current injections during the presentation of noise could also reveal noise-induced changes in neuronal excitability. Furthermore, studies in awake behaving animals that must discriminated FM sweep stimuli in the presence of noise would allow one to determine the relation between the responses of neurons tuned to different signal-to-noise ratios and psychophysical thresholds. Here too, training in a specific noise condition may emphasize neurons tuned to that noise level and thereby demonstrate the functional importance of this property.

References:

Atencio CA, Schreiner CE (2008) Spectrotemporal processing differences between auditory cortical fast-spiking and regular-spiking neurons. J Neurosci 28:3897-3910.

Atencio CA, Blake DT, Strata F, Cheung SW, Merzenich MM, Schreiner CE (2007) Frequency-modulation encoding in the primary auditory cortex of the awake owl monkey. J Neurophysiol 98:2182-2195.

Bakin JS, Weinberger NM (1990) Classical conditioning induces CS-specific receptive field plasticity in the auditory cortex of the guinea pig. Brain Res 536:271-286.

Behnam SE, Zeng FG (2003) Noise improves suprathreshold discrimination in cochlear-implant listeners. Hear Res 186:91-93.

Bendor D, Wang X (2007) Differential neural coding of acoustic flutter within primate auditory cortex. Nat Neurosci 10:763-771.

Britten KH, Shadlen MN, Newsome WT, Movshon JA (1992) The analysis of visual motion: a comparison of neuronal and psychophysical performance. J Neurosci 12:4745-4765.

Britten KH, Newsome WT, Shadlen MN, Celebrini S, Movshon JA (1996) A relationship between behavioral choice and the visual responses of neurons in macaque MT. Vis Neurosci 13:87-100.

Buracas GT, Zador AM, DeWeese MR, Albright TD (1998) Efficient discrimination of temporal patterns by motion-sensitive neurons in primate visual cortex. Neuron 20:959-969.

Cheung SW, Bedenbaugh PH, Nagarajan SS, Schreiner CE (2001) Functional organization of squirrel monkey primary auditory cortex: responses to pure tones. J Neurophysiol 85:1732-1749.

Destexhe A, Contreras D (2006) Neuronal computations with stochastic network states. Science 314:85-90.

Destexhe A, Rudolph M, Pare D (2003) The high-conductance state of neocortical neurons in vivo. Nat Rev Neurosci 4:739-751.

Engineer CT, Perez CA, Chen YH, Carraway RS, Reed AC, Shetake JA, Jakkamsetti V, Chang KQ, Kilgard MP (2008) Cortical activity patterns predict speech discrimination ability. Nat Neurosci 11:603-608.

Escabi MA, Nassiri R, Miller LM, Schreiner CE, Read HL (2005) The contribution of spike threshold to acoustic feature selectivity, spike information content, and information throughput. J Neurosci 25:9524-9534.

Godey B, Atencio CA, Bonham BH, Schreiner CE, Cheung SW (2005) Functional organization of squirrel monkey primary auditory cortex: responses to frequency-modulation sweeps. J Neurophysiol 94:1299-1311.

Haider B, Duque A, Hasenstaub AR, Yu Y, McCormick DA (2007) Enhancement of visual responsiveness by spontaneous local network activity in vivo. J Neurophysiol 97:4186-4202.

Hernandez A, Zainos A, Romo R (2000) Neuronal correlates of sensory discrimination in the somatosensory cortex. Proc Natl Acad Sci U S A 97:6191-6196.

Ho N, Destexhe A (2000) Synaptic background activity enhances the responsiveness of neocortical pyramidal neurons. J Neurophysiol 84:1488-1496.

Jenkins WM, Merzenich MM (1987) Reorganization of neocortical representations after brain injury: a neurophysiological model of the bases of recovery from stroke. Prog Brain Res 71:249-266.

Lampl I, Reichova I, Ferster D (1999) Synchronous membrane potential fluctuations in neurons of the cat visual cortex. Neuron 22:361-374.

Lu T, Liang L, Wang X (2001) Temporal and rate representations of time-varying signals in the auditory cortex of awake primates. Nat Neurosci 4:1131-1138.

Luna R, Hernandez A, Brody CD, Romo R (2005) Neural codes for perceptual discrimination in primary somatosensory cortex. Nat Neurosci 8:1210-1219.

Malone BJ, Scott BH, Semple MN (2007) Dynamic amplitude coding in the auditory cortex of awake rhesus macaques. J Neurophysiol 98:1451-1474.

McAdams CJ, Maunsell JH (1999a) Effects of attention on orientation-tuning functions of single neurons in macaque cortical area V4. J Neurosci 19:431-441.

McAdams CJ, Maunsell JH (1999b) Effects of attention on the reliability of individual neurons in monkey visual cortex. Neuron 23:765-773.

Mendelson JR, Schreiner CE, Sutter ML (1997) Functional topography of cat primary auditory cortex: response latencies. J Comp Physiol [A] 181:615-633.

Mesgarani N, David SV, Fritz JB, Shamma SA (2008) Phoneme representation and classification in primary auditory cortex. J Acoust Soc Am 123:899-909.

Mickey BJ, Middlebrooks JC (2003) Representation of auditory space by cortical neurons in awake cats. J Neurosci 23:8649-8663.

Miller LM, Schreiner CE (2000) Stimulus-based state control in the thalamocortical system. J Neurosci 20:7011-7016.

Moss F, Ward LM, Sannita WG (2004) Stochastic resonance and sensory information processing: a tutorial and review of application. Clin Neurophysiol 115:267-281.

Narayan R, Best V, Ozmeral E, McClaine E, Dent M, Shinn-Cunningham B, Sen K (2007) Cortical interference effects in the cocktail party problem. Nat Neurosci.

Nelken I, Chechik G, Mrsic-Flogel TD, King AJ, Schnupp JW (2005) Encoding stimulus information by spike numbers and mean response time in primary auditory cortex. J Comput Neurosci 19:199-221.

Panzeri S, Petersen RS, Schultz SR, Lebedev M, Diamond ME (2001) The role of spike timing in the coding of stimulus location in rat somatosensory cortex. Neuron 29:769-777.

Poulton EC (1979) Composite model for human performance in continuous noise. Psychol Rev 86:361-375.

Recanzone GH (2000) Response profiles of auditory cortical neurons to tones and noise in behaving macaque monkeys. Hear Res 150:104-118.

Recanzone GH, Schreiner CE, Merzenich MM (1993) Plasticity in the frequency representation of primary auditory cortex following discrimination training in adult owl monkeys. J Neurosci 13:87-103.

Recanzone GH, Guard DC, Phan ML, Su TK (2000) Correlation between the activity of single auditory cortical neurons and sound-localization behavior in the macaque monkey. J Neurophysiol 83:2723-2739.

Recanzone GH, Schreiner CE, Sutter ML, Beitel RE, Merzenich MM (1999) Functional organization of spectral receptive fields in the primary auditory cortex of the owl monkey. J Comp Neurol 415:460-481.

Reich DS, Mechler F, Purpura KP, Victor JD (2000) Interspike intervals, receptive fields, and information encoding in primary visual cortex. J Neurosci 20:1964-1974.

Schreiner CE, Mendelson JR (1990) Functional topography of cat primary auditory cortex: distribution of integrated excitation. J Neurophysiol 64:1442-1459.

Shu Y, Hasenstaub A, Badoual M, Bal T, McCormick DA (2003) Barrages of synaptic activity control the gain and sensitivity of cortical neurons. J Neurosci 23:10388-10401.

Spitzer H, Desimone R, Moran J (1988) Increased attention enhances both behavioral and neuronal performance. Science 240:338-340.

Stecker GC, Harrington IA, Middlebrooks JC (2005) Location coding by opponent neural populations in the auditory cortex. PLoS Biol 3:e78.

Steriade M, Timofeev I, Grenier F (2001) Natural waking and sleep states: a view from inside neocortical neurons. J Neurophysiol 85:1969-1985.

Tan AY, Zhang LI, Merzenich MM, Schreiner CE (2004) Tone-evoked excitatory and inhibitory synaptic conductances of primary auditory cortex neurons. J Neurophysiol 92:630-643.

Volkov IO, Galaziuk AV (1985) [Reactions of neurons of the auditory cortex of unanesthetized cats to tones of a characteristic frequency]. Neirofiziologiia 17:500-508.

Wallace MN, Palmer AR (2008) Laminar differences in the response properties of cells in the primary auditory cortex. Exp Brain Res 184:179-191.

Wang X, Lu T, Snider RK, Liang L (2005) Sustained firing in auditory cortex evoked by preferred stimuli. Nature 435:341-346.

Wehr M, Zador AM (2003) Balanced inhibition underlies tuning and sharpens spike timing in auditory cortex. Nature 426:442-446.

Zeng FG, Fu QJ, Morse R (2000) Human hearing enhanced by noise. Brain Res 869:251-255.

Publishing Agreement

It is the policy of the University to encourage the distribution of all theses and dissertations. Copies of all UCSF theses and dissertations will be routed to the library via the Graduate Division. The library will make all theses and dissertations accessible to the public and will preserve these to the best of their abilities, in perpetuity.

Please sign the following statement:
I hereby grant permission to the Graduate Division of the University of California, San Francisco to release copies of my thesis or dissertation to the Campus Library to provide access and preservation, in whole or in part, in perpetuity.

06/11/08

Author Signature Date